論文 / 著書情報
Article / Book Information

題目(和文)	
Title(English)	Kinetic studies on calcium release by the inositol 1,4,5-trisphosphate receptor
著者(和文)	廣田順二
Author(English)	Junji Hirota
出典(和文)	学位:博士（工学）, 学位授与機関:東京工業大学, 報告番号:甲第3086号, 授与年月日:1995年9月30日, 学位の種別:課程博士, 審査員:
Citation(English)	Degree:Doctor of Engineering, Conferring organization: Tokyo Institute of Technology, Report number:甲第3086号, Conferred date:1995/9/30, Degree Type:Course doctor, Examiner:
学位種別(和文)	博士論文
Type(English)	Doctoral Thesis

Kinetic Studies on Calcium Release by the Inositol 1,4,5-Trisphosphate Receptor

by

Junji Hirota

A DOCTORAL THESIS

submitted to the

Department of Bioengineering

Tokyo Institute of Technology

1995

Department of Bioengineering
Tokyo Institute of Technology
Nagatsuta 4259, Midori-ku
Yokohama 226
Japan

SUMMARY

Inositol 1,4,5-trisphosphate is a second messenger, responsible for the release of Ca^{2+} from intracellular Ca^{2+} stores. In this study, the kinetics of inositol 1,4,5-trisphosphate (IP_3)-induced Ca^{2+} release by the immunoaffinity-purified IP_3 receptor type 1 (IP_3R1), reconstituted into lipid vesicles, was investigated using the fluorescent Ca^{2+} indicator fluo-3. IP_3R1 was purified type-specifically from mouse cerebellar microsomal fraction by using an immunoaffinity column conjugated with an anti-IP_3R1 antibody. The immunoblotting analysis revealed that the purified IP_3R was chiefly composed of homotetramers of IP_3R1. Ca^{2+} efflux from the proteoliposomes induced by IP_3 was monitored as fluorescence changes of 10 μM fluo-3, whose concentration was high enough to buffer released Ca^{2+} and to keep deviations of extravesicular free Ca^{2+} concentration within 30 nM, excluding the possibility of Ca^{2+}-mediated regulation of IP_3-induced Ca^{2+} release. We also examined IP_3-induced Ca^{2+} release using 1 μM fluo-3, where the deviations of free Ca^{2+} concentration were within 300 nM. At both fluo-3 concentrations, IP_3-induced Ca^{2+} release showed similar kinetic properties, i.e., little Ca^{2+} regulation of Ca^{2+} release was observed in this system. IP_3-induced Ca^{2+} release of the purified IP_3R1 exhibited positive cooperativity; the Hill coefficient was 1.8 ± 0.1. The half maximal initial rate for Ca^{2+} release occurred at 100 nM IP_3. At the submaximal concentrations of IP_3, the purified IP_3R1 showed quantal Ca^{2+} release, revealing that a single type of IP_3R (IP_3R1) is capable of producing the phenomenon of quantal Ca^{2+} release. The profiles of the IP_3-induced Ca^{2+} release of the purified IP_3R1 were found to be biexponential with the fast and slow rate constants ($k_{fast} = 0.3 \sim 0.7\ s^{-1}$, $k_{slow} = 0.03 \sim 0.07\ s^{-1}$), indicating that IP_3R1 has two states to release Ca^{2+}. The amount of released Ca^{2+} by the slow phase was constant, whereas that by the fast phase increased in proportion to added IP_3. This provides evidence to support the view that the fast phase of Ca^{2+} release is mediated by the low affinity state and the slow phase by the high affinity state of the IP_3R1. This also suggests that the fast component of Ca^{2+} release is responsible for the process of quantal Ca^{2+} release.

Kinetics of Ca^{2+} release by adenophostin B, a novel agonist of inositol 1,4,5-trisphosphate (IP_3) receptor, in the purified and reconstituted IP_3 receptor type 1 (IP_3R1) was also investigated. Adenophostin B-induced Ca^{2+} release by the purified IP_3R1 exhibited a high positive cooperativity (n_H = 3.9 ± 0.2, EC_{50} = 11 nM), whereas the IP_3-induced Ca^{2+} release did a moderate one (n_H = 1.8± 0.1, EC_{50} = 100 nM). Submaximal concentrations of adenophostin B caused the quantal Ca^{2+} release from the purified IP_3R1 as IP_3 did. Inhibition of $[^3H]IP_3$ binding to the purified IP_3R1 by adenophostin B and IP_3 exhibited a positive cooperativity (n_H = 1.9, Ki = 10 nM) and no cooperativity (n_H = 1.1, Ki = 41 nM), respectively. These results suggested that the difference in the cooperativity of ligand-binding resulted in the difference in the cooperativity of Ca^{2+} release.

A polyclonal antibody (designated αM2) against a peptide corresponding to the splicing region (SII) of IP_3R1 was raised and was characterized. The αM2 antibody recognizes the splicing region (SII) of IP_3R1. The immunoblotting analysis with the αM2 showed immunoreactivity only to the neuronal tissues but not to the non-neuronal tissues, confirming the previous observation by RNase protection assays that IP_3R1 containing SII region is a neuronal type and IP_3R1 lacking SII region is a non-neuronal type. The αM2 antibody is found to be useful to purify IP_3R1.

ACKNOWLEDGMENT

I would like to take this opportunity to thank everyone who has helped me over the last three years. First of all I would like to thank my supervisor, Prof. Ichiro Okura, for his continuous support and encouragement since I began my research works in 1989 and especially for putting up with my bad moods (I was afraid that he was fed up with my selfishness.). Under his supervision, I thoroughly enjoyed my works and felt that the several years of my research at his laboratory was the most meaningful. I would also like to thank Prof. Katsuhiko Mikoshiba (Univ. of Tokyo, Inst. of Med. Sci.) for allowing me to study in his laboratory and continuous support and discussion throughout this study. The last two years at his laboratory was really academically profitable period for me. I would also like to express my extreme gratitude to Prof. Teiichi Furuichi (Univ. of Tokyo, Inst. of Med. Sci.) for continuous encouragement and valuable discussion (and his wife for making (feeding me?) heartwarming and delicious foods), to Drs. Atsushi Miyawaki (Univ. of Tokyo, Inst. of Med. Sci.) and Takayuki Michikawa (Univ. of Tokyo, Inst. of Med. Sci.) for their excellent guidance, assistance and fruitful discussion on my research work. I am grateful to Drs. Michio Niinobe (Osaka Univ.) and Shinji Nakade (Ono Pharmaceutical Company, Ltd.) for their assistance and valuable discussion in the purification of IP_3R1 (especially to Dr. Niinobe for drinking with me so many times, I always had a terrible hangover the day after drinking). I would like to thank Dr. Lee G. Sayers for his critical reading of the thesis and for the useful English slang he has taught me. I engrave the kindness of the members in Okura laboratory and Mikoshiba laboratory on my mind.

June 1995

Junji Hirota

This thesis is dedicated to the late Prof. Nobumasa Kitajima who was a constant source of encouragement and inspiration over the past six years. His death has made me so sad and I will miss the frequent discussions we had together. He often talked to me about his many excellent works and his exciting and wonderful dreams. I have learned a lot from him. I would not have finished my doctoral degree without his continuous encouragement.

Junji Hirota

CONTENTS

ABBREVIATIONS

ATP	Adenosine 5'-triphosphate
B_{max}	Maximum binding
BSA	Bovine serum albumin
Ca^{2+}	Calcium ion
CaM	Calmodulin
CaMKII	Ca^{2+}/CaM dependent protein kinase II
CHAPS	3-[(3-cholamidopropyl) dimethylammonio]-1-propanesulfonic acid
CICR	Ca^{2+}-induced Ca^{2+} release
cAMP	Adenosine 3,5'-cyclic monophosphate
DAG	sn-1,2-Diacylglycerol
EC_{50}	Median effective concentration
EDC	1-ethyl-3-(3-dimethylaminopropyl) carbodiimide
EDTA	Ethylenediaminetetraacetic acid
EGF	Epidermal growth factor
EGTA	Ethylene glycol-bis(β-amino-ethyl ether) N,N,N',N'-tetra acetic acid
ER	Endoplasmic reticulum
FGF	Fibroblast growth factor
GTP	Guanosine 5'-triphosphate
HEPES	*N*-(2-hydroxyethyl) piperizine-*N'*-2-ethanesulfonic acid.
IC_{50}	Median effective concentration
IICR	IP_3-induced Ca^{2+} release
IP_3	D-*myo*-inositol 1,4,5-trisphosphate
IP_3R	Inositol 1,4,5-trisphosphate receptor
IP_3R1	Inositol 1,4,5-trisphosphate receptor type 1
IP_3R2	Inositol 1,4,5-trisphosphate receptor type 2
IP_3R3	Inositol 1,4,5-trisphosphate receptor type 3

K_D	Dissociation constant
mAbs	Monoclonal antibody
n_H	Hill coefficient
PBS	Phosphate-buffered saline
PDGF	Platelet-derived growth factor
PKA	cyclic AMP-dependent protein kinase
PKC	Protein kinase C
PKG	cGMP-dependent protein kinase
PLC	Phospholipase C
RyR	Ryanodine receptor
SDS-PAGE	Sodium dodecyl sulfate polyacrylamide gel electrophoresis
SR	Sacroplasmic reticulum
Tris	Tris[hydrosyethyl]aminomethane

The numbering of atoms in myo-inositol.

Inositol containing compounds are numbered according to the recommendations of the IUPAC-IUB in Biochemical Journal 1988, 258, 1-2, therefore all inositol phosphates the D-enantiomers unless otherwise stated.

CHAPTER I

INTRODUCTION

I - 1 General Overview of Intracellular Ca^{2+} Signaling Mediated by Inositol 1,4,5-Trisphosphate

External signals, such as hormones, neurotransmitters and growth factors, arriving at the cell surface receptors initiate intracellular signal transduction systems which induce a variety of biochemical and physiological responses in the cells. There are two major pathways for signal transduction according to the nature of the stimuli. One pathway is initiated through stimulation of a family of G protein-linked receptors, the other is tyrosine kinase-linked receptors. Both pathways couple with phosphoinositide (PI) turnover in which D-*myo*-inositol 1,4,5-trisphosphate (IP_3) and diacylglycerol (DAG) are formed by the hydrolysis of phosphatidylinositol 4,5-bisphosphate (Figure 1-1) [1, 2]. Both of these molecules function as intracellular second messengers. DAG activates protein kinase C (PKC), which then exerts its physiological function through phosphorylation, whereas IP_3 binds to a specific IP_3 receptor (IP_3R) and induces the release of Ca^{2+} into the cytoplasm from intracellular Ca^{2+} stores such as endoplasmic reticulum (ER). The increase in the cytoplasmic Ca^{2+} concentration modulates the functions of various Ca^{2+} associated proteins, such as calmodulin (CaM), protein kinases (Ca^{2+}/CaM dependent protein kinase II (CaMKII), Ca^{2+}-sensitive protein kinase C (PKC)), protein phosphatase (calcineurin), protease (calpain), ion channels (Ca^{2+}-dependent K^+ and Cl^- channel, IP_3R itself and another intracellular Ca^{2+} releasing channel/ryanodine receptor (RyR)), cytoskeleton (actin) and transcription factors (immediate-early genes), leading to various cellular responses. The intracellular IP_3-induced Ca^{2+} signals indeed operates throughout life, beginning with fertilization, cell proliferation, metabolism, secretion, contraction and neural signals.

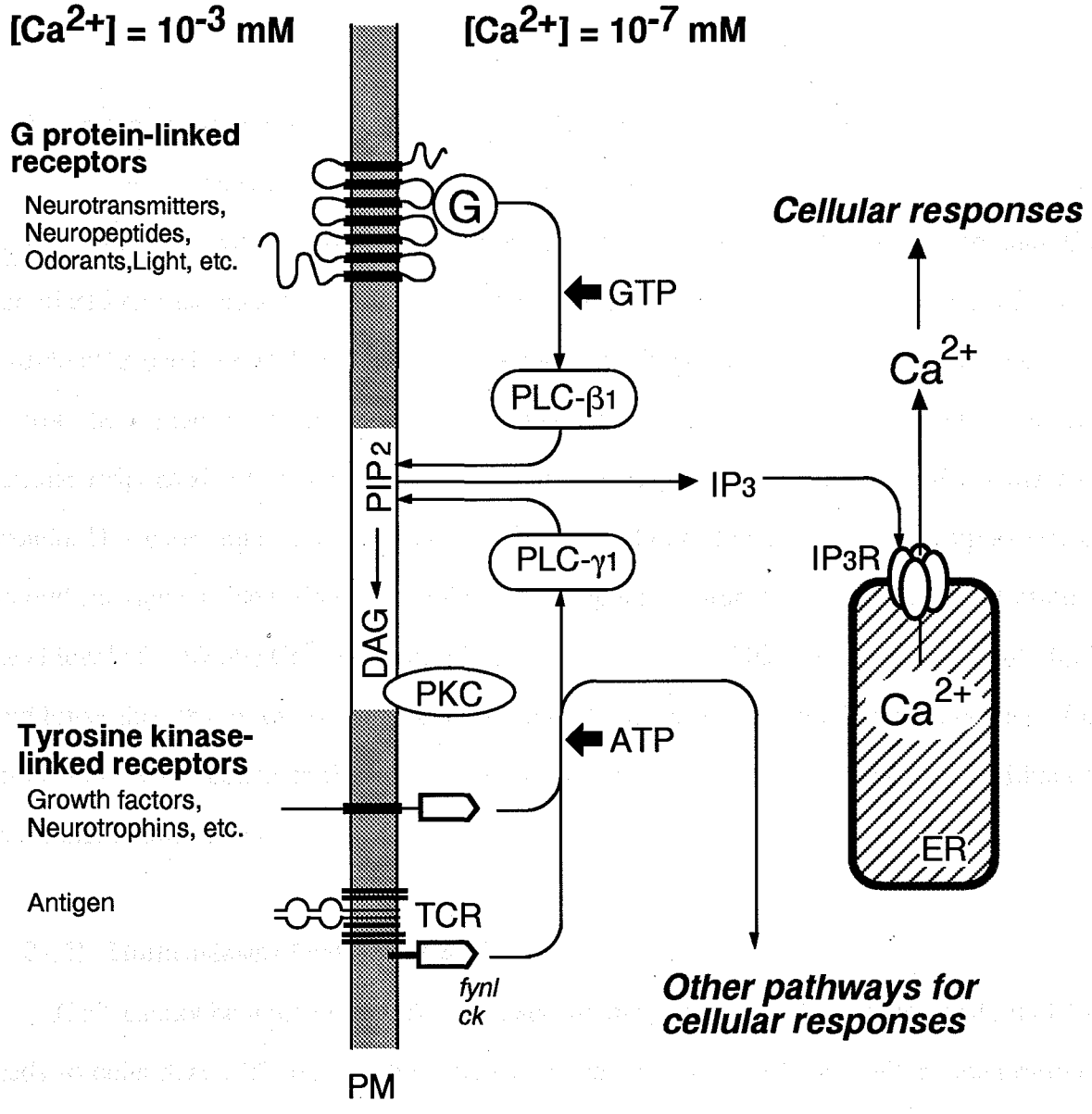

Figure 1-1. IP_3 / Ca^{2+} signal transduction cascades.
Scheme of the formation of Inositol 1,4,5-trisphosphate (IP_3) and diacylglycerol (DAG) by the hydrolysis of phosphatidylinositol 4,5-bisphosphate (PIP_2) in response to extracellular stimuli. There are two major pathways for the formation of IP_3 and DAG, depending on the extracellular stimuli. One is stimulated by neurotransmitters (glutamate, acetylcholine, dopamine, serotonin, ATP, etc.), neuropeptides (neuropeptide Y, substance P, etc.), ordrants and light, etc., which bind to their specific receptors (7-membrane-spanning receptors). Upon binding, the receptor use the GTP-binding protein (G protein) to activate phospholipase C-β1 (PLC-β1) which catalyses the hydrolysis of PIP_2 to produce IP_3 and DAG. IP_3 binds to IP_3 receptor releasing Ca^{2+} form intracellular Ca^{2+} store, such as the endoplasmic reticulum (ER), whereas DAG activates protein kinase C (PKC).The other pathway uses PLC-γ1, which is activated by the tyrosine kinase-linked receptors (stimuli: growth factors (PDGF, EGF, etc.), neurotrophins (NGF, BDNF and NT-3,4,5) and antigen). The tyrosine kinase-linked receptors also activate other effectors such as the phosphatidylinositol 3-OH kinase and GTPase activating protein (Modified Figure 1 of ref. [2] and [3]).

I - 2 Ca^{2+} is the Element for Signal Transduction

Ca^{2+} is the most common and unique second messenger in cells. The physiological role of Ca^{2+} in cells was firstly demonstrated by Sydney Ringer who discovered that Ca^{2+} stimulated cardiac muscle contraction in the nineteenth century. Although the role of Ca^{2+} in muscle cells has been well understood since then, that in non-muscle cells is more obscure and is now the subject of intensive studies. Elevations of cytosolic Ca^{2+} are known to mediate cellular responses, where Ca^{2+} itself and Ca^{2+} binding proteins trigger to affect the target protein. However, high concentration of Ca^{2+} can lead to cell death despite its importance as a second messenger. Therefore, the cells tightly regulate intracellular Ca^{2+} concentration. At basal level of cytosolic Ca^{2+} concentration is kept low (about 100 nM), which is about 10,000-fold lower than that of extracellular concentration (1 mM). As a result, this maintenance of low intracellular Ca^{2+} concentration also gives an excellent environment to the cells to utilize Ca^{2+} as the signal transduction element.

I - 2 - 1) Homeostasis of cytosolic Ca^{2+}

Ca^{2+} cannot be metabolized like other second messengers and high concentration of Ca^{2+} leads to cells death. Therefore, the cells tightly regulate intracellular Ca^{2+} concentration by Ca^{2+} pumps located on the plasma membrane and on the intracellular Ca^{2+} stores which extrude Ca^{2+} from the cytosol out of the cell or into intracellular Ca^{2+} stores. Ca^{2+} uptake systems proceed against its chemical gradient and require energy to operate. To maintain low cytosolic Ca^{2+} concentration, there are several systems involved in Ca^{2+} homeostasis as follows.

I - 2 - 1. 1) ATP-driven Ca^{2+} pump

To maintain low cytosolic Ca^{2+} concentration, Ca^{2+} pumps transport intracellular Ca^{2+} into extracellular or ER/SR space spending one or two ATP molecules per one Ca^{2+} to remove. Both smooth ER and plasma membrane Ca^{2+} pumps are P type ATPase, defined by an obligatory phosphorylated intermediate in the pump cycle [4] [5].

I - 2 - 1. 2) Mitochondrial Ca^{2+} electrogenic uniport

Mitochondria accumulates Ca^{2+} at up to 0.5 mM levels in the mitochondrial matrix utilizing the H^+ elctrochemical gradient created by H^+-ATPase as the driving force. Under physiological conditions, the mitochondrial H^+ electrochemical gradient is largely dominated by the electrical component about 180 mV negative inside. Ca^{2+} possesses an active electrogenic transport system that permits its rapid accumulation, driven by the membrane potential. However, mitochondrial Ca^{2+} uniporters have lower affinities for Ca^{2+} than Ca^{2+} pumps and probably are only significant when cytosolic Ca^{2+} rises above 0.5 μM [5].

I - 2 - 1. 3) H^+ - Ca^{2+} antiporters

Some intracellular acidic organelles have an H^+ - Ca^{2+} antiporter to accumulate Ca^{2+} at the expense of its H^+ gradient. A gradient of 2 pH units, acidic inside, should permit a 10,000-fold accumulation of Ca^{2+} in their lumen [6]. Chloroplasts, lysosomes, trans Golgi cisternae, secretory granules and endosomes might accumulate Ca^{2+}. Such a mechanism, however, remains a controversial issue [5].

I - 2 - 1. 4) Ca^{2+} binding proteins

Ca^{2+} binding proteins buffer Ca^{2+} to reduce its intracellular levels, and some of them act as Ca^{2+} sensing protein to trigger functions (summarized in Table 1-1)

I - 2 - 1. 5) Plasma membrane Ca^{2+} channels

Ca^{2+} channels located on the plasma membrane mediate Ca^{2+} entry into cells. There are three classes of plasma membrane Ca^{2+} channels:

(1) Voltage operated Ca^{2+} channels, which can be further subdivided into L-type, N-type and T-type voltage-dependent Ca^{2+} channels. Depolarization from the resting membrane potential (-70 mV) initiates conformational changes in Ca^{2+} selective ion channels on the plasma membrane, resulting in Ca^{2+} flux from extracellular space into the cells according to its electrochemical gradient.

(2) Receptor operated Ca^{2+} channels, which are characterized by a ligand binding domain present on the same polypeptide or molecular complex. The binding of the ligand at the

extracellular binding site induces a conformational change to open the channel and to follow Ca^{2+} entry into cell. The most characterized receptor operated Ca^{2+} channel is the NMDA receptor of neuronal tissue which opens in response to the excitatory amino acid, glutamate.

(3) Second messenger operated Ca^{2+} channels, which have not been well characterized yet. An obvious candidate is the plasma membrane IP_3R.

I - 2 - 1. 5) Intracellular Ca^{2+} channels

Two intracellular Ca^{2+} release channels, IP_3 receptor and ryanodine receptor, have been identified. Intracellular Ca^{2+} channels are characterized by their ability to release Ca^{2+} from intracellular stores into the cytosol in response to stimulation by their specific ligand.

(1) IP_3 receptor (see section I - 4)

(2) Ryanodine receptor (RyR), which was first studied in skeletal and cardiac muscle and was characterized by its ability to tightly bind the plant alkaloid ryanodine [7]. There are at least three RyR isoforms, RyR type 1 represents skeletal type located in skeletal muscle [8]; RyR type 2 is cardiac type located in cardiac muscle and in several non-muscle tissues [9, 10]; RyR type 3 is a much shorter RyR identified in some non-muscle cells [11, 12]. RyR release Ca^{2+} from intracellular Ca^{2+} stores induced by low [Ca^{2+}] (0.1 - 1.0 μM) and also inhibited at high [Ca^{2+}] (10 - 100 μM) [13]. The RyR, like IP_3R exists as a tetramer of non-covalently linked polypeptide subunits, each subunits having four transmembrane regions and a molecular weight of approximately 500 kD.

The RyR is gated either by electromechanical coupling to the plasma membrane dihydropyridine receptor in skeletal muscle, by Ca^{2+} or by cADP-ribose in some cell types [14]. The RyR is regulated by ATP, Mg^{2+} and Ca^{2+}, although Mg^{2+} and Ca^{2+} inhibit it in mM range. FKBP-12, a *cis-trans* peptidylprolylisomerase that binds the immunosuppressant FK506 and rapamycin, is copurified with RyR and modulate the channel opening of RyR [15]. A newly discovered second messenger, cADP-ribose, release Ca^{2+} in see urchin eggs and may be a RyR agonist in cardiac and pancreatic cells (RyR type 2 and 3) [16, 17].

I - 2 - 2) Increases in cytosolic Ca^{2+} for signal transduction

There are several mechanisms to introduce Ca^{2+} into the cytosol for signal transduction. Ca^{2+} ions from the two Ca^{2+} sinks, the extracellular space and the ER, are injected into the cytosol either across the plasma membrane (see section I - 2 - 1. 5) or from the ER through ion channels (see section I - 2 - 1. 6), resulting in increases in cytosolic Ca^{2+} to trigger cellular responses (Fig. 1-1 and Table 1-1).

I - 2 - 2. 1) Nonexcitable Cells

Activation of G protein-linked and tyrosine kinase-linked cell surface membrane receptors by various extracellular stimuli (summarized in Table 1-2) produce IP_3 via hydrolysis of phosphatidylinositol 4,5-bisphosphate. G protein-linked receptors, the seven transmembrane-spanning receptors, activate phospholipase Cβ (PLCβ), while tyrosine kinase-linked receptors stimulate phospholipase Cγ (PLCγ), to convert phosphatidylinositol 4,5-bisphosphate into IP_3 and diacylglycerol [1]. IP_3 acts as an intracellular second messenger by binding to the specific receptor, i.e., the IP_3 receptor (IP_3R), which is an IP_3-induced Ca^{2+} releasing channel located on intracellular Ca^{2+} stores such as the endoplasmic reticulum. Either of these IP_3-mediated pathways can increase intracellular [Ca^{2+}] form 100 nM to 1 μM.

Ca^{2+} can also enter nonexcitable cells by crossing the plasma membrane. Nonexcitable cells enhance Ca^{2+} entry by hyperpolarization. Open potassium channels force the membrane potential to more negative, drawing Ca^{2+} more rapidly across the plasma membrane Ca^{2+} enters through specialized voltage-independent Ca^{2+} selective channels triggered by second-messenger molecules [18].

I - 2 - 2. 2) Excitable Cells

In addition to the system described for nonexcitable cells, excitable cells contain voltage-dependent Ca^{2+} channels that enable these cells to increase cytosolic Ca^{2+}. These can be further subdivided into L-type, N-type and T-type voltage-dependent Ca^{2+} channels. Depolarization from the resting membrane potential (-70 mV) initiates conformational changes in Ca^{2+} selective ion channels on the plasma membrane, resulting in Ca^{2+} flux from

extracellular space into the cells according to its electrochemical gradient [18]. Ca^{2+} entering through voltage-dependent Ca^{2+} channels may directly activate ryanodine receptors (RyR) to release Ca^{2+} from intracellular Ca^{2+} stores.

Table 1-1. Proteins Triggered by Ca^{2+} and Their Functions.

Protein	Function
Troponin C	Modulator of muscle contraction
Calmodulin	Ubiquitous modulator of protein kinases and other enzymes
Calretinin, retinin, visinin	Activator of guanylyl cyclase
Calcineurin B	Phosphatase
Calpain	Protease
Inositol phospholipid-specific PLC	Generator of IP_3 and DAG
α-Actinin	Actin-binding protein
Annexin	Implicated in endo- and exocytosis
Phospholipase A2	Producer of arachidonic acid
Protein kinase C	Protein kinase
Gelsolin	Actin-severing protein
Ca^{2+}-dependent K^+ channel	Effector of membrane hyperpolarization
IP_3 receptor	Effector of intracellular Ca^{2+} release
Ryanodine receptor	Effector of intracellular Ca^{2+} release
Na^+/Ca^{2+} exchanger	Effector of the exchange of Ca^{2+} for Na^+ across the plasma membrane
Ca^{2+} ATPase	Pump of Ca^{2+} across membranes
Ca^{2+} antiporters	Exchanger of Ca^{2+} for monovalent ions
BoPCAR	G protein-linked Ca^{2+}-sensing receptor
Caldesmon	Regulator of muscle contraction
Villin	Actin organizer
Arrestin	Terminator of photoreceptor response
S100β	Unknown
Calreticulin	Ca^{2+} buffer/modulator of nuclear hormone receptor
Parvalbumin	Ca^{2+} buffer
Calbindin	Ca^{2+} buffer
Calsequestrin	Ca^{2+} buffer

Modified Table 1 of ref. [18]

Table 1-2. Receptors Increasing Intracellular Ca^{2+}.

via PLCβ	via PLCγ	Directly
Stimuli	Stimuli	
α1-Adrenergic	EGF	Nicotinic Ach channels
Muscarinic m1, m3, m5	PDGF	Glutamate receptor family
Purinergic P2y, P2u, P2t	FGF	
Serotonin 5HT1C	ErbB2	
H1	Antigen	
GnRH		
TRH		
Glucagon		
Cholecystokinin		
Vasopressin V-1a, V-1b		
Oxytocin		
Angiotensin II		
Thrombin		
Bombesin		
Vasoactive intestinal peptide		
Bradykinin		
Tachykinin		
Thromboxanes		
Platelet activating factor		
F-Met-Leu-Phe		
Endothelin opiate		
BoPCAR		

Modified Table 2 of ref. [18]

I - 3 Inositol 1,4,5-Trisphosphate is a Second Messenger to Mobilize Ca^{2+}

The function of D-*myo*-inositol 1,4,5-trisphosphate (IP_3) (Figure 1-2) as a second messenger was revealed by Streb *et al.* [19] who demonstrated that IP_3 released Ca^{2+} from non-mitochondrial intracellular Ca^{2+} stores of permeabilized pancreatic acinar cells. Since then, our knowledge of this second messenger, IP_3, has been accumulated using a variety of experimental systems, such as the permeabilized and intact cells and microsome systems. It is now well established that IP_3 acts as an intracellular second messenger to mobilize Ca^{2+} from non-mitochondrial Ca^{2+} stores, such as the endoplasmic reticulum, by binding to the specific receptor, i.e., the IP_3 receptor (IP_3R).

I - 3 - 1) Formation of IP_3

It is now well established that IP_3 is derived from the hydrolysis of phosphatidylinositol 4,5-bisphosphate via activation of phospholipase C, whose activity is enhanced by activation of G protein-linked and tyrosine kinase-linked cell surface membrane receptors by various extracellular stimuli, such as hormones, growth factors, neurotransmitters, odorants, lights, etc. [2] (Figure 1-1) (see section I - 2 - 2).

I - 3 - 1. 1) G protein-linked receptors.

At least 30 G protein-linked receptors initiate Ca^{2+} release through the activation of PLCβ (Table 1-2). The majority of G protein-linked receptors are characterized by seven membrane spanning helices connecting an extracellular ligand binding domain to an intracellular domain. Activation of G protein-linked receptor results in conformational change to activate the G protein. The heterotrimeric G protein then dissociates into Gα and Gβγ, both of which appears to interact with different the PLCβ isozymes, implicating independent regulation by both effector arms. However, little is known about the specificity of Gβγ subunits in activating PLCβ, except that transducin Gβγ is less effective than other dimmer combinations.

I - 3 - 1. 1) Tyrosine kinase-linked receptors.

Tyrosine kinase-linked receptors activate PLCγ, which are single transmembrane-spanning receptor molecules, via a direct interaction with the enzyme itself. Growth factors such as platelet-derived growth factor (PDGF), epidermal growth factor (EGF) and fibroblast growth factor (FGF), once bound, cause their receptors to dimerize. This allows their cytoplasmic kinase domains to phosphorylate each other on specific tyrosine residues, creating docking sites for the PLCγ SH2 domains. The activated receptor then binds to the SH2 domains, bringing PLCγ into proximity with phosphatidylinositol 4,5-bisphosphate to produce IP_3 and DAG. In general, tyrosine kinase-activated PLCγs increase Ca^{2+} more slowly and for longer duration than do G protein-mediated PLCβs.

Both G protein-mediated and tyrosine kinase-mediated activation of PLC are energy dependent processes; GTP hydrolysis is necessary to inactivate Gαq leading to the reassociation of Gαqβγ, and the stimulation of PLCγ requires ATP hydrolysis during the phosphorylation of tyrosine residues both on the activated receptor and PLC.

I - 3 - 2) Metabolism of IP_3

The IP_3 concentration depends on the activities of PLC and two IP_3-metabolizing enzymes that either phosphorylate or dephosphorylate IP_3. Following the removal of the extracellular stimuli to the cell surface receptor and subsequent inactivation of PLC, the metabolism of IP_3 represents a fundamental mechanism terminating the action of this second messenger ("off-switch"). There are two metabolic routes of IP_3 (Figure 1-3): phosphorylation by a 3-kinase and dephosphorylation by a 5-phosphatase. The metabolism of IP_3 to inositol 1,4 bisphosphate ($Ins(1,4)P_2$) by 5-phosphatase is generally considered to predominate. Alternatively IP_3 can be phosphorylated by 3-kinase producing inositol 1,3,4,5-tetrakisphosphate ($Ins(1,3,4,5)P_4$). 3-kinase has a relatively high affinity for IP_3 [K_m = 0.2 - 1.5 mM] but its V_{max} is considerably less than that of the 5 phosphatase [20 - 23].

I - 3 - 3) Intracellular IP_3 concentration

The prevailing levels of IP_3 are regulated by an enormously complex series of control processes that finely balance its rates of synthesis and metabolism (Figure 1-3). The concentration of IP_3 in basal cells is generally reported to be about 0.1 to 0.2 μM, rising to less than 1 μM except during stimulation with the most extreme concentrations of agonists [24 - 27]. This is a classic response of a second messenger, whereby a relatively small change in its concentration has an enormous impact on cell physiology. IP_3-induced Ca^{2+} release was found to have a sensitivity, EC_{50} for IP_3 = 0.1 μM.

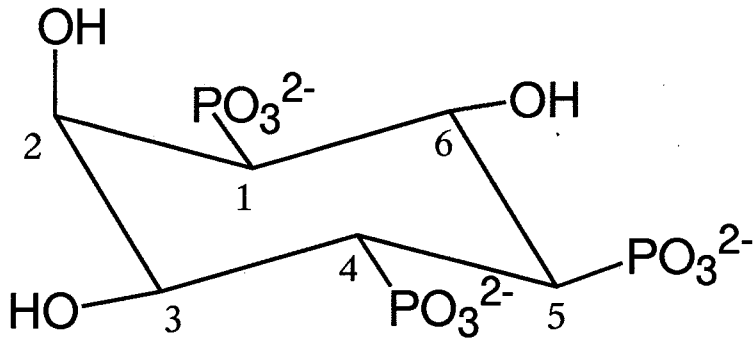

Figure 1-2. Structure of D-*myo*-inositol 1,4,5-trisphosphate.

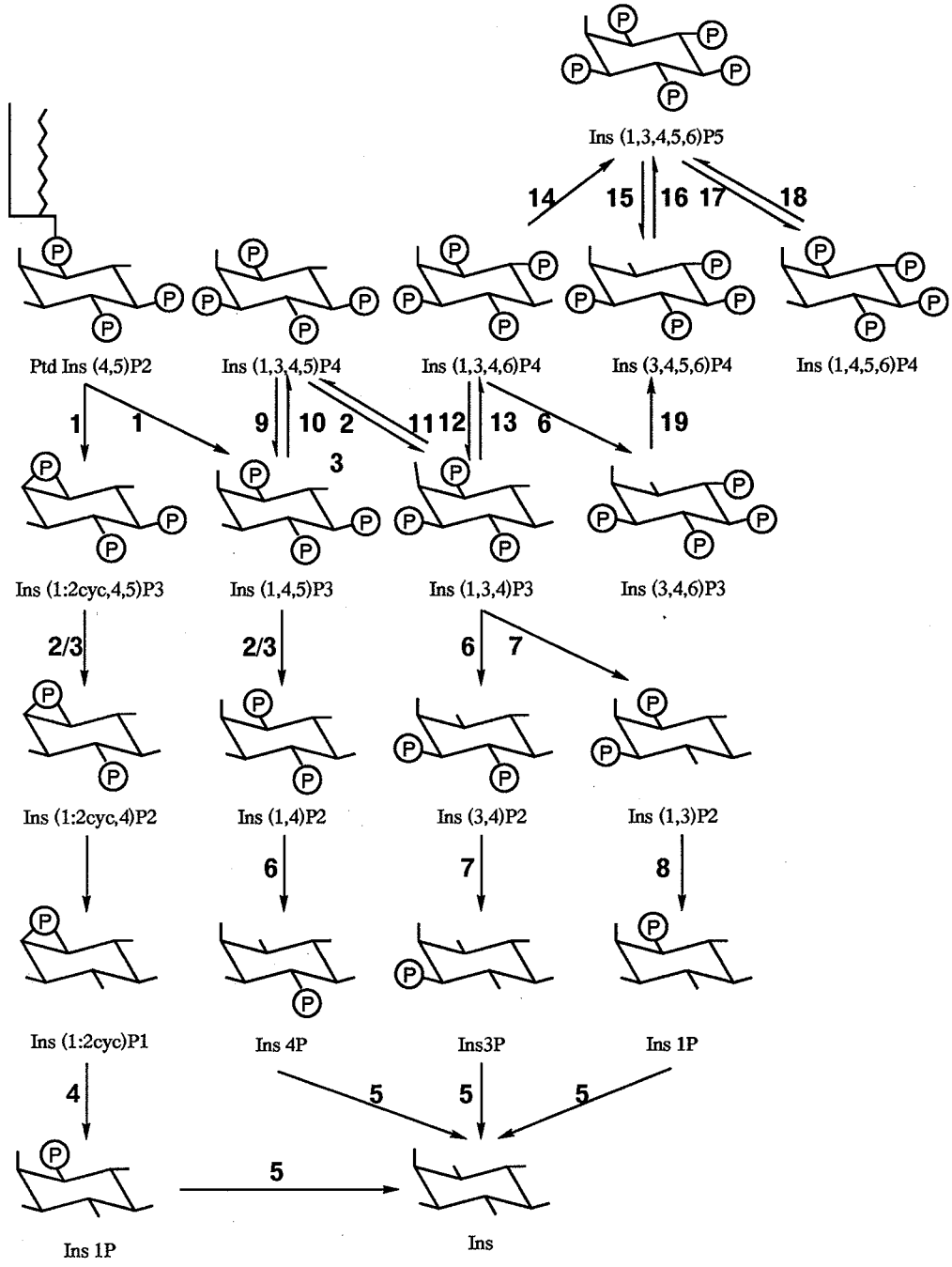

Figure 1-3. Scheme of the metabolism of inositol phosphates.
Phosphatidylinositol (4,5)bisphosphate (Ptd Ins(4,5)P_2) turnover leads to the accumulation of a number of inositol phosphates. The pathway that the phospholipase C (PLC) might also hydrolyze Ptd Ins(4,5)P_2 to Ins(1,4)P_2 and Ptd is omitted in this figure. The enzymes are 1, Phospholipase C; 2, Ins (1,4,5)P_3 / Ins(1,3,4,5)P_4-5-phosphatase; 3. Ins(1,4,5)P_3-5-phosphatase; 4, Ins(1:2cyc)P phosphodiesterase; 5, InsP phosphatase; 6, inositolpolyphosphate-4-phosphatase; 7, inositolpolyphosphate-4-phosphatase; 8, Ins(1,3)P_2-3-phosphatase; 9, Ins(1,3,4,5)P_4-3-phosphatase; 10, Ins(1,4,5)P_3-3-kinase; 11, Ins(1,3,4)P_3-5-kinase; 12, Ins(1,3,4,6)P_4-6-phosphatase; 13, Ins(1,3,4)P_3-6-kinase; 14, Ins(1,3,5,6)P_4-5-kinase; 15, Ins(1,3,4,5,6)P_5-1-phosphatase; 16, Ins(3,4,5,6)P_4-1-kinase; 17, Ins(1,3,4,5,6)P_5-3-phosphatase; 18, Ins(1,4,5,6)P_4-3-kinase [1].

I - 4 IP_3 Receptor as Ca^{2+} releasing Ca^{2+} channel [28]

I - 4 - 1) Discovery of IP_3 receptor

The first demonstration of the Ca^{2+} mobilizing properties of IP_3 by Streb *et al* has lead to much interest in its specific receptor, i.e. IP_3 receptor (IP_3R) as well as its Ca^{2+} releasing properties. IP_3R was first characterized in 1979 as a protein called P_{400} that is abundant in normal mice cerebella but virtually absent in the cerebella from Purkinje cell-deficient mutant mice, long before the importance of IP_3, as a second messenger to release Ca^{2+} from the intracellular stores, was recognized [29 - 31]. The mouse cerebellum contains five types of neuron. The Purkinje cell, one of them, plays an important role in information processing, because it is the target of all inputs into the cerebellar cortex and is the only neuron that sends outputs from the cerebellar cortex. In the course of biochemical analysis, a protein termed P_{400} was found to be enriched in Purkinje cells, but greatly reduced in the cerebella of Purkinje cell-deficient ataxic mutants. The content of P_{400} protein decreases in the cerebella from *pcd* and *nervous* mutants, where most of the Purkinje cells degenerate selectively. Purkinje cells of the *staggerer* mutant have a withered dendritic arbor lacking the tertiary branched spines which serve as the sites of synapse between the parallel fibers and the dendrites of Purkinje cells. In the *staggerer* cerebellum only a small amount of P_{400} protein persists.

Purification of P_{400} protein allowed to obtain three independent anti-P_{400} monoclonal antibodies (mAbs 4C11, 10A6 and 18A10) [31 - 32]. Immunological analyses using the monoclonal antibodies revealed that P_{400} protein is abundantly distributed in the cell body, dendrite and axon of the Purkinje cell, and was also detected at low densities in other parts of nervous system and in non-neural tissues. Digestion of P_{400} protein with endo-β-acetylglucosaminidase F caused small changes in the electrophoretic mobility, indicating that P_{400} has a small number of asparagine-linked oligosaccharide chains [31]. The purified P_{400} protein was phosphorylated in vitro by the catalytic subunit of PKA at only seryl residue and by CaMKII [33].

In 1988, IP_3 binding protein (IP_3R) was purified from the rat cerebellum by another group using IP_3 binding activity as a marker [34]. This protein was also enriched in cerebellar Purkinje cells [35] and its biochemical properties were similar to those of P_{400}. To confirm this, Maeda *et al.* purified IP_3R from a postnuclear fraction of mouse cerebellum by solubilizing with Triton X-100, followed by sequential column chromatography on DE-52, heparin-agarose, lentil lectin-Sepharose and hydroxylapatite [36]. The purified IP_3R was a 25K protein with IP_3 binding activity and fractionated completely with the P_{400} protein in sequential chromatography and cross-reacted with three anti-P_{400} monoclonal antibodies [36]. These results demonstrated that P_{400} protein was identical to IP_3R.

I - 4 - 2) Primary structure of IP_3 receptor

Cloning the cDNA for the mouse IP_3R provided us a substantial information about the receptor structure [37]. On the basis of the cDNA sequence, IP_3R is predicted to comprise 2749 amino acids (M 313kDa). IP_3R is structurally divided into three parts, a large N-terminal cytoplasmic arm (2275 amino acids, 83% of the receptor molecule), a putative six membrane-spanning domain clustered near the C-terminus, and a short C-terminal cytoplasmic tail (160 amino acids, 5.3%). The amino acid sequence deduced from the cDNA sequence of mouse [37], rat [38], *Drosophila melanogaster* [39], *Xenopus* [40]and human IP_3R [41] showed that the general structure of the receptor is highly conserved among these different species.

Functionally, IP_3R is composed of the following domains (Figure 1-4) [37 - 38]:

(1) Ligand binding domain containing about 650 N-terminal amino acid residues in the large cytoplasmic domain which binds the ligand (IP_3) [38]. Deletion of any small fragment within this region abolished IP_3-binding activity, suggesting that this region is critical for IP_3 binding [42]. In fact, the sequence of this region is highly conserved among different species.

(2) Modulatory domain containing binding sites for various modulators, such as Ca^{2+} [43], CaM [44] and ATP [45], two sites phosphorylated by PKA [33, 46], one site

phosphorylated by cGMP-dependent protein kinase (PKG) [47] and potential sites phosphorylated by PKC [48] and CaMKII [33, 48]. Interestingly, other second messengers such as cAMP, cGMP and DAG can effect on this modulatory domain via their transduction cascades (PKA, PKG and PKC, respectively [49]). This modulatory domain may function as the transducing domain in the transduction of IP_3-binding to the channel opening and IP_3-induced Ca^{2+} release may be regulated by various modulators [50].

(3) **Channel domain** with the putative six membrane spanning segments clustered near the C-terminus which functions as the Ca^{2+} channel. The primary sequence of the IP_3R shares no homology with the Ca^{2+} channel on the plasma membrane but shares significant partial homology with the ryanodine receptors, which mediate Ca^{2+} release from the sacroplasmic reticulum of skeletal muscle and cardiac muscle.

I - 4 - 3) Structural properties of IP_3 receptor

I - 4 - 3. 1) Tetrameric complex structure of IP_3R

Agarose-PAGE analysis after cross-linking of the purified IP_3R revealed four distinct bands of Mr 320K, 650 K 1000K 1250K, indicating that IP_3R is composed of four subunits each with Mr 320K [45]. Deletion analysis suggested that formation of the tetrameric IP_3R complex involves the transmembrane domains and/or successive C-termini and that IP_3 binding is independent of the intermolecular conformation [42]. The electron microscopic observation of the purified IP_3R revealed that IP_3R consists of four subunits and exists in a square form of 25 nm on each side [36].

I - 4 - 3. 2) Transmembrane topology of IP_3R

Two models have been proposed for the transmembrane topology of IP_3R. Mikoshiba *et al.* have previously proposed that IP_3R traverses the membrane six times (Figure 1-4) [39, 40], while others have suggested eight [50 - 52]. Michikawa *et al.* studied the subcellular location of the hydrophilic segment (residues 2463-2529 of the mouse IP_3R) to define the transmembrane

topology of IP_3R [53]. This segment is predicted to be on the luminal side of the ER membrane in the six transmembrane model and is on the cytosolic side in the eight-transmembrane model. They revealed that this region locates in the intracisternal space of the ER by the electron microscopic immunocytochemical study. In addition, this region has two consensus sites for N-glycosylation (Asn-2475 and Asn-2503). If these potential sites for N-glycosylation are really in the intracisternal space, these sites could be glycosylated. By analyzing some site directed mutant receptors with substitutions of these consensus sites (Asn to Gln) for N-glycosylation, both sites are found to be glycosylated. These results indicate that the residues of 2504-2523 are exposed to the ER lumen, supporting the six transmembrane segments. According to the transmembrane topology, Michikawa *et al.* suggested that IP_3R is a member of the superfamily of voltage- and second messenger-gated ion channels and has a putative pore-forming region between M5 and M6 region (residues 2529-2552) [53].

I - 4- 4) Localization of IP_3 receptor

Immunohistochemistry and *in situ* hybridization clarified the localization of IP_3R. IP_3R is mostly enriched in the cerebellar cortex [31, 32, 37, 54, 55]. In this region, Purkinje cells are the predominant sites of IP_3R. It also widely localizes throughout brain at very low to moderate levels (moderate: cerebral cortex, nucleus accumbens, caudate-putamen, cerebellar nuclei and the CA1 region of the hippocampus; low: amygdaloid cortex, prepiriform cortex, white matter; very low dentate gyrus, corpus callosum, olfactory tubercle, precommissural hippocampus, hypothalamus, substantia nigra, pons) [54]. These cell-types and regions agree with the sites for IP_3 binding [35]. The IP_3R mRNA and proteins are also located in peripheral tissues; thymus, heart, lung, liver, spleen, kidney, uterus, oviduct, testis [31, 56]. A considerable amount of the IP_3R mRNA are located in smooth muscle cells, such as those of the arteries, bronchioles, oviduct and uterus. Localization of IP_3R in invertebrates is quite different. In *Drosophila melanogaster* the receptor is more enriched in antenna and legs than in brain. In the head of the *eya* mutant, which is missing the retinae, there was a great decrease in IP_3R content. These data

suggest that IP_3R plays an important role not only in the brain but also in sensory systems (visual and olfactory tissue) and in muscular function in invertebrates.

Subcellular localization of IP_3R in mouse cerebellar Purkinje cells was studied using immunogold with the anti-IP_3R mAbs [57]. The IP_3R was detected abundantly on the smooth ER (especially on the stacks of flattened smooth ER, subplasma membrane cisternae and spine apparatus), a little on rough ER and the outer nuclear membrane [57 - 62].

Some reports suggest the presence of IP_3R in the plasma membrane (PM-IP_3R) of olfactory neurons, olfactory cilia and human T lymphocytes [63 - 67]. However, no information on the molecular aspects of PM-IP_3R is available nor do we know whether IP_3R on ER is sorted into the plasma membrane. The widely distribution of IP_3R in central nervous system and peripheral tissues suggest the functional importance of the IP_3-second messenger system in many cells.

I - 4 - 5) Biochemical Properties of IP_3 receptor

I - 4 - 5. 1) IP_3 binding activity

The purified IP_3R from mouse cerebella has [^{3}H]Ins(1,4,5)P_3-binding activity with the K_D of 83 nM and a B_{max} of 2.1 pmol/μg of protein [36]. The purified receptor from rat cerebella also has similar characters [34]. Stoichiometric binding of IP_3 is that one purified receptor protein binds one IP_3 molecule (Hill coefficient is one). Ins(2,4,5)P_3 is a relatively potent competitor for [^{3}H]Ins(1,4,5)P_3 binding and Ins(1,3,4,5)P_4 is less effective. Ins(1,2)P_2 and Ins(1)P_1 are inactive at the concentration of 10 μM. The following rank of potency for displacement of [^{3}H]Ins(1,4,5)P_3 binding to the purified IP_3R is found: Ins(1,4,5)P_3 > Ins(1,4,5)P_3 > Ins(2,4,5)P_3 > Ins(1,3,4,5)P_4 > Ins(1,2,3,4,5,6)P_6 > Ins(1,4)P_2 > Ins(1,3,4)P_3 > Ins(1,3,4,5,6)P_5 > Ins, Ins(1)P_1, Ins(2)P_1, Ins$(SO_4)_6$ [34, 45, 68, 69].

For optimum [^{3}H]Ins(1,4,5)P_3 binding, alkaline pH (pH 8.5 - 9.5) is most effective [34, 70]. Heparin potently inhibits [^{3}H]Ins(1,4,5)P_3 binding. The IP_3R expressed from its cDNA in NG 108-15 [37, 42] and L cells [71] showed similar binding properties to the purified receptor.

I - 4 - 5. 2) Modulators of IP_3R

IP_3R has the modulatory domain in the large cytoplasmic domain. Various modulators may regulate the Ca^{2+} channel activity of IP_3R upon binding to or phosphorylating this domain. Relations between some of them and IP_3R has been studied.

(1) **Phosphorylation**: IP_3R has potential sites of phosphorylation. IP_3R can be phosphorylated by the catalytic subunit of cyclic AMP-dependent protein kinase [46, 72 - 75] and slightly by CaMKII. PKG and PKC also phosphorylates the receptor. These results suggest that IP_3-induced Ca^{2+} release is regulated by PKA and also slightly by CaMKII and PKC.

(2) **ATP**: ATP binds the purified IP_3R with K_D and B_{max} values of 17 μM and 2.3 pmol/μg, respectively. There are three putative ATP-binding sites in the receptor sequence and two of them overlap with each other. Binding kinetics indicated that one purified receptor binds one ATP molecule [45, 76].

(3) **CaM**: The transfection experiments of cDNA of IP_3R and deletion mutant demonstrate that IP_3R binds CaM, but no more information is yet available.

(4) **Ca^{2+} binding**: It was demonstrated that Ca^{2+} binds IP_3R [43]. Some experiments shows that IP_3R mediated Ca^{2+} release activity is depending on the Ca^{2+} concentration (see below) [44].

(5) **Ankyrin**: The amino acid residues 2546-2556 the putative pore forming region shares a great deal of structural homology with the ankyrin-binding domain located in well characterized ankyrin-binding proteins such as the cell adhesion molecule, CD44. Recently, ankyin (a cytoskeletal protein known to link membrane proteins such as erythrocyte band 3 [77] and lymphocyte GP85 (CD44)) [78] has been shown to bind IP_3R in brain [79] and lymphoma cells [80]. The ankyrin binding to the IP_3R inhibit IP_3 binding and IP_3-induced Ca^{2+} release [81]. These finding support that the cytoskeleton is involved in the regulation of the function of IP_3R.

(6) FKBP-12: IP_3R is found to associate with FKBP-12, a *cis-trans* peptidylprolylisomerase that binds the immunosuppressant FK506 and rapamycin, as well as RyR. The association of these two proteins is disrupted by FK506 and rapamycin. The FKBP-12 binding to the IP_3R decreases IP_3-induced Ca^{2+} release activity of IP_3R [82].

(7) Chromogranin A: Chromogranin A (CGA) is a Ca^{2+} binding protein with high capacity and low affinity for Ca^{2+} located in the intracellular Ca^{2+} stores. IP_3R is found to interact with CGA in a pH-dependent manner. Indeed, it was found that one of the intraluminal loops of the IP_3R interacted with CGA at the intravesicular pH 5.5 but not at pH 7.5 [83].

I - 4 - 6) Functional properties of IP_3R as Ca^{2+} releasing channel

Several experiments demonstrate that IP_3R is a Ca^{2+} channel. In particular: (1) the purified IP_3R reconstituted into lipid vesicles medicates $^{45}Ca^{2+}$ flux [75, 76, 84]; (2) reconstitution experiment of the purified IP_3R into planar lipid bilayers showed IP_3-dependent cation selective channel activity (Ca^{2+} conductance, 26 pS in 54 mM Ca^{2+}; Na^+ conductance, 21 pS in 100-500 mM asymmetric Na^+ solution) with several subconductance states [45]; (3) The expressed IP_3R has Ca^{2+} releasing activity [71]. In this expression system, $Ins(1,4,5)P_3$ is the most potent ligand for Ca^{2+} releasing activity, whereas $Ins(2,4,5)P_3$ and $Ins(1,3,4,5)P_4$ are much less effective. Newly found IP_3R agonists, referred to "adenophostin A and B", are 100 fold more potent than IP_3 in terms of Ca^{2+} release [85].

I - 4 - 7) Heterogeneity of IP_3 receptor / Subtypes of IP_3 receptor

I - 4 - 7. 1) Splicing variants of IP_3R

Heterogeneity due to alternative splicing has been found in the rat [50], human [72] and mouse [55] IP_3Rs. One alternatively-splicing segment (named SI for the mouse receptor subtype) is a 45-nucleotide sequence coding for 15 amino acids within the IP_3 binding domain. In the mouse brain, a relative quantity of an mRNA containing the SI (SI^+ subtype) is high in

the cerebral cortex (88%) and hippocampus (69%), whereas and mRNA lacking the SI (SI^- subtype) is dominant in the cerebellum (85%) and spinal cord (75%) [55]. During the postnatal development of the cerebellum, the SI^- mRNA level is a little higher than the SI^+ mRNA during the early stages. At two weeks after birth, the ratio of the SI^+ and SI^- is reversed. The SI^- and SI^+ expression continue to increase and gradually reduce, respectively. The change of splicing pattern in the IP_3 binding region may be involve in the development and neuronal function of the cerebellar Purkinje cells, probably by changing the binding affinity of the receptor for IP_3. In peripheral tissues, ratios of the SI^+ and SI^- splicing subtypes differ from tissue to tissue. Recently, the alternative splicing of the SI region showed, however, no significant differences of the IP_3 binding affinity [86].

The other alternatively splicing segment (SII) is a 120-nucleotide sequence (40 amino acids) between the two potential PKA phosphorylation sites [55](Figure 5-1). Within the SII segment, additional splicing events occur in combination with three more segments, A, B and C coding for 23, 1 and 16 amino acids, respectively [55]. This combination of alternative splicing produces for splicing variants, i.e., SII(A+B+C segments), $SIIB^-$(A+C segments), $SIIBC^-$ (A segment only) and $SIIABC^-$ (deletion of A, B and C). In the mouse central nervous system, the $SIIB^-$ subtype is predominant (50 - 54%), and the $SIIABC^-$ is a predominant splicing subtype in spinal cord (54%). In the peripheral tissues tested, we observed only the $SIIABC^-$-type mRNA. Thus, the SII, $SIIB^-$ and $SIIBC^-$ subtypes may be brain-specific receptors and IP_3R lacking SII is known to be ubiquitous isoform. [55]. This segment is located between the two potential sites for PKA phosphorylation as described above. *In vitro* PKA phosphorylation demonstrated that the rat cerebellar receptor (SII^+) is highly phosphorylated at Ser-1756 (Ser-1755 in the mouse receptor) and to a much less extent at Ser-1589 (Ser-1588 in the mouse receptor). By contrast, the rat receptor from the vas deferens (SII^-) is phosphorylated exclusively at Ser-1589 [72]. These results suggested that the phosphorylation of the receptor at the different sites is coupled with the efficiency of the receptor activities.

It is clear that there are heterogeneity due to heteromeric formations of IP_3R isoforms arising from alternative splicing, which may display different properties from that of homotetramer.

I - 4 - 7. 2) New types of IP_3R

New types of IP_3R from distinct genes have been reported. The original IP_3R is therefore now called the IP_3 receptor type 1 (IP_3R1). IP_3 receptor type 2 (IP_3R2) is comprised of 2701 aminoacids and shares 68-69% sequence homology with IP_3R1 (rat IP_3R2 [52]; human IP_3R2 [87]). IP_3 receptor type 3 (IP_3R3) contains 2670 amino acids and 2671 amino acids in rat and human, respectively, and has 62% and 65% homology with IP_3R1 and IP_3R2, respectively (rat IP_3R3 [88]; human IP_3R2 [87, 89]). The details of each receptor types are summarized as follows (Figure 1-6);

(1) IP_3R Type 1 (IP_3R1), 2749 amino acids (SI^+/SII^+ splicing subtype) from the mouse and rat, 2695 amino acids (SI^-/SII^-) from human and 2693 amino acids (SI^-/SII^-) from *Xenopus*. In contrast to the rodent SI^-/SII^- splicing subtype, h-Ser is a human specific insertion (Ser-666 in human) between residues 681 and 682 in the rodent SI^+ subtype. The following sites and regions are revealed: splicing segments SI (residues 318-332) and SII (residues 1692-1731, subsegments A, 1692-1714; B, 1715; C, 1716-1731); *ligand-binding domain* : IP_3-binding site, N-terminal 650 amino acids. *Modulatory & transducing domain including*: CaM (CaM-binding site), PKA (Ser residues, 1588 and 1755, for PKA phosphorylation), ATP (potential ATP-binding sites, 1773-1778, 1775-1780 and 2016-2021, and another potential site, 1768-1773, detected by completely splicing out the SII segment), and Ca^{2+}-binding (Ca^{2+}-binding site, residues 1961-2219). The CaMKII and PKC phosphorylation sites have not been identified yet. *Channel domain* : six putative membrane spanning regions M1-M6, between residues 2276-2589 in the mouse, including two N-glycosylation sites (Asn residues 2475 and 2503) and one putative 'pore' forming sequence (residues 2530-2552) between M5 and M6.

(2) IP_3R Type 2 (IP_3R2), 2701 amino acids from the rat and human. *Drosophila* IP_3R (2833 amino acids) is, if anything, similar to mammalian IP_3R2. The putative ligand-binding domain (N-terminal 649 amino acids in human) homologous to that of IP_3R1. Putative binding sites for ATP (ATP, residues 1968-1973) and Ca^{2+} (Ca^{2+}, residues 1914-2173) are conserved. The following sites and regions are indicated: h-P-PKA, potential PKA phosphorylation site in human IP_3R2 (Ser residue 1687); the putative channel domain, M1-M6 (between residues 2230-2541) in man; two putative N-glycosylation sites (Asn residues 2430 and 2456 in human).

(3) IP_3R Type 3 (IP_3R3) The putative ligand-binding domain (N-terminal 650 amino acids) homologous to that of IP_3R1 is indicated by a dotted box. The following sites and regions are indicated: putative binding sites for ATP (residues 1921-1926 in the rat) and Ca^{2+} (residues 1865-2147 of rat receptor that include a large insertion of 29 amino acids, however); two potential PKA phosphorylation sites in the rat (r-P-PKA, Ser residues 1130 and 1457) and human (h-P-PKA, residues 934 and 1133); putative channel domain, M1-M6 (between residues 2205-2517 or 2203-2520) in human; one putative N-glycosylation site (Asn residue 2405) in human.

The ligand binding domain (72-77%) and channel domain (66-71%) are relatively conserved among the receptor types in the IP_3R family. The cDNA transfection experiments have showed no significant difference in binding affinity and specificity [37, 38, 41, 52, 87, 88], although more precise comparisons of the binding activity of all of the types remain to be performed. No data concerning the IP_3-induced Ca^{2+} releasing properties of IP_3R2 and IP_3R3 has been available. The modulatory domain located between the IP_3-binding domain and the channel domain are less similar (56-65%). Most of the putative modulator-binding sites and phosphorylation sites are diversified among the family, except that the putative ATP-binding site on the C-terminal side is conserved (summarized in Figure 2) [3]. These differences in the modulatory systems of the individual receptor types may cause different Ca^{2+} release activities. Moreover the expression of multiple types of IP_3Rs in individual cells suggests that a

heterotetrameric IP_3R complex, which may display different IP_3 binding and channel opening properties from the homotetramer, may cause more complicated IP_3 / Ca^{2+} signaling. Future investigations into the biochemical properties of individual IP_3R isoforms may allow us to establish a relationship between the structure and Ca^{2+} releasing activities of each IP_3R type.

Chromosomal mapping showed that the genes coding the different IP_3R are located on different chromosomes. Type 1, 2 and 3 were mapped to human chromosome 3p25-26, 12p11 and 6p21, respectively [41]. Although the gene locus of each IP_3R was mapped, we do not know of any human genetic disease caused by mutations of these IP_3R subtypes. Linkage analysis of the pedigrees will give us some clues for the identification of human diseases associated with IP_3R mutations.

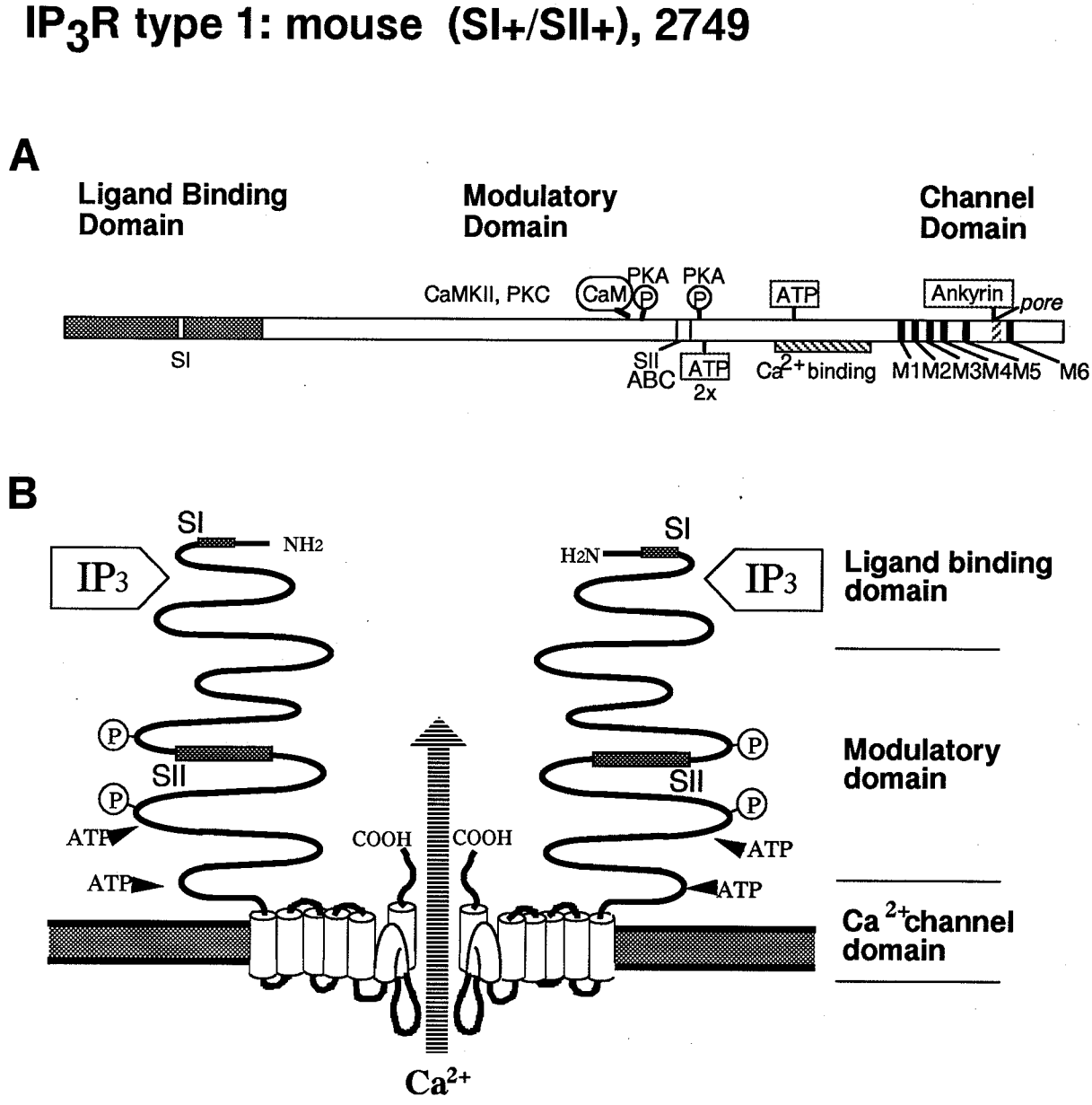

Figure 1-4. Structure of IP_3 receptor.

A: The primary structure of mouse IP_3R, illustrating the three functional domains. P, phosphorylation sites. SI and SII represent alternative splicing sites. M1-M6 represent membrane spanning regions.

B: schematic representation of the transmembrane topology of IP_3R, illustrating half of the homotetrameric structure. The splicing sites are shaded and ATP binding sites are shown, P, phosphorylation sites.

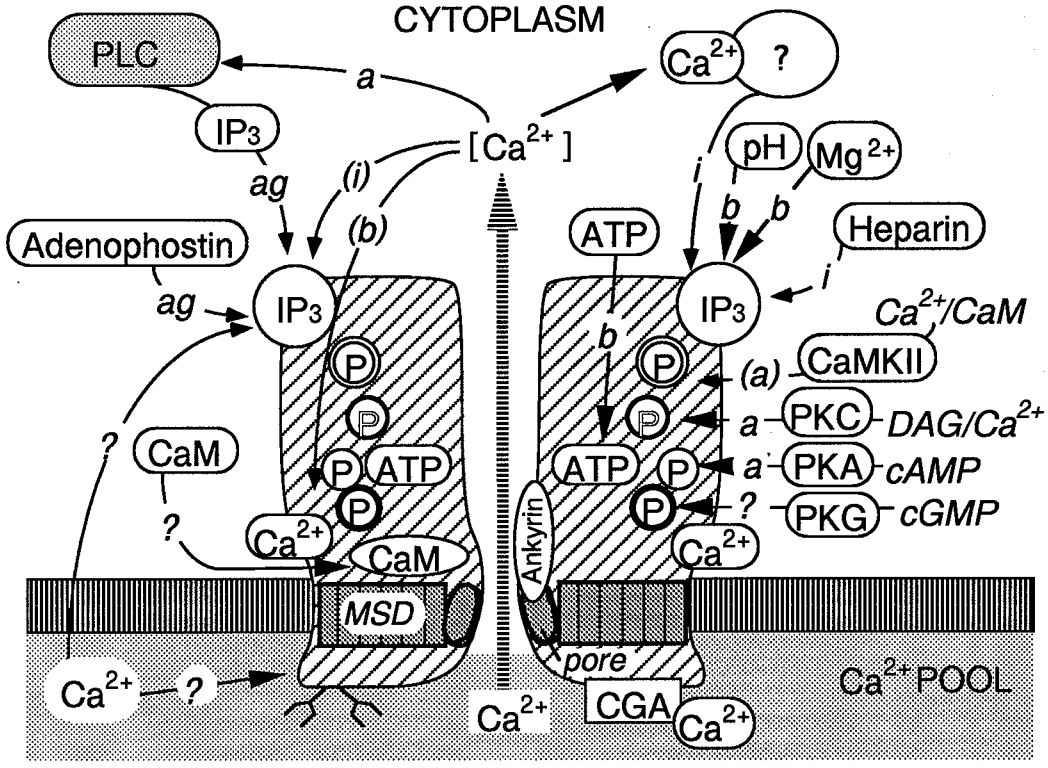

Figure 1-5. Regulation of IP_3R.

The IP_3R is illustrated by two separated shaded parts. Various functional sites on the IP_3R are illustrated in circles: IP_3, IP_3-binding site; P, phosphorylation sites; ATP, ATP-binding site; CaM. CaM-binding site; Ca^{2+}, Ca^{2+}-binding site. Adenophostin is the novel agonist of IP_3R. IP_3-binding is affected by pH, Ca^{2+}, Mg^{2+} and heparin. Chromogranin A (CGA) interact with the intraluminal portion at acidic pH. Ankyrin binds to the putative pore-forming region. Letters with arrows indicate target sites of actions; ag, agonist activity; a, activation; i, inhibition; b, regulation in biphasic manner (dose depend); ?, not well characterized yet (modified Fig. 3 of ref. [49]).

IP3R Family

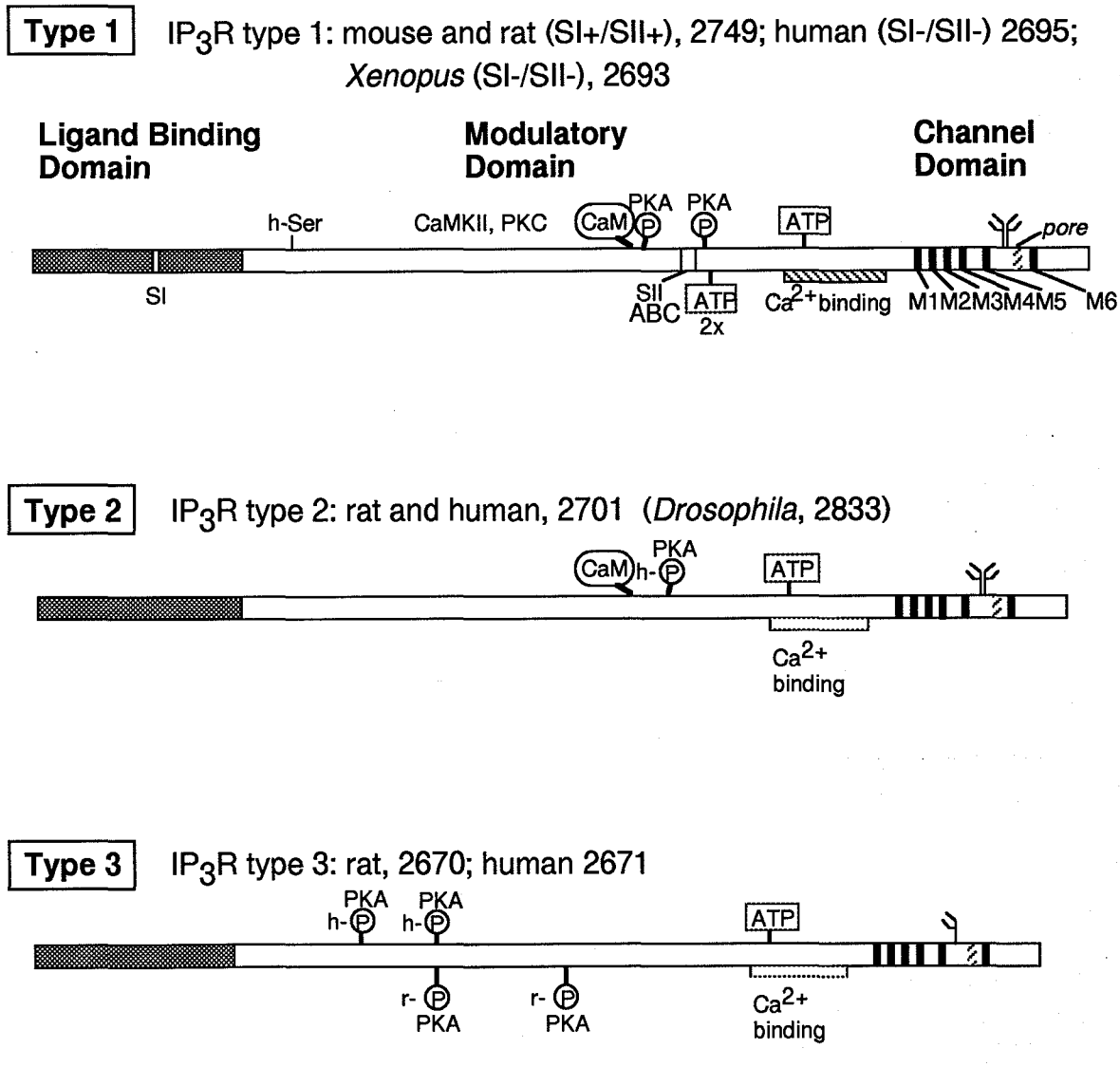

Figure 1-6. The primary structures of various types of IP_3R [3].

I - 5 Kinetics of Ca^{2+} Release by IP_3 Receptor

Following the first observation of the Ca^{2+} mobilizing properties of IP_3, our knowledge of IP_3-induced Ca^{2+} mobilization has currently benefited from a variety of experimental systems used, including the permeabilized and intact cells and microsome systems. There have been many studies on the kinetics of IICR; they describe the channel opening mechanism of the IP_3R [90 - 94], the regulation of IICR by modulators such as PKA [46, 74, 75], ATP [45, 76], GTP [95, 96], Ca^{2+} [92, 97 - 102], FKBP-12 [82] and the cytoskeleton, and the phenomenon of "quantal Ca^{2+} release" originally described by Muallem *et al.* [103], where sub-maximal concentrations of IP_3 cause the partial release of Ca^{2+} from intracellular stores.

I - 5 - 1) Fundamentals

I - 5 - 1. 1) Cooperativity of IP_3-induced Ca^{2+} release

The IP_3R functions as Ca^{2+} channel in its tetramer formation, thus there are four IP_3-binding sites per one channel, which may act cooperatively. The degree of the cooperativity of Ca^{2+} release is an important and fundamental issue for understanding the channel opening mechanism. However, there have been discrepancies among the reports. Some reports show no cooperativity of IICR ($n_H = 1$) [92, 104] others show positive cooperativity ($n_H = 2$) [90, 93] ($n_H = 4$) [91, 105, 106].

In the first detailed study of the kinetics of IP_3-induced Ca^{2+} release using rat basophilic leukemia (RBL) cells, the opening of Ca^{2+} channels was steeply dependent on IP_3 concentration ($n_H > 3$) [105]. In further analysis of the kinetics of IICR, they investigated a lag between addition of IP_3 and the onset of Ca^{2+} release, which was found to decrease from 1.5 sec at the lowest IP_3 concentration to 64 msec at the highest concentration [91]. The inverse correlation between the latency and IP_3 concentration suggests that IP_3 binding is the rate limiting for the channel opening step. And they have suggested that the latency represent the time between IP_3 binding to the receptor and channel opening and that at least four IP_3 molecules are required for the channel opening.

In liver [90] and skeletal muscle [93], initial rates of Ca^{2+} release have been reported to show a moderate positive cooperativity ($n_H = 2$), but in these experiments, as author suggested, the response to low IP_3 concentrations may have been more attenuated by continued Ca^{2+} pumping than that to high concentration, resulting artificial steeping the dose response curve.

No cooperativity ($n_H = 1$) of Ca^{2+} release have also been reported in some studies [92, 104]. However, in these study, they plotted above submaximal doses of IP_3 to calculate a Hill coefficient, resulting in the underestimation of the value. Generally speaking, the Hill plot should be drawn at submaximal doses of the ligand to evaluate an accurate Hill coefficient.

Anyway, the discrepancy in the degree of cooperativity of Ca^{2+} release have remained, which is probably due to the different experimental systems used, i.e., different micro-environments surrounding the IP_3R and Ca^{2+} pools assayed (e.g., different constitution of PLC, IP_3-metabolizing enzymes, Ca^{2+}-binding proteins, Ca^{2+}-pumps, modulators in each cell type and different types of IP_3R).

I - 5 - 1. 2) Biphasic nature of IP_3-induced Ca^{2+} release

The time course of Ca^{2+} release was found to be biphasic. Champeil *et al.* explained the biphasic nature of IP_3-induced Ca^{2+} release in terms of switching of the IP_3R from a low affinity/high conductance state, giving rise to the rapid phase of Ca^{2+} release, to a high affinity/low conductance state, producing the second slower phase of Ca^{2+} release. The rise in cytosolic Ca^{2+} concentration may provide a possible trigger for the interconversion of these two states. Indeed the [^{32}P] IP_3 binding experiment suggested that the interconversion between high affinity state and low was mediated by the cytosolic Ca^{2+} concentration [107]. In Champeil's study, the activity of the Ca^{2+} ATPase was not inhibited which could account for the biphasic nature of Ca^{2+} release. However, the demonstration of biphasic Ca^{2+} release in the absence of Ca^{2+} ATPase activity and IP_3 degradation is highly suggestive that biphasic nature of IP_3-induced Ca^{2+} release mediated by IP_3R is an intrinsic property [91].

I - 5 - 1. 3) IP_3-induced Quantal Ca^{2+} release

Quantal Ca^{2+} release was first described by Muallem *et al.*, who demonstrated that low hormone concentrations were unable to evoke the complete release of the IP_3-sensitive Ca^{2+} stores in pancreatic acinar cells, even under conditions preventing Ca^{2+} uptake system [103]. Quantal Ca^{2+} release was not caused by rapid metabolism of IP_3, since such phenomenon was demonstrated using a poorly-metabolizable IP_3 analogue [108 - 110]. In addition, since Ca^{2+} ATPase activity was inhibited in these studies, quantal Ca^{2+} release was not due to the equilibration between IP_3-induced Ca^{2+} release and Ca^{2+} uptake [108]. Furthermore, classical channel desensitization seems not to be involved in this phenomenon, since the IP_3 sensitive Ca^{2+} stores retained their responsiveness to further additions of IP_3 following partial depletion of the store, called incremental detection [94, 106]. This phenomenon has now been observed in a variety of cell types, pancreatic acinar cells [103], endothelia and HeLa cells [111, 112], hepatocytes [90, 108, 113, 114], cerebellar microsomes [115] and synaptosomes [92]. As the purified and reconstituted IP_3R-mediated Ca^{2+} release showed quantal release process [116], the quantal release is found to be an intrinsic and fundamental property of IP_3R (see section I - 6 - 1).

The physiological significance of quantal Ca^{2+} release is not clear. What is clear that IP_3-induced Ca^{2+} release can provide an obvious mechanism for allowing cells to have a graded response to different agonist concentrations. It seems likely that revealing the mechanism underlying these quantal responses will help us to more clearly understand the generation of complex Ca^{2+} signaling.

I - 5 - 2) Regulation of IP_3-induced Ca^{2+} release

It is now well known that the activity of the IP_3R is regulated by a variety of intracellular factors (see section I - 4 - 5. 2). Due to IP_3R type heterogeneity, regulatory elements may exert different effects on different IP_3R isoforms and types. In addition, the different environment of IP_3R due to different cells could provide differential distribution of the modulators, leading to differences in IP_3R activity. It is now apparent that IP_3-induced Ca^{2+} release is modulated by

various factors, such as other second messenger-signaling ("cross-talk regulation"), ATP and cAMP-dependent protein kinase (PKA) and Ca^{2+} signal itself ("feedback regulation"). These diverse modulations of IP_3R suggest that the complicated Ca^{2+} signaling appears to be involved in the intracellular IP_3/Ca^{2+} signaling.

I - 5 - 2. 1) The effects of cytosolic Ca^{2+}

Cytosolic Ca^{2+} is believed to regulate the IP_3R activity in a biphasic manner [97, 98, 117]. IICR showed a bell-shaped curve depending on the Ca^{2+} concentration using the cerebellar microsomal fraction incorporated into the lipid bilayer [117]. Increasing the cytosolic Ca^{2+} concentration up to 300 nM increases the Ca^{2+} releasing activity of IP_3R, whereas that the higher Ca^{2+} concentration inhibits the Ca^{2+} release. The feedback regulation of subsequent IICR by initially increased Ca^{2+} may be important to generate spatio temporal dynamics of cytosolic Ca^{2+} (Ca^{2+} wave or oscillation).

The stimulatory effect of cytosolic Ca^{2+} on the IP_3R is exerted instantaneously [98] and seems to be dependent on the content Ca^{2+} in its store [99]. It is generally assumed that the effects of cytosolic Ca^{2+} on the IP_3R is exerted directly [118], although a recent report suggests the involvement of the Ca^{2+} and calmodulin-dependent protein kinase [119]. On the other hand, the inhibitory effect of cytosolic Ca^{2+} on the IP_3R is slower than the stimulatory effect. There have been suggestions that the inhibition could be exerted indirectly through binding of Ca^{2+} to inositol phosphate [120], through activation of proteases [121], or through phosphatase 2E [119].

The fact that the effects of cytosolic Ca^{2+} is absent in some systems, including platelets [122], vas deferens [69], adrenal cortex [123], airway smooth muscle [124] and rat basophilic leukemia (RBL) [106], also suggest the possibility that such effects may mediate some Ca^{2+} sensing proteins or isoforms of IP_3R may exhibit a different effects of Ca^{2+}.

The effects of cytosolic Ca^{2+} are not generally considered to represent the mechanism of quantal Ca^{2+} release since this phenomenon is observed in cells that do not exhibit the

feedback regulation by the released Ca^{2+} and when cytosolic Ca^{2+} is strongly buffered [108, 111, 113, 114].

The Ca^{2+} feedback regulation is well related to the observation that the recombinant protein a part of coupling domain just preceding to the channel domain expressed binds Ca^{2+}. This analysis does not exclude the existence of other Ca^{2+} binding sites.

I - 5 - 2. 2) The effects of luminal Ca^{2+}

The effects of luminal Ca^{2+} on IP_3R have been reported in several systems, in which the stores with a low luminal Ca^{2+} concentration are less sensitive to IP_3 than more filled stores.

The finding that the IICR is activated by luminal Ca^{2+} provide an explanation for the phenomenon (see section I - 6 - 1). In the model, luminal Ca^{2+} determines the IP_3 sensitivity or slow down the Ca^{2+} release once pools become depleted. Indeed. Oldershow *et al.* reported that the partial Ca^{2+} release in permeabilized rat hepatocytes no longer occurred under conditions where the luminal free Ca^{2+} concentration was kept constant by pyrophosphate as Ca^{2+} buffer [114].

Little is known about the site of a putative intraluminal Ca^{2+} sensor sites in the IP_3R. Furthermore, it is not known whether luminal Ca^{2+} interact with IP_3R directly or indirectly.

I - 5 - 2. 3) The effects of cAMP-dependent protein kinase A

IP_3Rs have been shown to be phosphorylated by cAMP-dependent protein kinase A (PKA) at the serine residue as mentioned above, providing evidence to suggest that the cAMP signalling pathway can interact with and regulate the phosphoinositide pathway ("crosstalk").

IP_3R1 has two phosphorylation sites on either side of the SII splicing region. *In vitro* PKA phosphorylation demonstrated that the IP_3R containing SII^+ region is highly phosphorylated at Ser-1756 (Ser-1755 in the mouse receptor) and to a much less extent at Ser-1589 (Ser-1588 in the mouse receptor). By contrast, the IP_3R lacking SII^- is phosphorylated exclusively at Ser-1589 [72]. The functional significance of the phosphorylation of these individual sites has not been determined but it is possible that phosphorylation of different serine residues by PKA cause different activities of IP_3R.

In all of the studies examined so far, there are heterogeneous populations due to the different IP_3R types derived from distinct genes and isoforms by alternative splicing. Furthermore as they have investigated using crude systems such as microsomal fractions, the effects of PKA obtained could be not only attributed to the phosphorylation of the IP_3R itself but also the phosphorylation of an accessory molecule regulating the activities of IP_3R. To clarify the effect of PKA on IP_3R type 1 (IP_3R1), Nakade *et al.* have isolated and reconstituted IP_3R1, and investigated effects of PKA on the IP_3R1. In the study, PKA was shown to enhances the Ca^{2+} release activity of the IP_3R 1 [75]. Same tendencies were observed in intact platelets [125] and hepatocytes [126] and in cerebellar membranes [127]. However, the contrary results were obtained in some cells and crude preparations [48, 128]. Further studies of the effects of PKA on each IP_3R type and on each isoforms produced by the SII splicing are required.

I - 5 - 2. 4) The effects of phosphorylation by CaMKII, PKC and cGMP-dependent protein kinase

Although the IP_3R has been shown to be a substrate for phosphorylation by CaMKII [33], PKC [48] and PKG [47], the these effects on IICR are unknown. Effects of phosphorylation by CaMKII and PKC may be involved in immediate feedback mechanisms following IICR, since Ca^{2+} would stimulate CaMKII and the DAG produced during IP_3 production would activate PKC. However, details of the effects of these kinases have not been well characterized yet.

I - 5 - 2. 5) The effects of adenine nucleotides

ATP binds purified IP_3R with K_D and B_{max} values of 17 μM and 2.3 pmol/μg, respectively. There are three putative ATP-binding sites in the receptor sequence and two of them overlap with each other. Binding kinetics indicated that one purified receptor binds one ATP molecule. ATP enhanced IICR in a reconstituted IP_3R into planar lipid bilayers as well as in microsomal fraction from aorta. It is likely that ATP modifies the channel to reach the larger subconductance state. The channel opening was most effectively simulated at 0.6 mM ATP [45]. On the other hand, in the case of the reconstituted IP_3R into lipid vesicles, the IP_3-induced

$^{45}Ca^{2+}$ flux increased at 1-10 μM ATP but decreased at 0.1-1 mM ATP [76]. This discrepancy in the effective concentration of ATP may be due to differences among the methods of the preparation of IP_3R and the buffer composition used.

I - 5 - 2. 6) The effects of pH

Several studies have highlighted the pH dependence of IP_3R activity. For optimum [^3H] Ins(1,4,5)P_3 binding, alkaline pH (pH 8.5 - 9.5) is most effective [34, 70]. The enhancement of IP_3 binding as a function of pH appears to be mediated by a reversible increase in receptor affinity for IP_3, without change in the maximum number IP_3 binding sites. Ca^{2+} releasing activity of IP_3R in such high alkaline pH have not been investigated. However, the dependence on pH of IICR was studied in physiological range of pH using saponin-skinned smooth muscle cells [129]. Increasing pH between 6.7 and 7.3 enhanced the rate of IICR, suggesting that pH could modulate IICR.

I - 6 Complex Actions of IP_3-induced Ca^{2+} Signaling

I - 6 - 1) Quantal Ca^{2+} release

As the open probability of the IP_3R incorporated into lipid bilayer increases as a function of IP_3 concentration, one would expect that lower concentrations of IP_3 would cause the same degree of store emptying as higher ones but at a slower rate (Figure 1-7). However, submaximal concentrations of IP_3 fail to fully empty IP_3-sensitive Ca^{2+} stores, despite that there is still a large amount of Ca^{2+} left in the IP_3-sensitive Ca^{2+} store. Therefore submaximal doses of IP_3 induce a partial Ca^{2+} release, i.e., the extent of Ca^{2+} release is dependent on the IP_3 concentration. This phenomenon has been described as "quantal Ca^{2+} release".

Quantal Ca^{2+} release was first described by Muallem *et al.*, who demonstrated that low hormone concentrations were unable to evoke the complete release of the IP_3-sensitive Ca^{2+} stores in pancreatic acinar cells, even under conditions preventing Ca^{2+} uptake system [103]. As described in I-5-1.3, quantal Ca^{2+} release was not caused by rapid metabolism of IP_3, since such phenomenon was demonstrated using a poorly-metabolizable IP_3 analogue [108 - 110]. In

addition, since Ca^{2+} ATPase activity was inhibited in these studies, quantal Ca^{2+} release was not due to the equilibration between IP_3-induced Ca^{2+} release and Ca^{2+} uptake [108]. Furthermore, classical channel desensitization seems not to be involved, since the IP_3 sensitive Ca^{2+} stores retained their responsiveness to further additions of IP_3 following partial depletion of the store, called incremental detection [94, 106]. The phenomenon of the quantal Ca^{2+} release has now been observed in a variety of cell types, pancreatic acinar cells [103], endothelia and HeLa cells [111, 112], hepatocytes [90, 108, 113, 114], cerebellar microsomes [115] and synaptosomes [92]. As the purified and reconstituted IP_3R-mediated Ca^{2+} release showed quantal release process [116], the quantal release is found to be an intrinsic and fundamental property of IP_3R.

At present, mainly three hypotheses are proposed to explain the "quantal Ca^{2+} release". First, individual store have different IP_3 sensitivities to release Ca^{2+} and respond to IP_3 in an all-or none fashion, where a low IP_3 concentration may only induce Ca^{2+} release from the most sensitive stores and not cause any response from the less sensitive stores and as IP_3 concentration increase, less sensitive Ca^{2+} stores start to release Ca^{2+} (All-or-none model). Second, a low IP_3 concentration may release some Ca^{2+} from the stores which have equal sensitivity to IP_3, where following the Ca^{2+} release, the subsequent decrease in luminal Ca^{2+} concentration serves to close the channel (Steady state model). Third, IP_3-induced Ca^{2+} release may cause receptor desensitization-like process (not classical desensitization) to slow down Ca^{2+} release or stop.

I - 6 - 2) Models for the quantal Ca^{2+} release

I - 6 - 2. 1) All-or none model

Muallem *et al.* proposed an all-or-none mechanism for quantal Ca^{2+} release, where there are heterogeneous population of IP_3Rs which differ in their sensitivities to IP_3, and release their Ca^{2+} content in an all-or-none manner [103]. A low IP_3 concentration may only induce Ca^{2+} release from the most sensitive stores and not cause any response from the less sensitive stores

and as IP_3 concentration increase, less sensitive Ca^{2+} stores start to release Ca^{2+} (Figure 1-8). The heterogeneity of sensitivity of IP_3R to IP_3 could arise form the existence of isoforms of IP_3R due to alternative splicing, which may different affinities for IP_3. However, a possible site resulting in different affinities for IP_3, i.e., SI region, has not influenced the binding affinity. Alternatively, the heterogeneity due to different types of the IP_3Rs, which have different sensitivity to IP_3, may be responsible for the quantal release.

I - 6 - 2. 2) Steady state model

Irvine proposed a steady-state model for quantal Ca^{2+} release that IP_3-induced Ca^{2+} release may be regulated by the luminal content of the IP_3-sensitive Ca^{2+} [130]. A low IP_3 concentration may release some Ca^{2+} from the stores which have equal sensitivity to IP_3, where the subsequent decrease in luminal Ca^{2+} concentration following the Ca^{2+} release serves to close the channel (Figure 1-8). This model requires the existence of a Ca^{2+} binding site on the luminal side of the receptor or Ca^{2+} sensing protein which modulate the receptor from luminal side. Several studies using smooth muscle cells and hepatocytes have shown some dependence on luminal Ca^{2+} [109, 131], suggesting the existence of a Ca^{2+} binding site in IP_3R or a regulatory molecule which senses the luminal Ca^{2+} concentration. However, such Ca^{2+} binding site has not been identified yet. Other studies involving the manipulation of the intraluminal Ca^{2+} content of IP_3-sensitive Ca^{2+} stores have demonstrated that the luminal Ca^{2+} does not influence IP_3-induced Ca^{2+} release [114, 115, 132].

I - 6 - 2. 3) Inactivation / Interconversion

One can easily imagine that inactivation of the IP_3R, which slow down or stop IP_3-induced Ca^{2+} release, could contribute to the quantal Ca^{2+} release. The IP_3R is generally assumed not to be desensitized, for the following reasons. IP_3-sensitive Ca^{2+} stores retained their responsiveness to further additions of IP_3 following partial depletion of the store, called incremental detection.

Recently, Hajnoczky *et al.* [134], however, reported that IP_3R could inactivate upon IP_3 binding in the permeabilized hepatocytes. In Hajnoczky's experiments, the inactive state which

appeared after preincubation with IP_3 could response further stimulation but release Ca^{2+} very slowly. This is resemble to phenomenon of single channel adaptation observed in ryanodine receptor. Moreover, the degree of inactivation of IP_3R by IP_3 depends on both the duration of the preincubation with IP_3 and Ca^{2+} concentration. It seems to well relate the phenomenon of the interconversion of IP_3R, where IP_3R has two state with high affinity and low affinity and the interconversion between these states was mediated by the cytosolic Ca^{2+} concentration [107]. If the released Ca^{2+} rapidly rises near the channel pore and mediate the interconversion in cooperation with IP_3, the inactivation of the receptor reported by Hajnoczky *et al.* [134] may reflect an interconversion of the IP_3R. This hypothesis could be supported by the observations in Fig. 3 of ref. [134], where the degree of inactivation (interconversion) varied with the cytosolic free Ca^{2+} concentrations during the preincubation with IP_3 and IP_3R, whereas no significant change in IICR at various cytosolic free Ca^{2+} concentrations were observed without preincubation. In addition, very recent single channel recording of IP_3R of isolated Xenopus oocyte nuclei revealed that IP_3R could inactivate after more than 5 min continuous stimulation with IP_3 [135]. In addition, the phenomenon of single channel adaptation was described for the ryanodine receptor, which is an intracellular Ca^{2+} channel with much resemblance to the IP_3R. Single channel adaptation means that the channel activity during continuous stimulation progressively decreases, although the channel remains responsive to a more intense stimulation [133].

Therefore now it is the time for reconsideration and re-examination of the inactivation (interconversion) and adaptation of IP_3R for the mechanism underlying the quantal Ca^{2+} release.

I - 6 - 3) Complex Ca^{2+} signaling (Ca^{2+} wave and oscillation)

Many of the numerous cell types that respond to Ca^{2+}-mobilizing agonists are known to exhibit more complex patterns of Ca^{2+} release in the form of a wave of Ca^{2+}, which sweeps across the cell, and a repetitive pattern of Ca^{2+} spikes, the frequency of which is determined by

both the agonist concentration and level of external Ca^{2+} [136 - 139]. The spatial organization of such a spike is often complex; there is a specific initiation locus form which Ca^{2+} sweeps across the cell in the form of a regenerative wave [140, 141]. The propagation of a Ca^{2+} wave through the cell requires the presence of either IP_3R or RyRs; RyRs are believed to contribute to wave propagation of a Ca^{2+} wave in mouse eggs [142] whereas IP_3Rs have been implicated in the generation of Ca^{2+} waves [143] in Xenopus oocytes, hamster eggs [144] and in rat hepatocytes [145].

There have been several models proposed to explain the generation of a Ca^{2+} spike, and its propagation as a wave across the cell. Due to the great expanse of literature surrounding the spatial and temporal aspects of Ca^{2+} signalling, a model in which IP_3R are involved in the generation of a Ca^{2+} spike and how it may propagate through the cell as a wave has been proposed. In this model, both IP_3 and Ca^{2+} act through the IP_3R to trigger the regenerative release of Ca^{2+} from intracellular stores. The occupation of cell surface receptors, coupled to PLC activation , causes the release of IP_3 into the cytosol. This in turn stimulates Ca^{2+} release from stores lying closest to the site of IP_3 generation i.e. near to the plasma membrane. The resulting increase in Ca^{2+} concentration, as it diffuses from the initial site of release, is taken up by stores lying deeper within the cell. This increase in Ca^{2+} loading serves to increase their sensitivity to IP_3, allowing the stores to discharge their Ca^{2+} in response to the lower IP_3 concentrations likely to be found further away from the plasma membrane. Both IP_3 and the released Ca^{2+} may act as a trigger for the subsequent release of Ca^{2+} from neighboring stores and subsequent rise in cytosolic Ca^{2+} concentration will serve to inhibit the IP_3 receptor, allowing IP_3-sensitive stores to reaccumulate Ca^{2+}, and release their Ca^{2+} content once the stores regain their sensitivity to IP_3. Such a model can be used to explain how a single wave of Ca^{2+} can propagate across the cell. In a cell that contains RyR as well as IP_3R, the subsequent release of Ca^{2+} from one store may induce a neighboring store containing RyR, to release its Ca^{2+} content by a CICR mechanism.

The precise mechanisms by which cells generate Ca^{2+} wave and spikes are not entirely understood and the available models go some way to explain this phenomenon. However, we can begin to understand the mechanism underlying such phenomenon by fundamental studies on IP_3R as well as RyR.

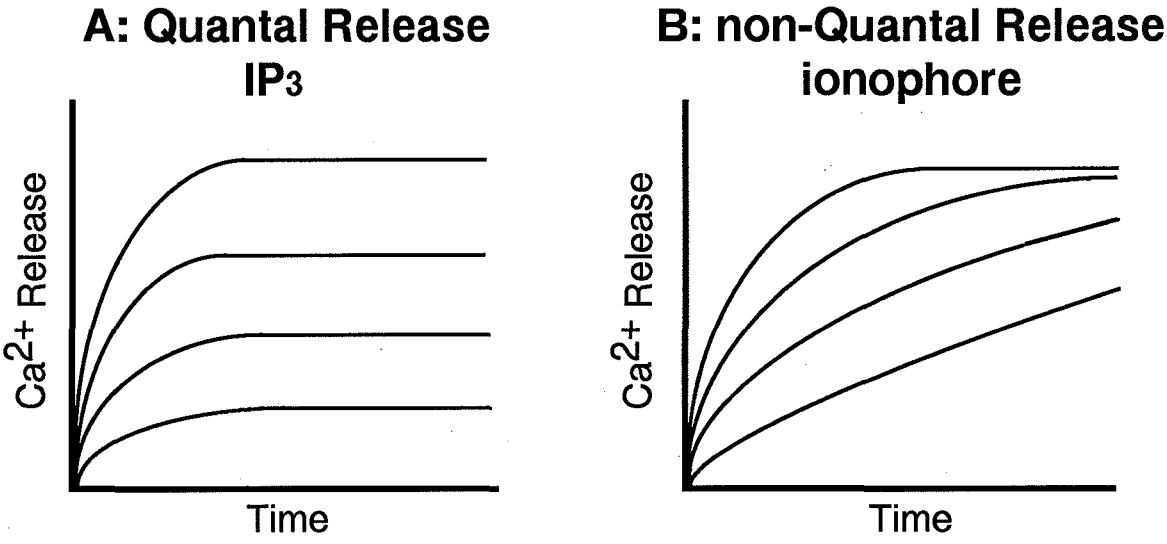

Figure 1-7. Quantal and non-quantal Ca^{2+} release.

Schematic representation of quantal Ca^{2+} release (A) and non-quantal Ca^{2+} release (B). The submaximal concentration of IP_3 induce partial Ca^{2+} release and no further effect on Ca^{2+} release. Inonomycin, by contrast, fully empties stores of Ca^{2+} at rates that increase with increasing inonomycin concentration.

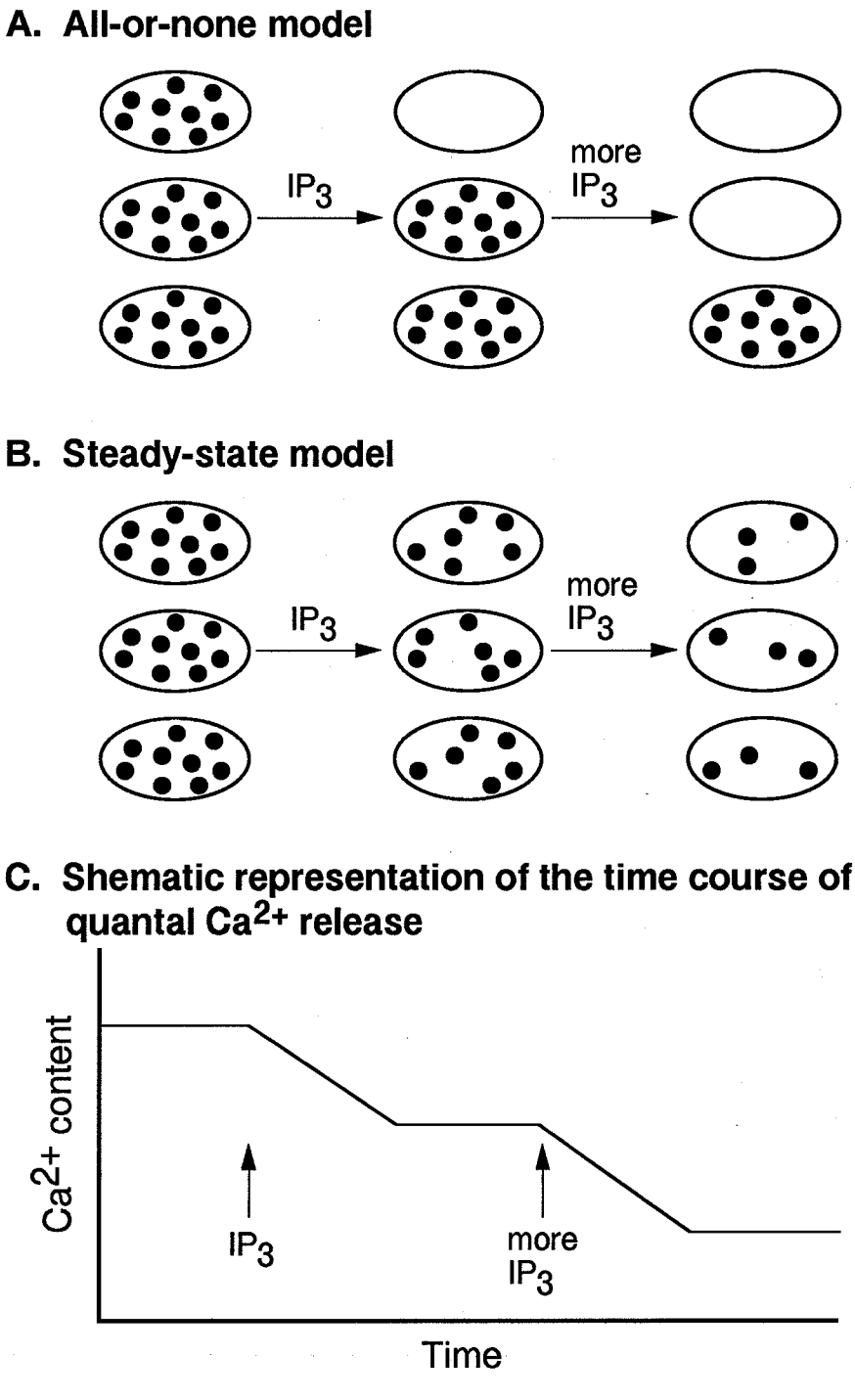

Figure 1-8. The models accounting for IP_3-induced quantal Ca^{2+} release.

A: All-or-none model, a low IP_3 concentration may only induce Ca^{2+} release from the most sensitive stores and not cause any response from the less sensitive stores and as IP_3 concentration increase, less sensitive Ca^{2+} stores start to release Ca^{2+}.

B: Steady state model, IP_3-induced Ca^{2+} release is regulated by the luminal Ca^{2+} concentrations, where following the Ca^{2+} release, the subsequent decrease in luminal Ca^{2+} concentration serves to close the channel.

I - 7 Purpose

As described above, IP_3R is an IP_3-induced Ca^{2+} releasing channel located on intracellular Ca^{2+} stores such as the endoplasmic reticulum. The IP_3-mediated Ca^{2+} signaling plays a critical role in a variety of cell functions, including fertilization, cell proliferation, metabolism, secretion, contraction of smooth muscle and neural signals [2]. The structural and biochemical properties of IP_3R have been well known by many intensive molecular biological studies. Our knowledge of functional properties of IP_3R, i.e., properties of IP_3-induced Ca^{2+} mobilization, has currently benefited from a variety of experimental systems used, such as the permeabilized and intact cells and microsome systems. These results, however, so often differ among the reports. In these studies, the arguments on some critical points of IP_3-induced Ca^{2+} release have often been complicated due to the different experimental systems used, i.e., different micro-environments surrounding the IP_3R and Ca^{2+} pools assayed (e.g., different constitution of PLC, IP_3-metabolizing enzymes, Ca^{2+}-binding proteins, Ca^{2+}-pumps, modulators in each cell type and heterogeneity of IP_3R types). Therefore, an investigation of IP_3-induced Ca^{2+} release by a "purified single type" of IP_3R allow us to reveal the fundamental properties of IP_3-induced Ca^{2+} release.

In this study, to investigate the functional properties of IP_3R1, we have purified IP_3R1 using immunoaffinity column conjugated with an antibody against IP_3R1 from mouse cerebellar microsomes and have established a novel system to investigate the kinetics of IP_3-induced Ca^{2+} release using the fluorescent Ca^{2+} indicator fluo-3. This study provides the first report of the kinetics of Ca^{2+} release by the purified single IP_3R type.

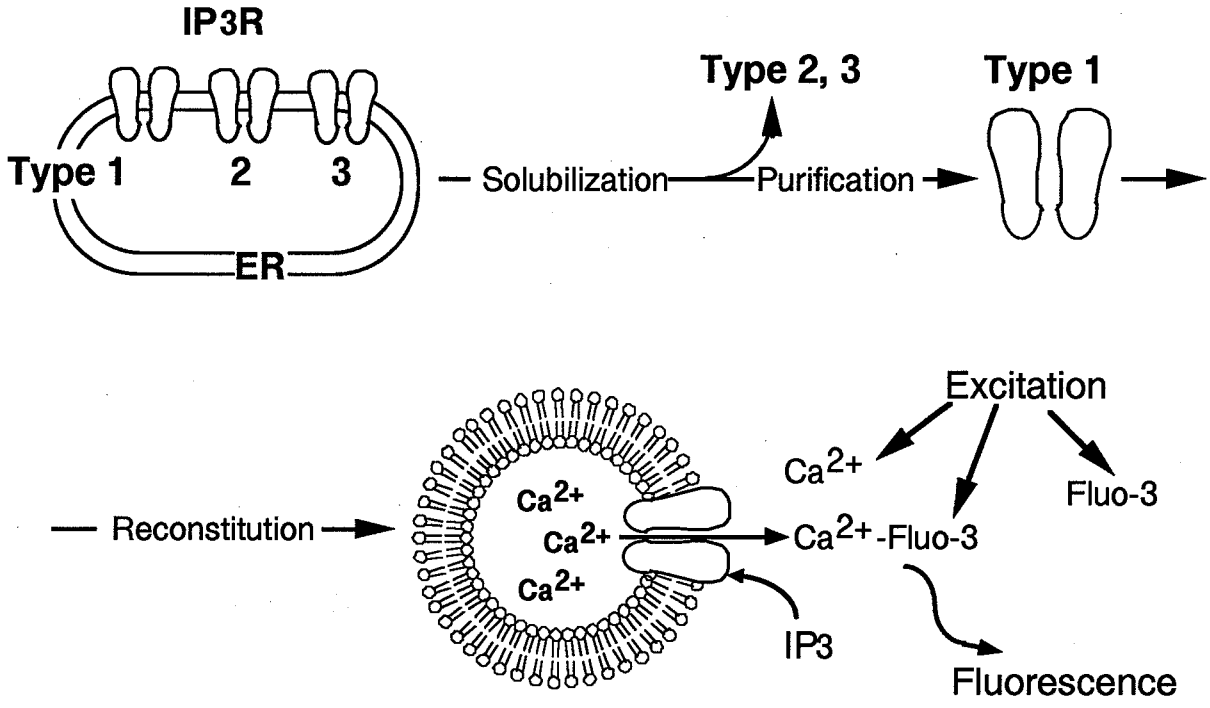

Figure 1-9. Scheme summarizing the experimental procedures.

IP_3R1 was purified form mouse cerebellar microsomes using a type-specific immunoaffinity column conjugated with an antibody against IP_3R1. The purified IP_3R1 was reconstituted into lipid vesicles to investigate the kinetics of IP_3-induced Ca^{2+} release using fluorescent Ca^{2+} indicator fluo-3.

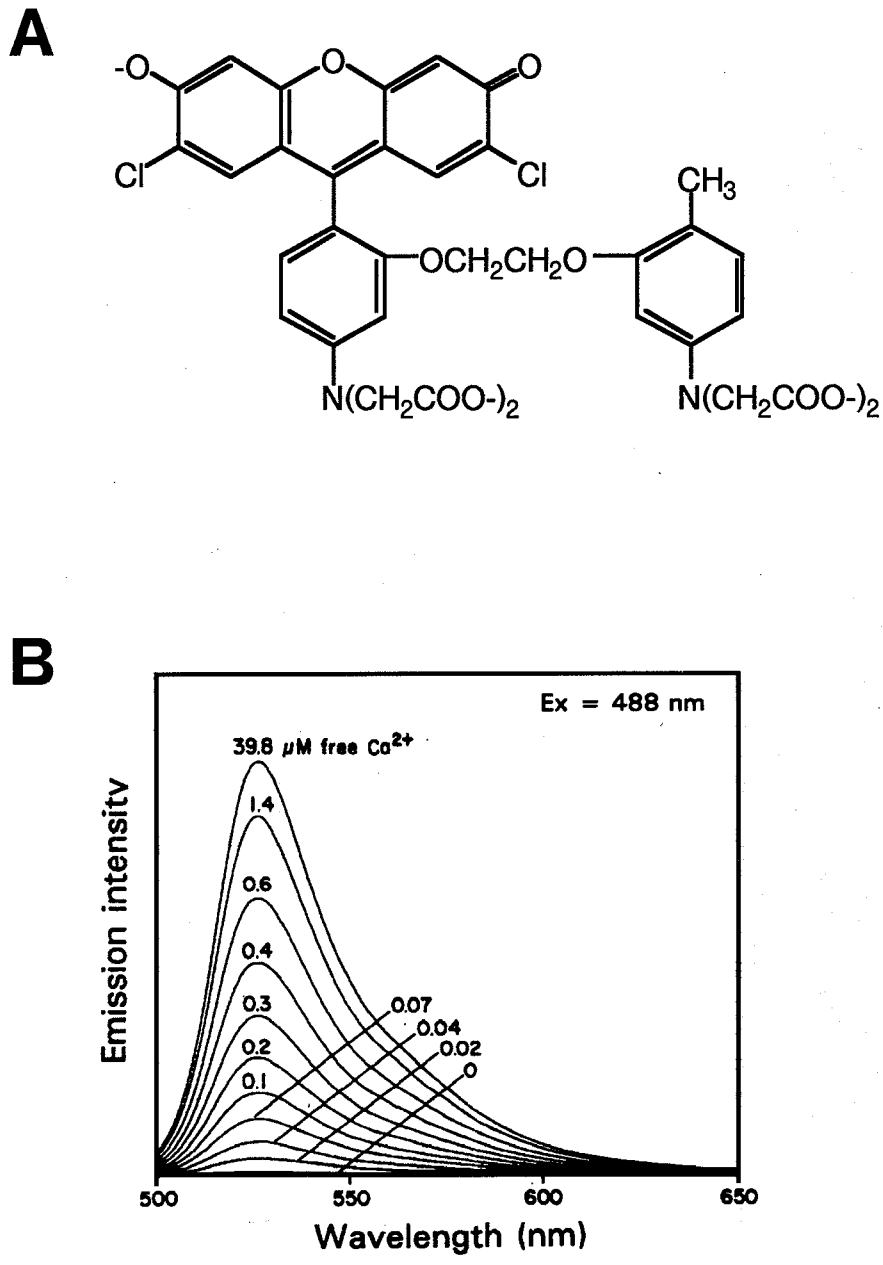

Figure 1-10. Structure (A) and fluorescence spectra obtained at various concentration of Ca^{2+} (B) of fluo-3.

The fluorescence intensity of fluo-3 increases in proportion to the Ca^{2+} concentrations.

CHAPTER II

PURIFICATION OF INOSITOL 1,4,5-TRISPHOSPHATE RECEPTOR TYPE 1

II - 1 Introduction

As described in Chapter I, inositol 1,4,5-trisphosphate (IP_3) is the second messenger derived from the hydrolysis of phosphatidylinositol bisphosphate via activation of phospholipase C, whose activity is enhanced by activation of G protein-linked and tyrosine kinase-linked cell surface membrane receptors by various extracellular stimuli, such as hormones, growth factors, neurotransmitters, odorants, lights, etc. [2]. The IP_3 signal is converted into a Ca^{2+} signal by binding to its specific receptor, i.e., the IP_3 receptor (IP_3R), which is an IP_3-induced Ca^{2+} releasing channel located on intracellular Ca^{2+} stores such as the endoplasmic reticulum. The IP_3-mediated Ca^{2+} signaling plays a critical role in a variety of cell functions, including fertilization, cell proliferation, metabolism, secretion, contraction of smooth muscle and neural signals [2]. For these multiple cell signaling, the mechanisms of transducing the IP_3 signal into a Ca^{2+} signal, i.e., IP_3 induced Ca^{2+} release (IICR), may be diverse in each cell type.

It is now well known that there are at least three types of the IP_3R from distinct genes [37, 52, 88]. The fundamental domains of the receptors, IP_3-binding (72-77% homology) and channel domains (66-71%), are relatively conserved, whereas the modulatory (coupling) domains (56-65%) are often interspersed with long stretches of diversified amino acids [3, 49]. As most of the putative modulator-binding sites and phosphorylation sites in the modulatory (coupling) domain are diversified among the IP_3R family, the properties of IICR may be different among the IP_3R types. Furthermore, the expression of multiple types of IP_3Rs in individual cells suggests that a heterotetrameric IP_3R complex, which may display different IP_3 binding and channel opening properties from the homotetramer, may cause more complicated IP_3/Ca^{2+} signaling.

Therefore, the investigations into the structural and functional properties of individual IP_3R isoforms may allow us to reveal new insights of the complex actions of IP_3/Ca^{2+} signaling. For example, Nakade *et al.* have isolated the IP_3R type 1 (IP_3R1) from mouse cerebellum and have found that Ca^{2+} releasing activity of the purified IP_3R1 is enhanced by

PKA phosphorylation. This is contrary to previous reports demonstrating inhibition of IICR from cerebellar microsomes [46] and platelet membranes [128] by PKA. Since cerebellar microsomes and platelet membranes may contain different IP_3R types and modulatory proteins, the effects of PKA on IICR may represent indirect effects on the IP_3R or different IP_3R types.

In this study, to investigate the functional properties of IP_3R1, we have purified IP_3R1 using immunoaffinity column [75, 146] form mouse cerebellar microsomes. The cerebellum is known to be the richest source of IP_3R type 1 (IP_3R1) among rodent tissues tested. A recent immunohistochemical study indicated that rat cerebellum contains three IP_3R types whose expressing cell-types are quite distinct; IP_3R1 is well known to be enriched in Purkinje cells, IP_3R type 3 (IP_3R3) is present in Bergmann glia and astrocytes and IP_3R type 2 (IP_3R2) is also present but not in neurons and astrocytes [147]. The differential localization of each IP_3R type in cerebellar cell types indicates that most IP_3R-channel complexes in the cerebellum are homotetramers within single cells. In the following section, isolation of the cerebellar IP_3R1 by a type-specific purification method using an immunoaffinity column coupled with an anti-IP_3R1 antibody is described. And homogeneity of the purified IP_3R1 have been also studied using monoclonal antibodies against each IP_3R type [157].

II - 2 Experimental Procedures

II - 2 - 1) Materials

Cerebella were dissected from adult ddY mice. The following reagents were purchased: 3-[(3-cholamidopropyl) dimethylammonio]-1-propanesulfonic acid (CHAPS) and 1-ethyl-3-(3-dimethylaminopropyl) carbodiimide (EDC) from Dojindo Laboratories (Kumamoto, Japan), bovine serum albumin fraction V (BSA), Freund's adjuvant complete, Freund's adjuvant incomplete and phosphatidylcholine from SIGMA, ECL Western blotting system, and Nitrocellulose hybridization transfer membranes Hybond ECL from Amersham Corp, Sephadex G-50 and CNBr-activated Sepharose 4B from Pharmacia LKB Biotechnology INC. All other reagents used were of analytical grade or the highest grade available.

II - 2 - 2) An antibody against a synthetic IP_3R1 C-terminal peptide

A peptide corresponding to the C-terminal region of the IP_3R1 (amino acid residues 2736 - 2747 designated pep 6: GHPPHMNVNPQQ), which is diverse in each receptor type, was custom-synthesized. The peptide (pep 6) was conjugated to bovine serum albumin (BSA) via EDC. Twenty milligram of pep 6 and 20 mg of BSA were dissolved in 5 ml of phosphate-buffered saline (PBS), pH 7.4, and 20 mg of EDC was added at 4 ^{o}C with constant stirring. The mixture was stirred over night. The remaining unreacted EDC and pep 6 were separated by gel filtration on a Sephadex G-50 column equilibrated in 50 mM ammonium acetate. The fractions containing of pep 6-BSA were collected, lyophilized and then dissolved with PBS at the protein concentration of 0.5 mg/ml. The pep 6-BSA conjugate solution was stored under -80 ^{o}C. New Zealand White rabbits were immunized by intradermal injection with a homogenate containing 1 ml of Freund's complete adjuvant and 1 ml of pep 6-BSA conjugate solution. Three weeks later, the rabbits were injected with a homogenate containing 1 ml of Freund's incomplete adjuvant and 1 ml of pep 6-BSA conjugate solution. Antiserum was collected each week thereafter. Booster injection was performed every 2 weeks until the titer of the antiserum was saturated [75].

II - 2 - 3) Immuno-affinity column (anti-pep 6 antibody-conjugated affinity column)

The IgG fraction from the anti-pep 6 serum was purified by ammonium sulfate precipitation and dialyzed against 0.1 M $NaHCO_3$ and 0.5 M NaCl, pH 8.3, and then 20 mg of IgG were conjugated to 2 ml of CNBr-activated Sepharose 4B according to the manufacturer's protocol. Briefly, CNBr-activated Sepharose 4B (2 ml) was washed with 120 ml of 1 mM HCl and then with 3 ml of the solution containing 0.5 M NaCl and 0.1M $NaHCO_3$. Twenty milligram of IgG was added to the solution and the mixture was incubated for over night at 4 ^{o}C. The beads were collected by centrifugation and 4 ml of the blocking buffer containing 0.1 M Tris-HCl were added to mask the unreacted ligand. After 2 hrs incubation, the beads were washed repeatedly with 10 ml of 0.1 M acetate buffer, pH 4.0, containing 0.5M NaCl and then 10 ml of 0.1M Tris-HCl, pH 8.0, containing 0.5 M NaCl three times. The anti-pep 6 antibody-Sepharose 4B beads were stored under PBS containing 0.05 % NaN_3 at 4 ^{o}C. For regeneration of the immunobeads, the beads were washed with the solution containing 1 M glycine and 1.5 M NaCl, pH 2.5 and then with PBS. The beads are equilibrated with the solution containing 1 mM EDTA, 1 mM 2-mercaptoethanol, 50 mM Tris-HCl, pH 7.4, 1 % CHAPS and 1 mg/ml phosphatidylcholine prior to use [75].

II - 2 - 4) Purification of IP_3R1

40 adult (10 weeks old) ddY mice were killed by decapitation, and the cerebella were dissected. The tissues were washed with PBS and then were mixed with 18 ml of the solution containing 0.32 M sucrose, 1 mM EDTA, 0.1 mM phenylmethylsulfonyl fluoride (PMSF), 10 μM leupeptin, 10 μM pepstatin A, 1 mM 2-mercaptoethanol, and 4 mM Tris-HCl, pH 7.4, and were homogenized in a glass-Teflon Potter homogenizer with 10 strokes at 850 rpm. The homogenate was centrifuged at 1000 x g for 5 min at 2 ^{o}C, and the pellet was homogenized again under the same condition. the combined supernatants were centrifuged at 105,000 x g for 1 hr at 2 ^{o}C to precipitate the membrane fraction. For the further functional studies of the

purified IP_3R1, we need to reconstitute it into lipid vesicles. Therefore, we used CHAPS for solubilization of the membrane fraction. The membrane fraction was resuspended with 1 mM EDTA, 1 mM 2-mercaptoethanol, 0.1 mM PMSF, 10 μM leupeptin, 10 μM pepstatin A, and 50 mM Tris-HCl, pH 7.4 (buffer A) and then solubilized with CHAPS to give final protein and detergent concentration of 3.0 mg / ml and 1.0 %, respectively, with gentle stirring for 20 min at 0 °C. The solution was centrifuged at 20,000 x g at 2 °C, and the supernatant was incubated with 2 ml of the anti-pep 6 antibody-Sepharose 4B beads for 3 hr at 4 °C with gentle stirring. The beads were transferred into a column and washed with 30 ml of buffer A containing 1 % CHAPS and 1 mg/ml phosphatidylcholine (buffer B), and then IP_3R was eluted with pep 6 at a concentration of 10 μM in buffer B. IP_3R was eluted by a batch method. Two milliliter of packed beads with 2 ml of eluting reagent were incubated for 30 min at 4 °C with gentle stirring and then the supernatant was collected as eluate. This elution step was repeated 10 times. The eluates were stored under -80 °C. The immuno-beads were regenerated with 1 M glycine and 1.5 M NaCl, pH 2.5 and washed with PBS. Figure 2-1 summarizes that procedure of the immuno-affinity purification of IP_3R1.

II - 2- 5) Monoclonal antibodies

Monoclonal antibodies, 18A10, KM1083 and KM1082 against IP_3R Type 1, IP_3R Type 2 and IP_3R Type 3, respectively, were prepared as described elsewhere [31, 36, 148].

II - 2 - 6) SDS-PAGE and Western blotting

Electrophoresis was carried out on a 5 - 12.5 % gradient polyzarylamide gel. The gel was stained with Coomassie Brilliant Blue R-250. To investigate a homogeneity of the purified IP_3R1 using monoclonal antibodies, the purified IP_3R1 was electrophoresed (5 % SDS-PAGE) and transferred to a nitrocellulose membrane. The blots were immunostained with the monoclonal antibodies, 18A10, KM1083 and KM1082 against IP_3R Type 1, IP_3R Type 2 and IP_3R Type 3, respectively, using western blotting system (Amersham) [157].

II - 3 Results

II - 3 - 1) Immunoaffinity purification of IP_3R1

A polyclonal antibody against a synthetic peptide corresponding to the C-terminal amino acids 2736-2747 (designated pep 6) of IP_3R1, whose sequences are different among the receptors, was raised and used for immunoaffinity chromatography. For the purpose of the reconstitution of the purified IP_3R1 into lipid vesicles, we used CHAPS for solubilization. IP_3R was solubilized from crude mouse cerebellar membrane fraction with 1 % CHAPS, and the fraction was incubated with immuno-beads with which anti-pep 6 antibody was conjugated. The beads were washed to remove unbound protein, as described in Experimental Procedures. For the specific elution of IP_3R1 from the beads without losing functional activity, the original antigen to the anti-pep 6 antibody, pep 6, was used to elute the IP_3R1.

Figure 2-2 shows the SDS-PAGE analysis of solubilized microsomal fraction and the eluate by pep 6 after immunoaffinity chromatography using anti-pep 6 antibody. As the purified IP_3R concentration is low, we concentrated it about ten times to detect IP_3R stained with Coomassie Brilliant Blue. The SDS-PAGE analysis showed that the immunoaffinity purified IP_3R1 comprised of a single band. Thus, the immunoaffinity purification enables us to isolate the single type of IP_3R rapidly and under a very gentle condition.

II - 3 - 2) Homogeneity of the purified IP_3R1

To investigate the homogeneity of the purified IP_3R1, existence of IP_3R type 2 (IP_3R2) and type 3 (IP_3R3) in the purified receptors was analyzed by immunoblotting with monoclonal antibodies to each type of IP_3R. The same amount of [^{3}H] IP_3 binding activity of cerebellar microsomal fraction and the purified IP_3R1 (1.5 pmol of IP_3R/ lane) were applied to the gel, followed by immunoblotting with the monoclonal antibodies (Figure 2-3). The cerebellar microsomal fraction showed strong immunoreactivity with mAb 18A10 against IP_3R1 and little with mAbs KM1083 and KM1082 against IP_3R2 and IP_3R3, respectively, as reported previously [147]. The purified IP_3R1 also showed strong immunoreactivity with mAb 18A10

and little with mAbs KM1083 and KM1082 and the contents of IP_3R2 and IP_3R3 in the purified receptors which might form heterotetramer with IP_3R1 [149] were very small and decreased after the immunoaffinity-purification in comparison with the cerebellar microsomal fraction. These results showed that the purified IP_3R was chiefly composed of homotetramers of IP_3R1.

II - 4 Discussion

II - 4 - 1) Immunoaffinity purification of IP_3R1

Recent molecular cloning studies have revealed that there are at least three types of the IP_3R from distinct genes [37, 52, 88]. The amino acid sequences of the receptors reveals that C-terminus regions are different among the receptors, suggesting that each C-terminal region exhibited different antigenicity. For the purpose of the kinetic study of the purified single type of the IP_3R, we have isolated IP_3R1 by the immunoaffinity chromatography conjugated with the polyclonal antibody against pep 6 peptide corresponding to C-terminus regions of IP_3R1. In the purification procedures, pep 6 was used for the specific elution, because the elution by low pH resulted in an irreversible inactivation or denature of IP_3R when pH of the eluate was adjusted to a neutral pH immediately after the elution (Nakade *et al.* personal communication). By the immunoaffinity purification described in this section, we could isolate the single type of IP_3R rapidly and under a very gentle condition.

II - 4 - 2) Homogeneity of the purified IP_3R1

The cerebellar microsomal fraction showed strong immunoreactivity with mAb 18A10 against IP_3R1 and little with mAbs KM1083 and KM1082 against IP_3R2 and IP_3R3, respectively, as reported previously [147]. The purified IP_3R1 also showed strong immunoreactivity with mAb 18A10 and little with mAbs KM1083 and KM1082 and the contents of IP_3R2 and IP_3R3 in the purified receptors were very small and decreased after the immunoaffinity-purification in comparison with the cerebellar microsomal fraction. These results showed that the purified IP_3R was chiefly composed of homotetramers of IP_3R1. A recent immunohistochemical study also indicated that rat cerebellum contains three IP_3R types whose expressing cell-types are quite distinct; IP_3R1 is well known to be enriched in Purkinje cells, IP_3R type 3 (IP_3R3) is in Bergmann glia and astrocytes and IP_3R type 2 (IP_3R2) is also present but not in neurons and astrocytes [147]. The differential localization of each IP_3R type in cerebellar cell types indicate that most IP_3R-channel complexes in the cerebellum are

homotetramers within single cells. The population of the purified IP_3R has been found to be almost homogeneous, containing little IP_3R2 and IP_3R3, therefore we can predict that the purified IP_3R exists in a homotetrameric structure of IP_3R1. However, isoforms of IP_3R1 by the alternative splicing are included.

The immunoblots of the purified IP_3R1 with monoclonal antibodies against IP_3R2 and IP_3R3 showed very weak immunoreactivities, suggesting IP_3R1 could form heterotetramers with IP_3R2 and IP_3R3. Recently, Monkawa *et al.* reported heterotetramer formation of IP_3Rs in several cell lines [149], where the all IP_3R types co-exist within a cell. Little immunoreactivities of monoclonal antibodies against IP_3R2 and IP_3R3 to the purified IP_3R1 is probably due to little expressions of these IP_3R types (type 2 and 3) in the cerebellum. Therefore, applications of this purification method to other types of the native IP_3R seem to be available, only if IP_3R2 or IP_3R3 exists dominantly in some tissues. If IP_3R2 or IP_3R3 expressed from their cDNAs is available, the purification method using an antibody against each type of IP_3R would become a strong tool to investigate individual receptor type.

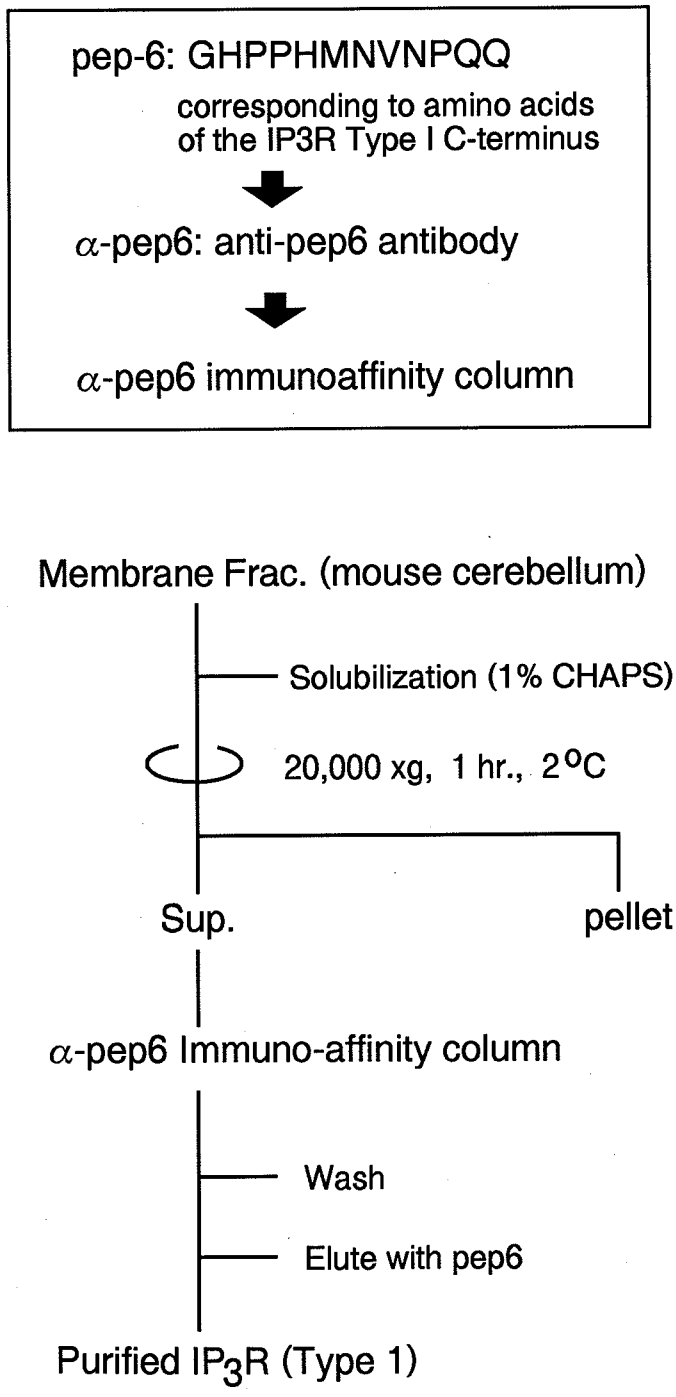

Figure 2-1. Scheme representing the immunoaffinity purification of IP_3R type 1

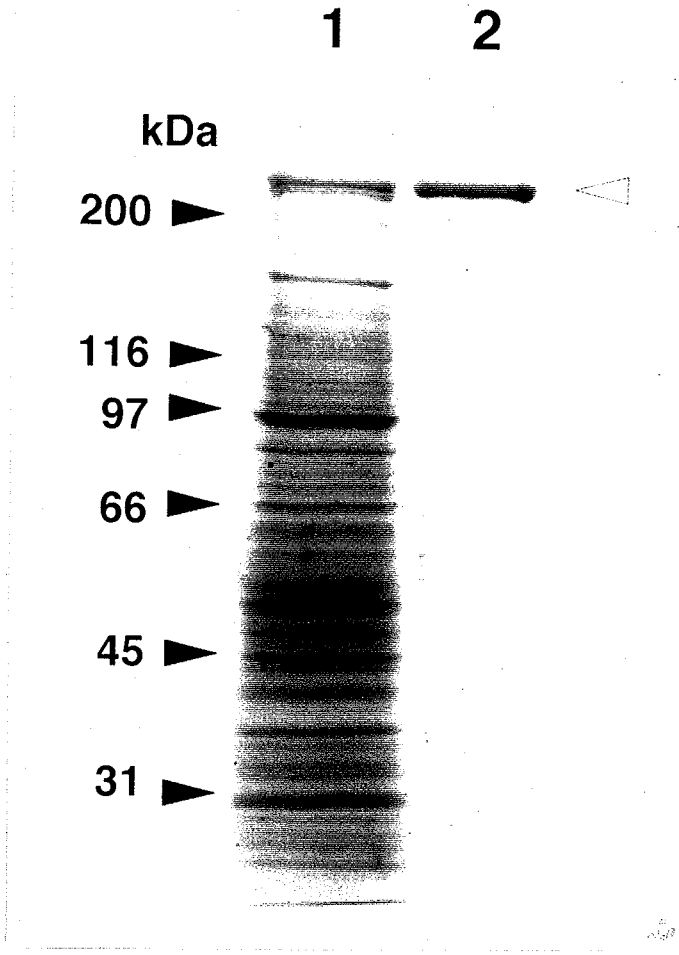

Figure 2-2. SDS-PAGE analysis of the purified IP_3R1.

Electrophoresis was carried out on a 5-12.5% gradient polyacrylamide gel. The gel was stained with Coomassie Brilliant Blue R-250. The positions of molecular weight markers (in kDa) are shown on the left. The open arrow indicates the position of IP_3R. *Lane* 1; the solubilized cerebellar membrane fraction with 1% of CHAPS. *Lanes* 2; the immunopurified IP_3R1.

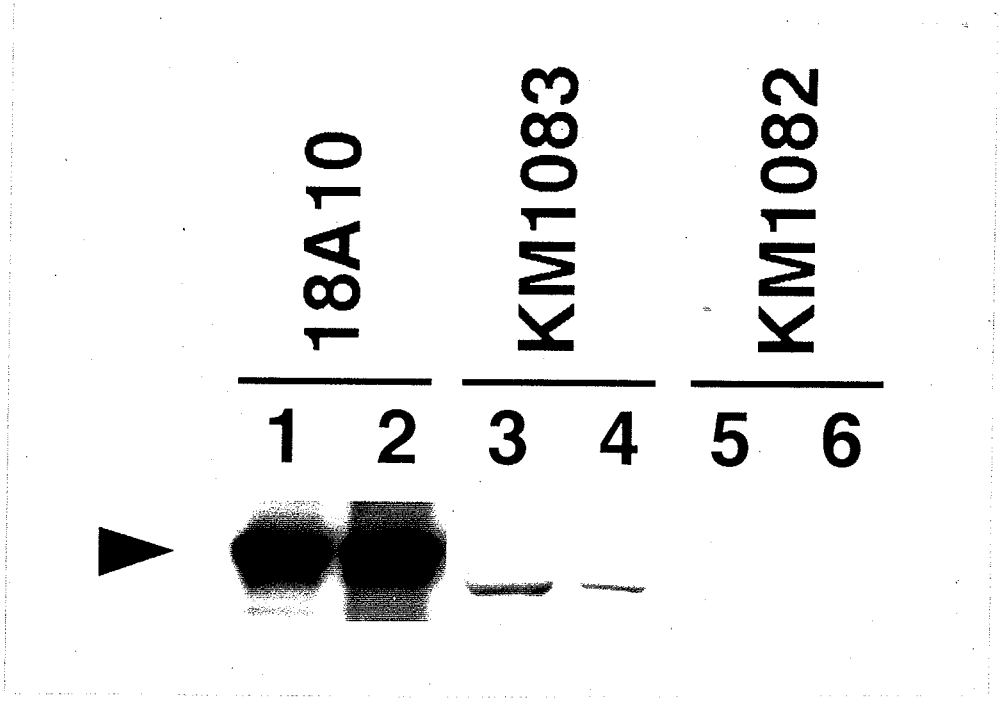

Figure 2-3. Immunoblots of the purified IP_3R1.

The purified IP_3R1 was analyzed by Western blotting to investigate its homogeneity. The same amounts of [^3H] IP_3 binding activity of cerebellar microsomal fraction and the purified IP_3R1 (1.5 pmol of IP_3R/ lane) were applied to the gel, followed by immunoblotting with monoclonal antibodies 18A10, KM1083 and KM1082 against IP_3R1, IP_3R2 and IP_3R3, respectively. *Lanes* 1, 3 and 5; the solubilized cerebellar membrane fraction with 1% of CHAPS. *Lanes* 2, 4 and 6; the immunopurified IP_3R1.

CHAPTER III

KINETICS OF Ca^{2+} RELEASE BY THE PURIFIED INOSITOL 1,4,5-TRISPHOSPHATE RECEPTOR TYPE 1

III - 1 Introduction

The development of the putch clamp techniques have enabled us to investigate functional (electrophysiological) properties of many channel proteins located on the plasma membrane. However, as IP_3R locates on intracellular Ca^{2+} stores such as endoplasmic reticulum, it makes the analysis of channel functions difficult. Because of the difficulties of analysis of channel activity of IP_3R using electrophysiological techniques except the lipid bilayer techniques, most studies have used the fluorescent Ca^{2+} indicators such as fura-2 and fluo-3. In deed, there have been many studies on the kinetics of IP_3-induced Ca^{2+} release (IICR); they describe the channel opening mechanism of the IP_3R [90 - 94], the regulation of IICR by modulators such as PKA [46, 74, 75], ATP [45, 76], GTP [95, 96] and Ca^{2+} [92, 97 - 102], and the "quantal release" originally described by Muallem *et al.* [103], where sub-maximal concentrations of IP_3 cause the partial release of Ca^{2+} from intracellular stores. They have often used permeabilized cells and microsomal preparations containing other proteins which might effect IP_3R activity, such as Ca^{2+} pumps and Ca^{2+} binding proteins, resulting in discrepancies among reports. In these studies, the arguments on some critical points of IICR have often been complicated due to the different experimental systems used, i.e., different micro-environments surrounding the IP_3R and Ca^{2+} pools assayed (e.g., different constitution of PLC, IP_3-metabolizing enzymes, Ca^{2+}-binding proteins, Ca^{2+}-pumps, modulators in each cell type and heterogeneity of IP_3R types).

Although the kinetics of IICR is fundamental to an appreciation of the dynamic intracellular signal transduction mechanisms, many studies of the kinetics of IICR in the crude systems also have led to different results. For example, the degree of the cooperativity of Ca^{2+} release, which is an important issue for understanding the channel opening mechanism, differed among the reports. Some reports show no cooperativity of IICR [92, 104], others show positive cooperativity [90, 91, 93]. Therefore, an investigation of IICR by a "purified single type" of IP_3R may allow us to reveal the fundamental properties of IICR. In this study, a single type of IP_3R (IP_3R type 1: IP_3R1) have been isolated by using immunoaffinity chromatography [75] (Chapter II) and have been reconstituted into lipid vesicles to investigate the kinetics of IICR

using the fluorescent Ca^{2+} indicator fluo-3. This study provides the first report of the kinetics of Ca^{2+} release by a single IP_3R type. In the following section, I describe a novel method for the analysis of the channel protein and also discuss the fundamental properties of the purified IP_3R1 [146, 157].

III - 2 Experimental Procedures

III - 2 - 1) Materials

The following reagents were purchased: IP_3, CHAPS and fluo-3 from Dojindo Laboratories (Kumamoto, Japan), Chelex-100 from Bio-Rad, diethylenetriaminepentaacetic acid (DTPA)-conjugated polymetal-sponge and Ca^{2+} calibration kit from Molecular Probes, phosphatidylcholine, phosphatidylserine and cholesterol from Avanti Polar-Lipids, INC. All of other reagents were of analytical grade or the highest grade available.

III - 2 - 2) Removal of Ca^{2+} contamination

Removal of Ca^{2+} contamination is necessary to measure the calcium release and to improve the sensitivity of the fluorometric measurements. We removed the Ca^{2+} contamination according to the method of Meyer *et al.* [91, 146]. Briefly, all solutions used in fluorometric measurements were passed over a polymetal-sponge and all labwares were successively washed with detergent, 0.1 N HCl, distilled water and the buffer to be used. Ca^{2+} contamination in all solutions, cuvettes and stir bars were checked using the Ca^{2+} indicator fluo-3 before the measurements. IP_3 stock solution was also passed over the polymetal-sponge to remove Ca^{2+}. Passing IP_3 stock solution over the polymetal-sponge did not cause any changes in IP_3 concentrations which was checked using IP_3 [^{3}H] radio receptor assay kit (Du Pont NEN).

III - 2 - 3) Purification of IP_3R1

IP_3R1 was purified type-specifically from mouse cerebellar microsomal fraction by using an immunoaffinity column conjugated with an anti-pep 6 antibody, a polyclonal antibody against IP_3R1 C-terminus, as reported in Chapter II

III - 2 - 4) Reconstitution of the purified IP_3R1

Phosphatidylcholine, phosphatidylserine and cholesterol dissolved in chloroform were mixed to give a concentration of 3, 1 and 0.8 mg/ml, respectively. The lipid mixture was dried to a thin film under a stream of nitrogen gas and then under vacuum. The lipid film was suspended at 2 mg/ml in buffer A (100 mM KCl, 1 mM 2-mercaptoethanol, 10 mM HEPES-KOH [pH 7.4] and 4 mM $CaCl_2$) containing 1 % CHAPS. The immunoaffinity purified IP_3R1 was concentrated by using Centriprep 100 (Amicon) to give a protein concentration of 100 μg/ml. The concentrated IP_3R1 solution was mixed with buffer A containing lipids and detergent to give final IP_3R1, lipids and CHAPS of 50 μg/ml, 0.5 mg/ml and 1%, respectively. After 20 min. incubation on ice with occasional gentle stirring, the IP_3R1-lipid mixtures were dialyzed for 72 hours against 8 changes of a 500-fold volume excess of buffer A at 4 °C. The resulting proteoliposomes (IP_3R1 in lipid vesicles) were pelleted by centrifugation at 100,000 x g for 30 min. at 2 °C, and were washed with buffer B(buffer A without Ca^{2+} + 10 or 1 μM fluo-3) twice, and were resuspended with buffer B in the same volume used before dialysis. After incubation for 10 min. at 25 °C, the resuspended proteoliposomes were passed over Chelex-100 to remove Ca^{2+}, and were used for IP_3-induced Ca^{2+} release (IICR) assay [146, 150, 157].

III - 2 - 5) Measurements of IP_3-induced Ca^{2+} release by the purified IP_3R1

Ca^{2+} efflux from the proteoliposomes was measured by monitoring the fluorescence changes of fluo-3. Fluorometric measurements of IICR were performed by using an F-2000 fluorometer (Hitachi, INC.) interfaced to a PC9801-VX computer (NEC, INC.). The excitation and emission wavelength were 500 and 525 nm, respectively, with 10 nm bandpass. Fluorescence signals were corrected for fluctuations in excitation light intensity. Measurements were made at 25 °C in a 0.5 x 0.5 cm quartz cuvette containing 0.4 ml of the proteoliposome solution with continuous-stirring by a Teflon stir bar. IICR was monitored after addition of 2 μl IP_3 to give the desired IP_3 concentration. The data was acquired every 200 ms. To exclude the possibility of Ca^{2+} regulation of IICR, we used 10 μM fluo-3, whose concentration was high enough to buffer the released Ca^{2+} and to keep deviations of extravesicular free Ca^{2+}

concentration within 10 to 30 nM. We also examined IICR using 1 μM fluo-3, where the deviations of free Ca^{2+} concentration were 150 - 300 nM, to compare the effects of changes in free Ca^{2+} concentration on IICR [146, 150].

III - 2 - 6) Calibration of Ca^{2+} concentration vs. fluorescence intensity

The fluorescent intensities of fluo-3 were calibrated to free Ca^{2+} concentrations using Ca^{2+}-calibration kit with modification of pH to 7.4 (Molecular Probes). The calibration curve (Figure 3-3, 10 μM fluo-3) gave the apparent dissociation constant of fluo-3 for Ca^{2+} of 170 nM.

III - 3 Results

III - 3 - 1) Reconstitution of the purified IP_3R1

The immunoaffinity purified IP_3R1 was reconstituted into lipid vesicles by the dialysis method (Figure 3-1) described previously [75]. The liposomes were observed using electron microscopy. The average diameter of the liposome was 170 ± 50 nm (n = 300) and the distribution of the size was represented in single peak (Figure 3-2). IP_3-induced Ca^{2+} release (IICR) from the proteoliposomes was monitored as fluorescence changes of fluo-3, whose values were used to calculate total Ca^{2+} concentrations outside the proteoliposomes. The profiles of IICR were highly reproducible. Free Ca^{2+} concentrations prior to addition of IP_3 were approximately 100 and 200 nM using 10 μM and 1 μM of fluo-3, respectively, throughout the experiments. Following the addition of maximal concentrations of IP_3, 10 μM of Ca^{2+} ionophore Br-A23187 was added to estimate the fraction of liposomes with the purified IP_3R1. About 6 % of the total released Ca^{2+} by Br-A23187 responded to IP_3, indicating approximately 6 % of the liposome were reconstituted with the purified IP_3R1.

III - 3- 2) Time course of IP_3-induced Ca^{2+} release by the purified IP_3R1

Figure 3-4 shows a typical profile of IICR by the immunoaffinity-purified IP_3R1 reconstituted into lipid vesicles. Five hundred nanomolar IP_3 induced Ca^{2+} release from the liposomes followed a constant leakage of Ca^{2+} (Figure 3-4A), which was linear over the time range of the experiments. The rate of leak from the liposomes was calculated to be about 1.5 nM/sec. The net IICR (Figure 3-4B) was obtained by extrapolating and subtracting the constant Ca^{2+} leakage (Figure 3-4, *the solid line*) from the profile. The net IICR could not be fitted by a single exponential but was found to be a biexponential (Eq. 1) (Figure 3-4C, *the solid line*) with the fast and slow rate constants (k_{fast} = 0.51 ± 0.01 sec^{-1} (71 ± 1 %), k_{slow} = 0.042 ± 0.001 sec^{-1} (29 ± 1 %)), indicating that the purified IP_3R1 has two states for IICR.

$$\Delta[Ca^{2+}]_{total} = T\,(1 - A_{fast}\cdot e^{-kfast\cdot t} - A_{slow}\cdot e^{-kslow\cdot t}) \qquad \text{(Eq. 1)}$$

where T represents a total amount of released Ca^{2+}, A is amplitude of the fast and slow components (%) ($A_{fast} + A_{slow} = 100$ %), k is rate constant (sec^{-1}) and t is time (sec).

III - 3- 3) Kinetic analysis of IP_3-induced Ca^{2+} release by the purified IP_3R1

III - 3 - 3. 1) Quantal Ca^{2+} release by the purified IP_3R1

Different concentrations of IP_3 were added to obtain dose-response curves. Figure 3-5 shows typical time courses of IICR observed using the same batch of proteoliposomes. Submaximal concentrations of IP_3 caused partial Ca^{2+} releases, and rates of Ca^{2+} release were dependent on the IP_3 concentration. Each profile of IICR consisted of the sum of two single exponentials as described in Figure 3-4C and Figure 3-8.

Relative amounts of released Ca^{2+} at various concentration of IP_3 are shown in Figure 6A (n = 3 - 4) and 6B (n = 2 - 5). The amount of released Ca^{2+} increased as a function of IP_3 concentration, indicating that the single type of the purified IP_3R1 is capable of producing the quantal response of Ca^{2+} release.

III - 3 - 3. 2) Cooperativity of IP_3-induced Ca^{2+} release

The initial rates of Ca^{2+} release varied with IP_3 concentrations and saturated above 1 μM IP_3 at both fluo-3 concentrations of 10 μM(Figure 3-7A, n = 3 - 4; deviations of $[Ca^{2+}]_{free}$ = 10 - 30 nM) and 1 μM (Figure 3-7B, n = 2 - 5; deviations of $[Ca^{2+}]_{free}$ = 150 - 300 nM). Both half-maximal initial rates of IICR in the presence of 10 μM and 1 μM fluo-3 occurred at 100 nM. We determined the degree of cooperativity of IICR by Hill plotting (Figure 3-7C, n = 3 - 4 and 5D, n = 2 - 5). The slopes in the Hill plot over the range of submaximal concentrations of IP_3 (20 - 200 nM) were calculated to be 1.8 ± 0.1 (Figure 3-7C and 7D), indicating that the IICR of the purified IP_3R1 exhibited positive cooperativity. As the EC_{50} value and the Hill coefficient of IICR at both concentrations of fluo-3 were calculated to be the same, the changes of free Ca^{2+} concentration by the released Ca^{2+} had no significant effect on the sensitivity for IP_3 and the cooperativity of IP_3R1-mediated IICR.

III - 3 - 3. 3) Analysis of biphasic nature of IP_3-induced Ca^{2+} release and

quantal Ca^{2+} release

To analyze the kinetic features of IICR in detail, we attempted to curve fit the profiles of IICR. As mentioned above, the profile of IICR could not be fitted by a single exponential but could be fitted to a biexponential with the fast and slow rate constants (Eq. 1) at both concentrations of fluo-3. The rate constants of the fast and slow components differed by a factor of about 10 (Figure 3-8A, n = 3 - 4 and 8B, n = 2 - 5). Both the fast and slow rate constants were influenced by the concentration of IP_3. The amplitudes of both states (A_{fast} and A_{slow}) were plotted as a function of the concentrations of IP_3 (Figure 3-8C, n = 3 - 4 and 8D, n = 2 - 5). A_{fast} increased as the concentration of IP_3 increased, whereas A_{slow} decreased. Considering these amplitudes with the amount of total released Ca^{2+} (Figure 3-6), the amounts of released Ca^{2+} by the fast and slow phases were then calculated. The amounts of released Ca^{2+} by the fast and slow components relative to the total released Ca^{2+} at 5 μM IP_3 were plotted as a function of the concentrations of IP_3 (Figure 3-9A, n = 3 - 4 and 9B, n = 2 - 5). The amount of released Ca^{2+} by the fast component increased as a function of the concentration of IP_3, whereas the amount by the slow component remained almost constant over the range of 10 - 5000 nM IP_3 at both concentrations of fluo-3. This result revealed that the fast phase of IICR, with the time constants of 0.3 - 0.7 sec^{-1}, was mainly responsible for the quantal Ca^{2+} release.

III - 4 Discussion

III - 4 - 1) Measurements of IP_3-induced Ca^{2+} release by the purified single type of IP_3R1

In order to understand the mechanisms of IP_3R channel gating and quantal Ca^{2+} release, it is essential that we study the kinetics of IICR. Although many studies of the kinetics of IICR were reported to reveal the mechanisms of channel opening, quantal Ca^{2+} release and the regulation by the modulators of IP_3R, the results differ from paper to paper. In these studies, permeabilized cells and microsomal preparations derived from different sources were often used, perhaps explaining the different results obtained. Thus, previous reports characterizing the properties of IICR have been complicated by the following factors;

(i) composition of subtypes of IP_3Rs; the presence of multiple IP_3R types in single cells possibly affects the kinetics of IICR, which has always been argued in many previous reports.

(ii) metabolism of IP_3; IP_3 could be easily metabolized by specific kinases and phosphatases which may be probably present in crude systems. The concentration of ligand during experiments is known to be one of the critical factors for IICR, since most IICR properties (multiple affinity sites on single IP_3Rs, quantal release by submaximal doses, inactivation by IP_3 itself) are dependent on IP_3 doses.

(iii) Ca^{2+} pump; the activity of the ATP-driven Ca^{2+} pump affects IICR by refilling Ca^{2+} stores following Ca^{2+} release. This prevents us from evaluating the cooperativity of IICR by reducing the net IICR to a great extent at low concentration of IP_3 than at high concentration [90].

(iv) molecules sensing changes in Ca^{2+} concentration; dynamic changes in cytosolic and luminal Ca^{2+} concentrations have been argued to be involved in functional regulation of IICR properties by modifying the function of the IP_3R itself and by activating IP_3R-modulator proteins (e.g., protein kinases [e.g., Ca^{2+}-calmodulin dependent protein kinase

and protein kinase C] and phosphatases [e.g., calcineurin] and Ca^{2+} binding proteins [e.g., calmedin] and IP_3-metabolizing enzymes [e.g., IP_3 kinase]).

(v) heterogeneity in IICR-Ca^{2+} pools; there is a subcellular heterogeneity in IP_3 sensitive Ca^{2+} stores, e.g., subsurface cisternae, calciosomes, nuclear membranes, etc. which may have different IICR properties. Artificial effects on IP_3-sensitive Ca^{2+} stores by experimental conditions must be considered, e.g., fusion of cisternae membranes by excess treatment with saponin [151] and induction of formation of cisternal stacks mediated by IP_3Rs by no-physiological treatment [152].

In this study, we have investigated the kinetics of IICR of a single member of the IP_3R family in artificial membrane vesicles, therefore excluding the possibility of modulation of IICR by factors other than Ca^{2+} and IP_3 itself. Due to the absence of IP_3 metabolizing enzymes, in our system, applied IP_3 doses should be constant throughout each experiment. However, we must consider the regulation of the IP_3R by changes in free Ca^{2+} concentration. Feedback regulations of IICR by the released Ca^{2+} have been observed in permeabilized cells [97, 98] and microsomal systems [92, 104]. On the other hand, the high concentrations of Ca^{2+} chelators and Ca^{2+} indicators caused artificial effects on IICR in those experiments [100, 153] In this study, to avoid problems concerning the regulation of IICR by the released Ca^{2+}, we used high enough concentration of fluo-3 to keep extravesicular free Ca^{2+} concentration within 100 - 130 nM. We also used 1 μM of fluo-3, 200 - 500 nM free Ca^{2+} concentration, to compare the effect of changes of extravesicular free Ca^{2+} by IICR on the kinetics of Ca^{2+} release. At both fluo-3 concentrations, where the extravesicular free Ca^{2+} concentration changed from 100 to 130 nM(10 μM of fluo-3) and from 200 to 500 nM (1 μM of fluo-3), the kinetics of the Ca^{2+} release was essentially the same, indicating little feedback regulation by the released Ca^{2+} in our system. We also observed similar kinetics of Ca^{2+} release at the initial extravesicular free Ca^{2+} concentration of 300 nM (data not shown), where Ca^{2+} release using cerebellar microsomes was shown to be inhibited [117]. Feedback regulation by the released Ca^{2+} or the regulation by

Ca^{2+} outside of pools may be mediated by the action(s) of other molecules which can sense changes of Ca^{2+} concentration.

III - 4 - 2) Fundamental properties of IP_3-induced Ca^{2+} release by the purified IP_3R1

The extent of cooperativity of Ca^{2+} release is an important and fundamental issue for understanding the channel opening mechanism. In previous reports, there are controversies, where some reports show no cooperativity of IICR [92, 104], others show positive cooperativity [90, 91, 93]. The Hill plot of the initial rates of Ca^{2+} release by the purified IP_3R1(Fig. 4B) shows evidence of a positive cooperativity ($n_H = 1.8 \pm 0.1$) of IICR at submaximal concentration of IP_3, indicating that at least two molecules of IP_3 are needed for channel opening and that positive cooperativity of IICR can be mediated by a single type of IP_3R.

The dose response curve of IICR shows that the amounts of released Ca^{2+} increased as a function of IP_3 concentrations (Fig. 3), revealing that the immunopurified single type of IP_3R (IP_3R1) shows the quantal response of Ca^{2+} release. Ferris *et al.* have also reported that conventionally purified and reconstituted IP_3R (they did not distinguish which types of IP_3Rs they investigated) showed quantal response [116]. In Ferris's study, they observed quantal Ca^{2+} entry into lipid vesicles reconstituted with the conventionally purified IP_3R. They suggested that the heterogeneity of IP_3R types was a possible mechanism underlying the phenomenon of the quantal release. Our results indicate that the heterogeneity due to the different types of the receptor is not responsible for quantal Ca^{2+} release and quantal Ca^{2+} release is an intrinsic property of IP_3R1.

III - 4 - 3) Detailed kinetic analysis of Ca^{2+} release

The profiles of IICR did not obey a single exponential but were found to be biexponential with the fast and slow rate constants, indicating that Ca^{2+} release occurred from two states of the IP_3R. The rate constants of the fast and slow components were 0.3 - 0.7 sec^{-1} and 0.03 -

0.07 sec^{-1}, respectively. We also analyzed the contribution of the fast and slow components to the total amounts of released Ca^{2+}. The amounts of released Ca^{2+} by the fast and slow components (Fig. 6) were easily estimated as described in Eq. 1. The amounts of released Ca^{2+} by the fast component increased as a function of the concentration of IP_3, whereas the amounts of Ca^{2+} released by the slow component were constant, i.e., already saturated at low concentration of IP_3. These results suggest that the fast component is kinetically the state of low affinity for IP_3 and high permeability of Ca^{2+} (active state) and the slow component is of high affinity and low permeability (inactive state). Consistent with this view, the studies of IP_3 binding in the permeabilized hepatocytes and a liver plasma membrane-enriched fraction displayed the existence of two states with the high and low affinity for IP_3 [107, 154]. Since the fast phase of Ca^{2+} release increases with increasing IP_3 concentrations and slow phase remains constant, it is the fast phase that determines the amount of Ca^{2+} release i.e., the fast component is responsible for the quantal Ca^{2+} release.

Two main cases could be considered for the two states of IICR. First, the two or more variants of the receptor exist in a single type of the receptor due to alternative splicing or secondly, the two different states of a single receptor exist due to an inactivation or an interconversion of the receptor.

One explanation for the former is that the two states may be caused by the alternative splicing included in the region of the IP_3 recognition site (SI) [50, 55]. In this case, the alternative splicing of SI region would influence the IP_3-binding affinity to produce the high and low affinity states. Recently, the alternative splicing of the SI region showed, however, no significant differences of the IP_3 binding affinity [86]. Alternatively, the heterogeneity of the receptors may be involved in the coupling between the IP_3 binding and the channel opening due to the alternative splicing of the modulatory (coupling) domain (SII) [55, 72]. Although such heterogeneity may cause the kinetically different components of IICR, there are too many splicing variants (four patterns) to explain the two phases. Considering the tetramer formation (an IP_3R channel unit) among these splicing variants, the effects of the splicing on IICR would

be more complicated. These possibilities could be investigated by using expressed IP_3R from its cDNA.

For the latter, an attractive explanation for the two states, which reflects the existence of two states in a single receptor, is based on the inactivation of the receptor [134] or the interconversion of the receptor mediated by Ca^{2+} [107]. The two phases of IICR could be the consequence of inactivation of the IP_3R by the ligand binding followed by the conversion from an active state (low affinity for IP_3 and high permeability of Ca^{2+}) into an inactive state (high affinity and low permeability). Indeed, the kinetic analysis revealed that the rate constants for the slow phase is the same as that for inactive state [134]. The interconversion between the low and high affinity for IP_3 mediated by cytosolic Ca^{2+} [107] could also be responsible for the two phases. In this case, two states may be already equilibrated before an application of IP_3 and the equilibration may be affected by cytosolic Ca^{2+}. Alternatively, the IP_3R may exist in the active state and the IICR may cause the interconversion from the active state into the inactive state followed by the changes in cytosolic Ca^{2+} concentration, i.e., by the released Ca^{2+}. To investigate whether the changes in cytosolic Ca^{2+} concentrations are responsible for the biphasic kinetics of IICR or not, the time courses of IICR by the purified IP_3R1 were measured under fluo-3 concentration of 10 μM, which could strongly buffer the released Ca^{2+} and keep the deviations of free Ca^{2+} concentration within 20 nM. The profiles of IICR by the purified IP_3R1 were also obeyed by the biexponential (data not shown), indicating that the changes in cytosolic free Ca^{2+} concentration may not be responsible for the biphasic kinetics of IICR. However, we can not ruled out the possibilities that the released Ca^{2+} causes rapid and local rises in Ca^{2+} concentrations near the channel pore, which can not be buffered by fluo-3, and mediate the interconversion of the receptor. Indeed, the interconversion of IP_3R reported by Pietri *et al.* [107] occurred by large changes in Ca^{2+} concentrations. If the released Ca^{2+} rapidly rises near the channel pore and mediate the interconversion in cooperation with IP_3, the inactivation of the receptor reported by Hajnoczky *et al.* [134] may reflect an interconversion of the IP_3R. This hypothesis could be supported by the observations in Fig. 3 of ref. [134], where

the degree of inactivation (interconversion) varied with the cytosolic free Ca^{2+} concentrations during the preincubation with IP_3 and IP_3R, whereas no significant change in IICR at various cytosolic free Ca^{2+} concentrations were observed without preincubation. The phenomenon of interconversion between the two states of the receptor could also be responsible for the Ca^{2+} feedback regulation of IICR [92, 97, 98], if the released Ca^{2+} causes rapid and local rises in Ca^{2+} concentrations near the channel pore and participates in the interconversion by cooperating with IP_3.

Recently, heterogeneity of IP_3R densities in pools, which had equal sensitivity to IP_3, was reported to be responsible for biphasic Ca^{2+} release [155]. If this is the reason for biphasic nature of IICR, the amplitudes of the fast and slow components in the curve fitting should be independent to the IP_3 concentrations, and the ratio of the amounts of released Ca^{2+} by the fast and slow components must be constant. However, in our experiments, the amplitudes of the fast and slow components, and the ratio of the total released Ca^{2+} were dependent on IP_3 concentrations, indicating that the biphasic nature of Ca^{2+} release was not due to such heterogeneity of receptor density. A possibility of heterogeneity in the size of individual Ca^{2+} pools was also excluded by the same reasons and by the direct observation using electron microscopy as described under the "Results". The present study has demonstrated that the purified IP_3R1 has two states with different affinity for IP_3, i.e., a low affinity and a high affinity state. This could arise from alternative splicing leading to the production of variants of IP_3R1 [55]. Alternatively, there may be two different states of a single IP_3R due to an IP_3-dependent inactivation or a Ca^{2+}-dependent interconversion.

Finally, the system reported here enables us to study kinetics of IICR by the "purified single" type of IP_3R. We demonstrated here the positive cooperativity of IICR and quantal Ca^{2+} release by a single type of IP_3R which had kinetically two states to release Ca^{2+}. Using this system, the purification and reconstitution of other types of IP_3Rs may reveal new insights into IICR as well as the effects of the modulators, such as PKA, ATP and Ca^{2+} etc. on IICR.

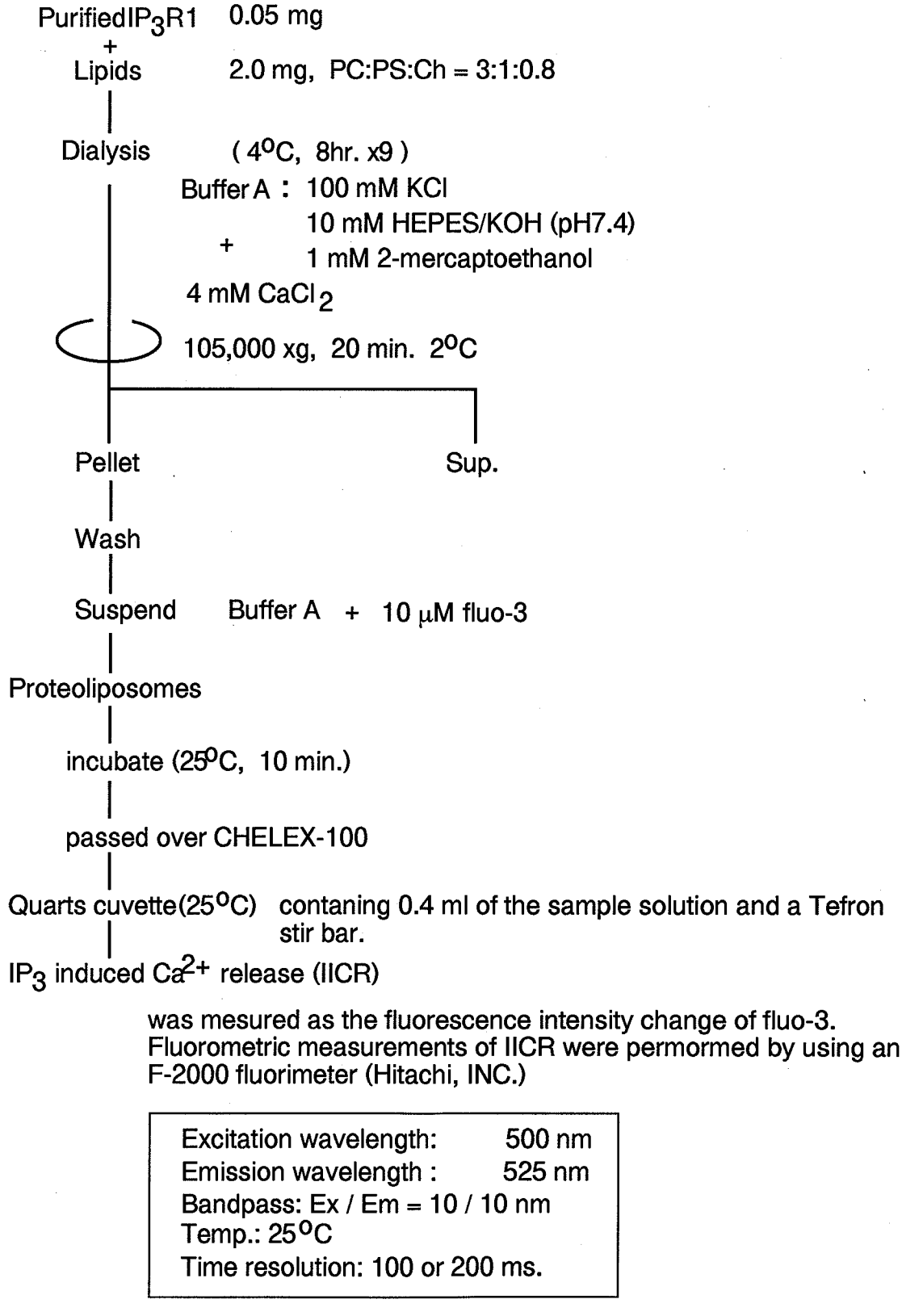

Figure 3-1. Scheme summarizing the reconstitution of the purified IP_3R1 and IICR assay.

A

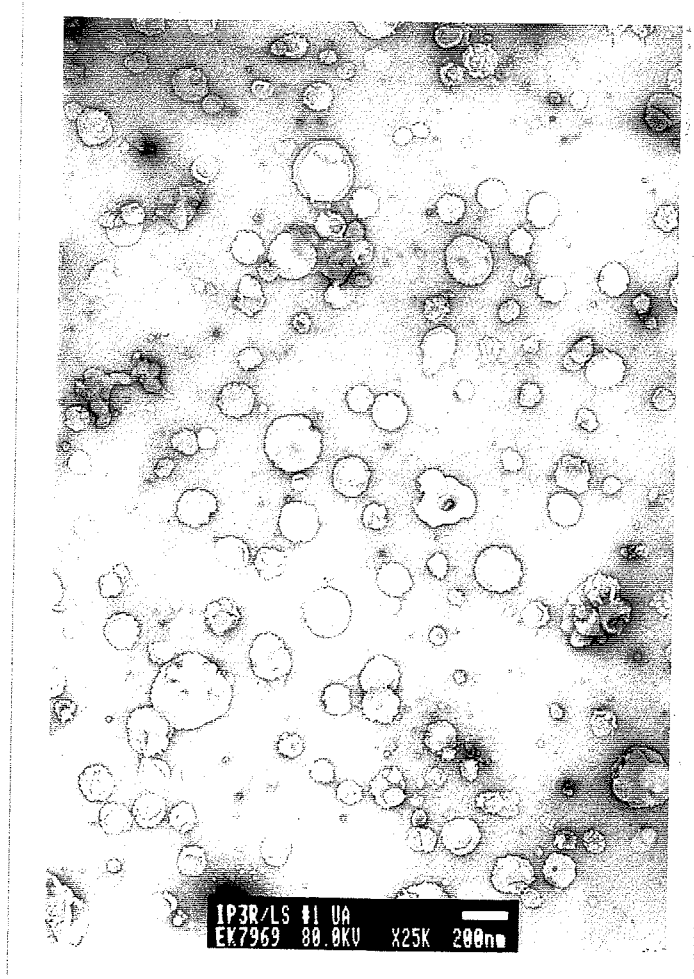

Figure 3-2A. Electron microscopic analysis of the proteoliposimes reconstituted with the purified IP_3R1.

A: The proteoliposomes reconstituted with the purified IP_3R1 were analyzed using the electron microscopy.

B

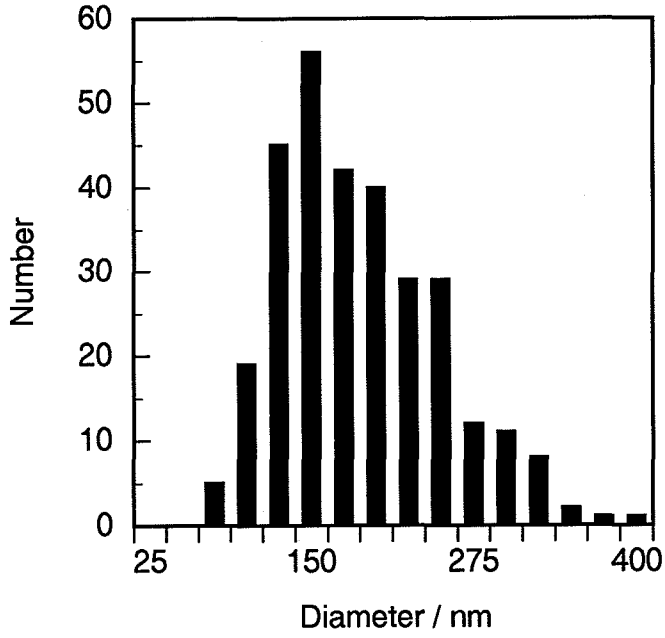

Figure 3-2B. Electron microscopic analysis of the proteoliposimes reconstituted with the purified IP_3R1.

B: The size distribution of the proteoliposomes. The average diameter of the liposome was 170 ± 50 nm (n = 300) and the distribution of the size was represented in single peak.

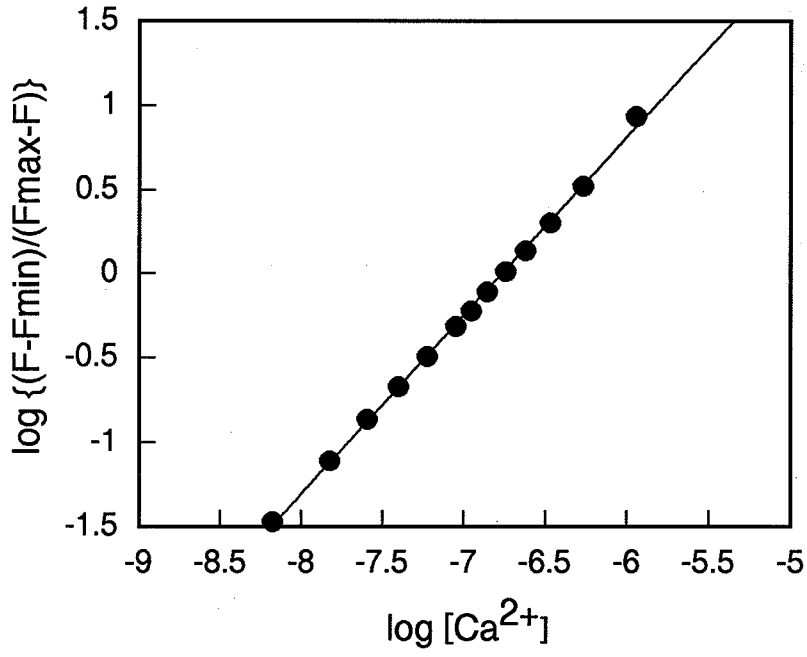

Figure 3-3. Calibration of Ca^{2+} concentration vs. fluorescence intensity.

The fluorescence intensities of 10 μM fluo-3 was calibrated against Ca^{2+} concentrations using Ca^{2+} calibration kit (Molecular Probes).

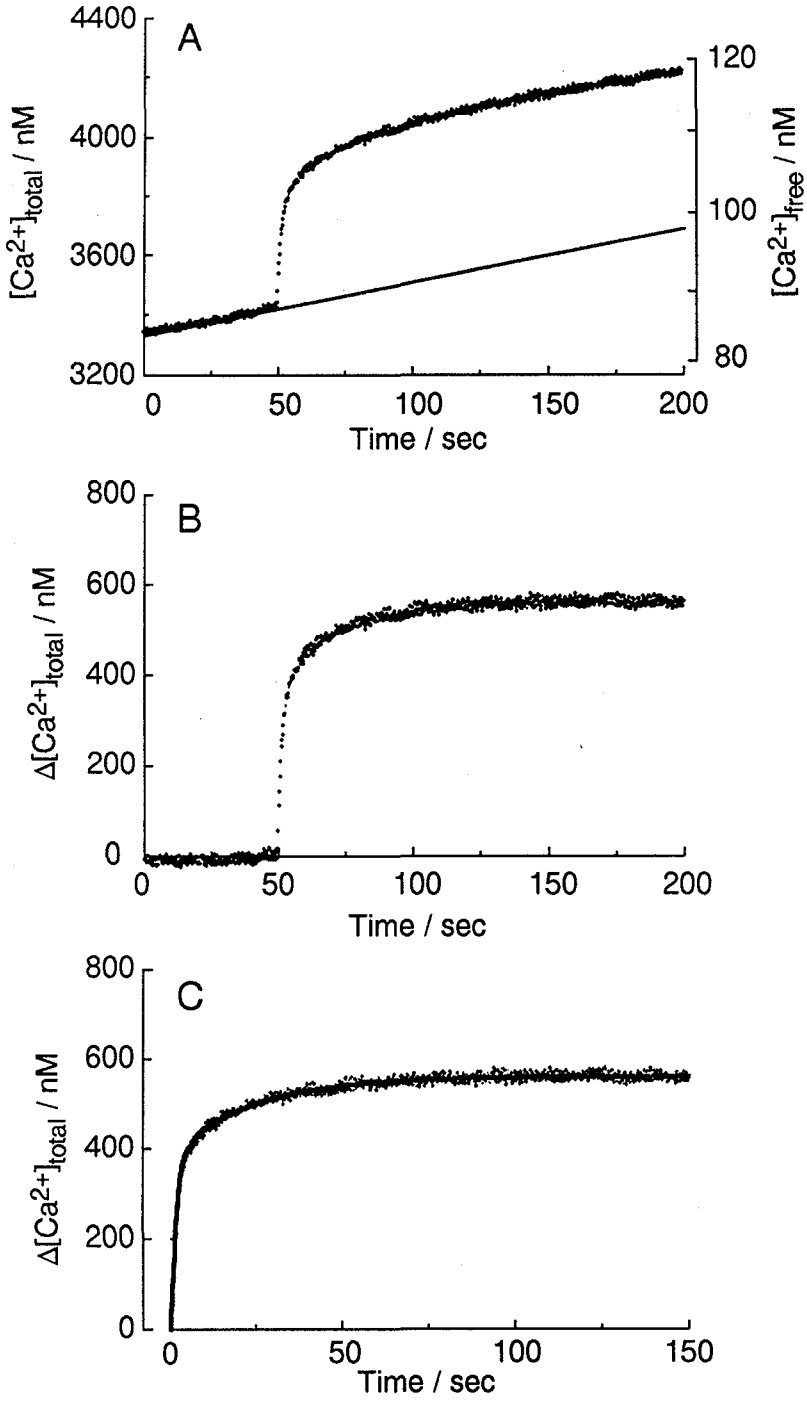

Figure 3-4. Typical profile of IP_3-induced Ca^{2+} release from proteoliposomes reconstituted with the purified IP_3R1.

Changes of fluorescence of the Ca^{2+} indicator fluo-3 ([fluo-3] = 10 μM) were recorded after injection of IP_3 (500 nM). The total Ca^{2+} concentration was estimated from the fluorescent intensity as described in the text. A, IP_3-induced Ca^{2+} release from the liposomes followed a constant leakage of Ca^{2+} (the *solid line*). B, The net IICR was obtained by extrapolating and subtracting the constant Ca^{2+} leakage from the profile. C, The net IICR was found to be well fitted by a biexponential (the *solid line*) with the fast and slow rate constants.

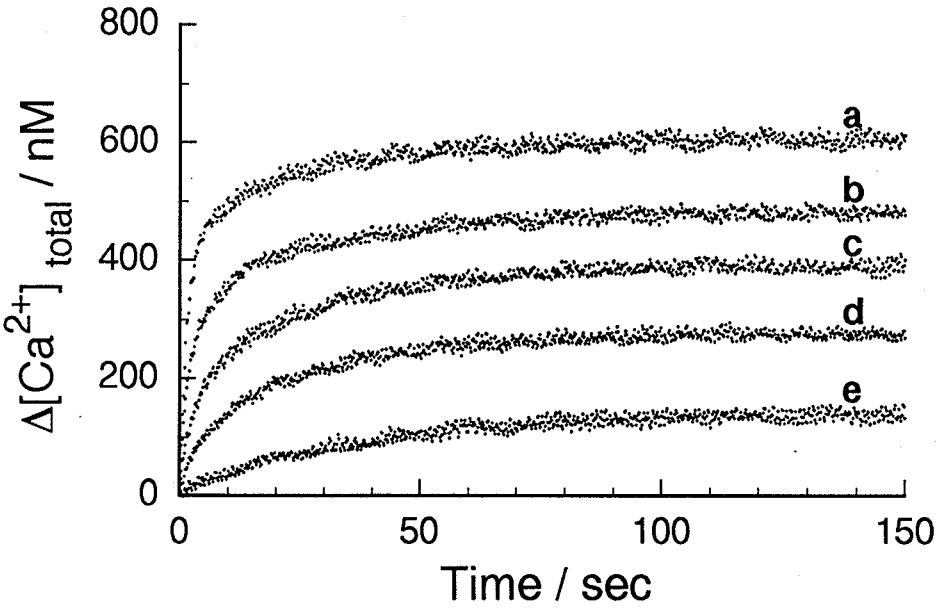

Figure 3-5. Time course of IP_3-induced Ca^{2+} release following the injection of different IP_3 concentrations.

IP_3-induced Ca^{2+} release at different concentrations of IP_3 were performed on a single batch of the proteoliposomes ([fluo-3] = 10 μM). 5 μM (a), 200 nM (b), 70 nM (c), 40 nM (d) and 20 nM (e) of IP_3.

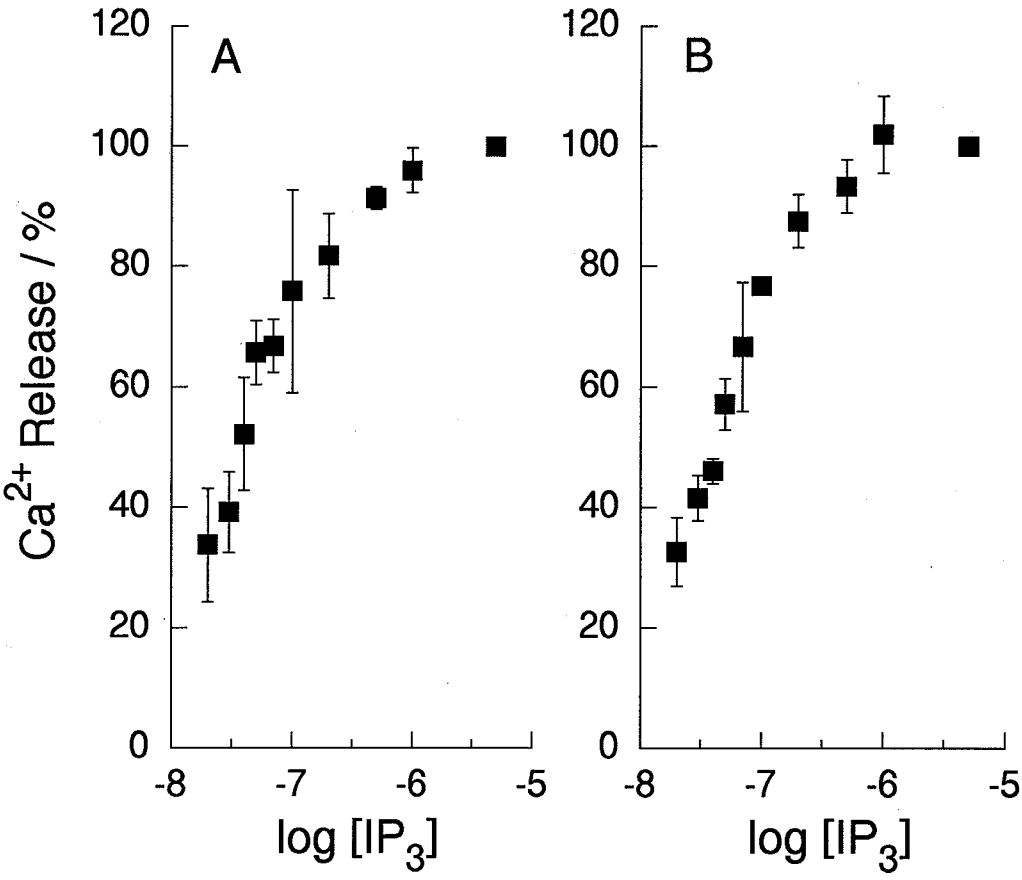

Figure 3-6. The amounts of released Ca^{2+} plotted as a function of IP_3 concentration.
The amounts of released Ca^{2+} were plotted as a function of IP_3 concentration. The data was normalized to the amplitude for 5.0 μM IP_3. A, 10 μM of fluo-3 (values are mean ± S. D., n=3 - 4, initial free Ca^{2+} concentration = 100 nM, deviations of free Ca^{2+} concentration by the released Ca^{2+} = 10 - 30 nM). B, 1 μM of fluo-3 (values are mean ± S. D., n=2 - 5, initial free Ca^{2+} concentration = 200 nM, deviations of free Ca^{2+} concentration by the released Ca^{2+} = 150 - 300 nM).

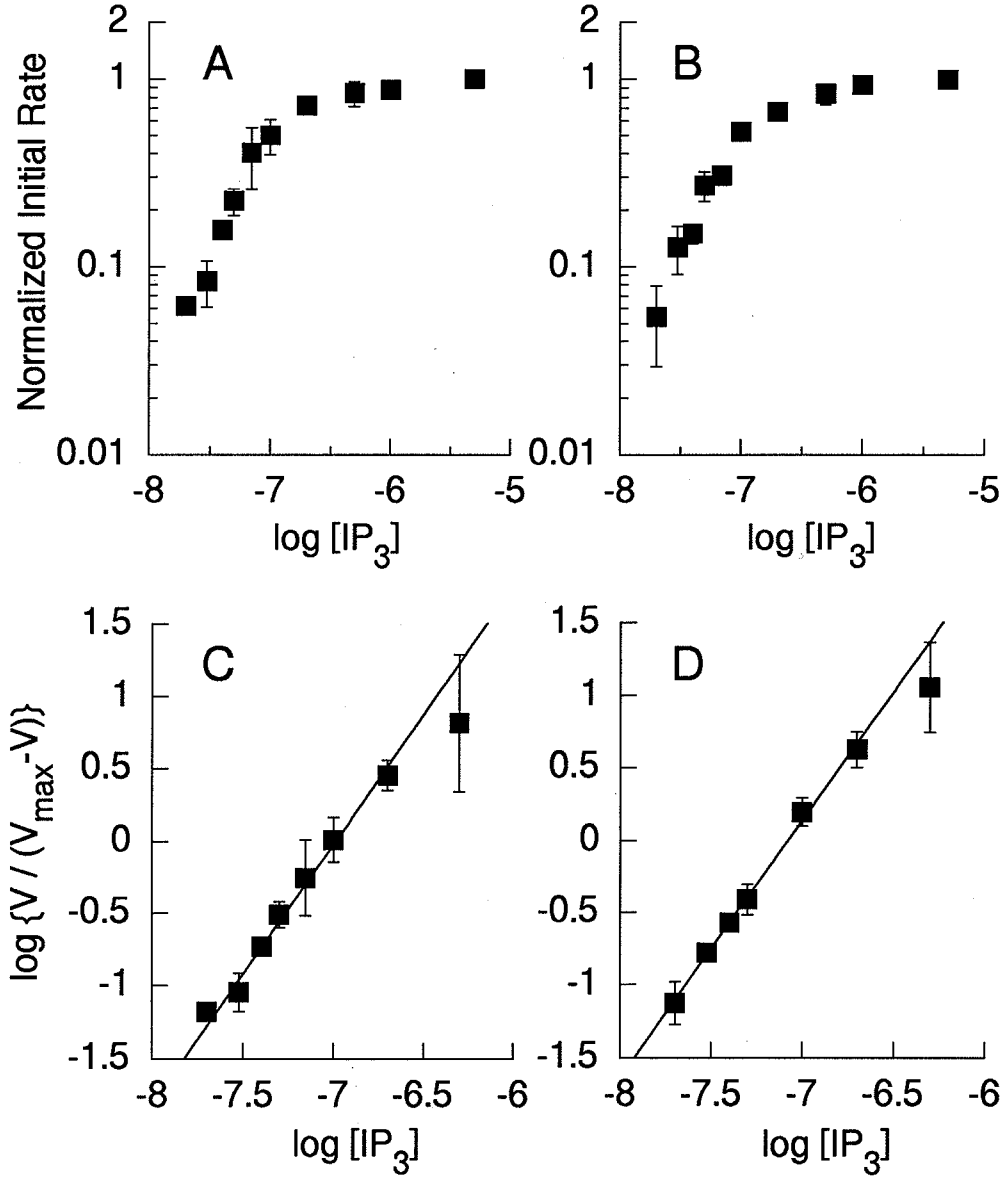

Figure 3-7. Analysis of IP_3-induced Ca^{2+} release.

Initial rates were measured from the initial and fast slope of IICR (values are mean ± S. D., n=2 - 5). A and B, Normalized initial rates of Ca^{2+} release were plotted as a function of the concentration of IP_3. C and D, Analysis of initial rates by a Hill plot shows the positively cooperativity of IICR. A and C were measured at 10 μM fluo-3 (values are mean ± S. D., n=3 - 4, initial free Ca^{2+} concentration = 100 nM, deviations of free Ca^{2+} concentration by the released Ca^{2+} = 10 - 30 nM), B and D at 1 μM fluo-3 (values are mean ± S. D., n=2 - 5, initial free Ca^{2+} concentration = 200 nM, deviations of free Ca^{2+} concentration by the released Ca^{2+} = 150 - 300 nM).

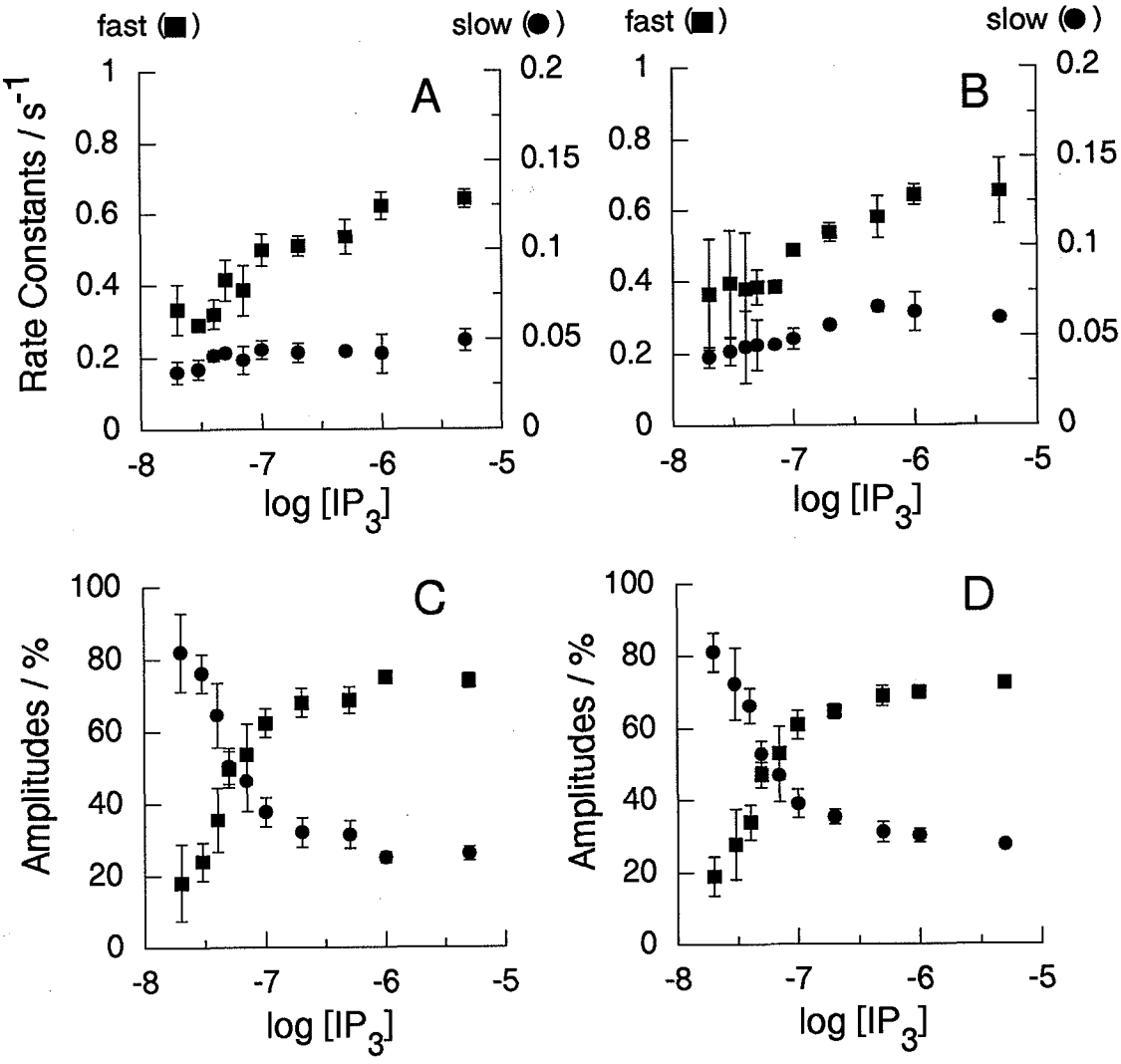

Figure 3-8. Biexponential analysis of IP_3-induced Ca^{2+} release: IP_3 dependence of the rate constants (A and B) and the amplitudes (C and D).

All profiles of IICR was found to be biexponential, with the fast and slow rate constants as described in Fig. 3-3 and the text (Eq. 1). A and B, the fast (squares) and slow (circles) rate constants and C and D, the amplitudes of the fast (squares) and slow (circles) were plotted as a function of the concentration of IP_3. A and C were measured at 10 μM fluo-3 (values are mean ± S. D., n=3 - 4, initial free Ca^{2+} concentration = 100 nM, deviations of free Ca^{2+} concentration by the released Ca^{2+} = 10 - 30 nM), B and D at 1 μM fluo-3 (values are mean ± S. D., n=2 - 5, initial free Ca^{2+} concentration = 200 nM, deviations of free Ca^{2+} concentration by the released Ca^{2+} = 150 - 300 nM).

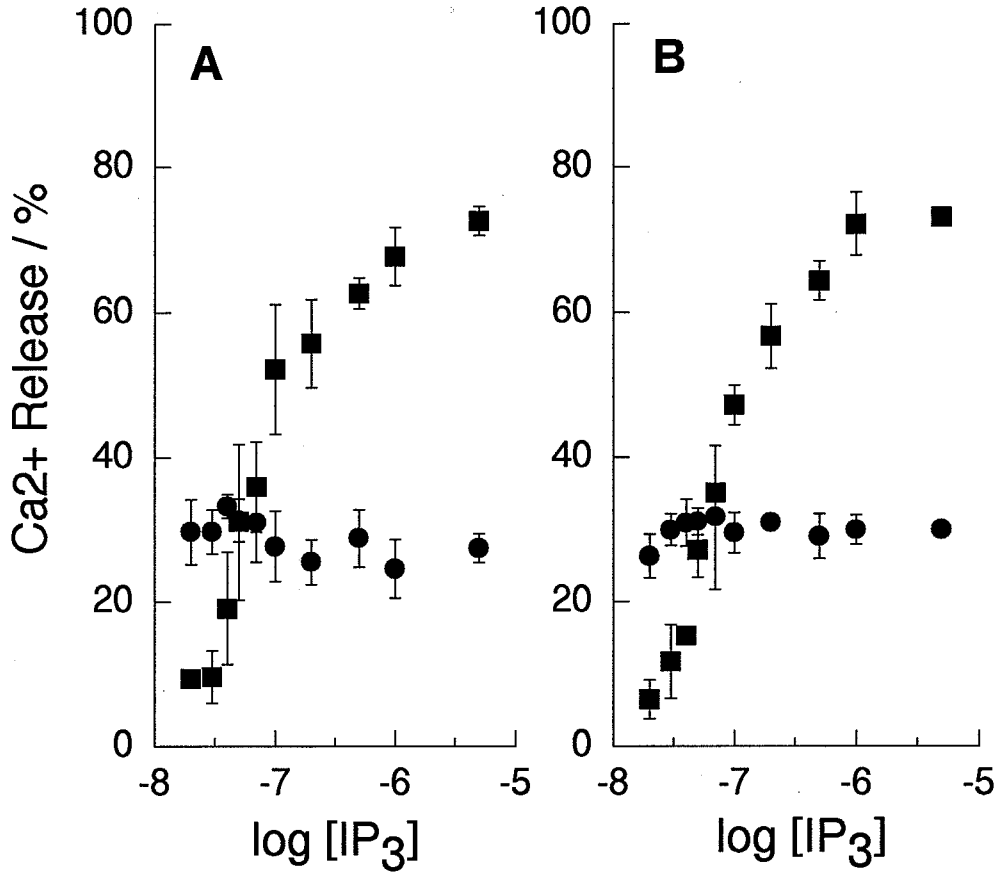

Figure 3-9. The amounts of released Ca^{2+} by the fast and slow components of IP_3-induced Ca^{2+} release.

The amounts of total released Ca^{2+} in Fig. 3-6 and the amplitude of the two components of IICR allowed us to calculate the amounts of released Ca^{2+} by the fast (squares) and slow (circles) components . A, 10 μM fluo-3 (values are mean ± S. D., n=3 - 4, initial free Ca^{2+} concentration = 100 nM, deviations of free Ca^{2+} concentration by the released Ca^{2+} = 10 - 30 nM). B, 1 μM fluo-3 (values are mean ± S. D., n=2 - 5, initial free Ca^{2+} concentration = 200 nM, deviations of free Ca^{2+} concentration by the released Ca^{2+} = 150 - 300 nM).

CHAPTER IV

ADENOPHOSTIN-MEDIATED QUANTAL Ca^{2+} RELEASE IN THE PURIFIED AND RECONSTITUTED INOSITOL 1,4,5-TRISPHOSPHATE RECEPTOR TYPE 1

IV - 1 Introduction

Inositol 1,4,5-trisphosphate (IP_3), a second messenger derived from the hydrolysis of phosphatidylinositol 4,5-bisphosphate, is responsible for Ca^{2+} release from intracellular calcium stores [2]. IP_3 receptor (IP_3R) is an IP_3-activated Ca^{2+} release channel and plays a crucial role in Ca^{2+} signaling in a variety of cell functions. Thus, kinetic studies of IP_3-induced Ca^{2+} release (IICR) are fundamental for elucidating the mechanisms underlying intracellular dynamics of Ca^{2+} signaling.

To understand the mechanisms and roles of IICR underlying intracellular Ca^{2+} signalling, development of specific agonists and antagonists with high affinity for IP_3R are needed. There are few pharmacological reagents available for analysis of IICR. No specific antagonist for IICR is known, but heparin inhibits IP_3 binding to the IP_3R in a non-specific manner. On the other hand, novel agonists, adenophostin A and B, have been isolated recently as fungal products [85]. Adenophostin is the most potent agonist, which has higher binding affinity and Ca^{2+} release activity than the native ligand, IP_3.

As described in Chapter III, I have established the novel system to investigate the kinetics of IP_3R type 1 (IP_3R1)-mediated IICR using the fluorescent Ca^{2+} indicator fluo-3, and reported that the IP_3R1-mediated IICR exhibited a positive cooperativity (n_H = 1.8), quantal Ca^{2+} release and biphasic nature [157]. In the following section, to define the properties of the new agonist adenophostin, the kinetics of Ca^{2+} release induced by adenophostin (adenophostin B) was investigated and was compared with that by IP_3 in terms of the cooperativity, quantal and biphasic nature of IP_3R1-mediated Ca^{2+} release [150].

IV - 2 Experimental Procedures

IV - 2 - 1) Materials

IP_3, fluo-3 and CHAPS were obtained from Dojindo Laboratories (Kumamoto, Japan), Chelex-100 from Bio-Rad, [^{3}H] IP_3 from NEN, DTPA-conjugated polymetal-sponge from Molecular Probes, phosphatidylcholine, phosphatidylserine and cholesterol from Avanti Polar-Lipids, INC. All other reagents used were of analytical grade or the highest grade available. Adenophostin (Figure 4-1) (adenophostin B), which was isolated from the culture broth of *Penicillium brevicompactum* SANK11991 [156], was kindly provided from Sankyo Co., Ltd.

IV - 2 - 2) Purification of IP_3R1

IP_3R1 was purified type-specifically from mouse cerebellar microsomal fraction by using an immunoaffinity column conjugated with an anti-pep 6 antibody, a polyclonal antibody against IP_3R1 C-terminus, as reported in Chapter II

IV - 2 - 3) Reconstitution of the purified IP_3R1

The purified IP_3R1 was reconstituted into lipid vesicles by the dialysis method described in Chapter III.

IV - 2 - 4) Measurements of adenophostin-induced Ca^{2+} release

Adenophostin- and IP_3-induced Ca^{2+} efflux from the proteoliposomes were measured by monitoring the fluorescence changes of fluo-3 as described in Chapter III. To exclude the possibility of feedback regulation by the released Ca^{2+}, we used 10 μM fluo-3, which was high enough to buffer the released Ca^{2+} and to keep deviations of extravesicular free Ca^{2+} concentration within 10 to 30 nM. Extravesicular free Ca^{2+} concentrations prior to addition of adenophostin or IP_3 were approximately 100 nM throughout the experiments [157].

IV - 2 - 5) [^{3}H] IP_3 binding assay

[^{3}H] IP_3 binding assay was performed by the polyethylene glycol precipitation method [36, 146]. The purified IP_3R1 (0.5 μg) was incubated in 50 μl of the solution containing 50 mM Tris-HCl, pH 8.0, 1 mM EDTA, 1 mM 2-mercaptoethanol, 9.6 nM [^{3}H] IP_3, and either adenophostin or IP_3, for 10 min at 4 ^{o}C, and then mixed with 2 μl of 50 mg/ml γ-globulin. Fifty microliters of the solution containing 30 % PEG6000, 1 mM 2-mercaptoethanol and 50 mM Tris-HCl, pH 8.0, was added to the sample, which was incubated for 5 min at 0 ^{o}C. After centrifugation at 10,000 xg for 5 min twice, the precipitate was dissolved in SOLVABLE (NEN) and radioactivity was measured with a liquid scintillation counter. Nonspecific binding was measured in the presence of 100 nM adenophostin or 2 μM IP_3 [150].

IV - 3 Results and Discussion

IV - 3 - 1) Measurement of Ca^{2+} release induced by adenophostin.

In this study, the kinetics of adenophostin- and IP_3-induced Ca^{2+} release by a single member of the IP_3R family in artificial membrane vesicles was investigated, thereby excluding the possibilities of modulation of Ca^{2+} release kinetics by factors such as IP_3 metabolism, Ca^{2+} pumping activity, molecules sensing changes in Ca^{2+} concentration and heterogeneity of IP_3R types. As high enough concentration of fluo-3 was used to keep extravesicular free Ca^{2+} concentration almost constant as described under the "Experimental Procedures", we could expect to rule out the possibility of the feedback regulation of the subsequent Ca^{2+} release activity by changes of extravesicular free Ca^{2+} concentrations, which have been observed in permeabilized cell systems [97, 98] and microsome assays [92, 104].

Figure 4-2 shows a typical profile of adenophostin-induced Ca^{2+} release by the immunoaffinity-purified IP_3R1 reconstituted into lipid vesicles. Fifteen nanomolar adenophostin-induced Ca^{2+} release from the liposomes followed a constant leakage of Ca^{2+} (Figure 4-2A), which was linear over the time range of the measurements, confirming that adenophostin is a true agonist of IP_3R1. The net Ca^{2+} release (Figure 4-2B) was obtained by extrapolating and subtracting the constant Ca^{2+} leakage (Figure 4-2A) from the profile. The net IICR could not be fitted by a single exponential but was found to be a biexponential (Figure 4-2B) with the fast and slow rate constants (k_{fast} = 0.63 ± 0.02 sec^{-1} (76 ± 1 %), k_{slow} = 0.050 ± 0.002 sec^{-1} (24 ± 1 %)), indicating that in response to adenophostin the purified IP_3R1 has two states to release Ca^{2+}.

$$\Delta[Ca^{2+}]_{total} = T\,(1 - A_{fast}\cdot e^{-kfast\cdot t} - A_{slow}\cdot e^{-kslow\cdot t}) \qquad \text{(Eq. 1)}$$

where T represents a total amount of released Ca^{2+}, A is amplitude of the fast and slow components (%) ($A_{fast} + A_{slow}$ = 100 %), k is rate constant (sec^{-1}) and t is time (sec).

IV - 3 - 2) Kinetics of adenophostin-induced Ca^{2+} release

Different concentrations of adenophostin and IP_3 were added to obtain dose response curves. Figure 4-3A and 3B show typical time courses of Ca^{2+} release by adenophostin and IP_3, respectively, from the same batch of the proteoliposomes. These profiles were found to be biexponential. Submaximal concentrations of adenophostin and IP_3 caused partial Ca^{2+} release, and rates of Ca^{2+} release were dependent on the adenophostin and IP_3 concentrations. After full Ca^{2+} release by maximal concentrations of adenophostin and IP_3, no additional Ca^{2+} release was evoked by additions of IP_3 and adenophostin, respectively (data not shown). The amounts of released Ca^{2+} by maximal doses of adenophostin and IP_3 were identical.

Relative amounts of released Ca^{2+} at various concentrations of adenophostin and IP_3 are shown in Figure 4-4 (n = 3 - 4). The amount of released Ca^{2+} increased as a function of adenophostin and IP_3 concentrations, indicating that adenophostin is capable of producing the quantal response of Ca^{2+} release by the purified IP_3R1 as IP_3 did. These results suggest that the quantal Ca^{2+} release is not a unique phenomenon to the native ligand, IP_3, but is an intrinsic property of IP_3R1.

The initial rates of Ca^{2+} release varied with adenophostin and IP_3 concentrations and saturated above 20 nM adenophostin and 1 μM IP_3 (Figure 4-5A). Half-maximal initial rates of Ca^{2+} release occurred at 11 nM adenophostin and 100 nM IP_3, indicating that adenophostin was approximately 10-fold more potent than the native ligand, IP_3, in Ca^{2+} releasing activity. However, in the previous experiments using rat cerebellar microsomes, adenophostin was 100-fold more potent than IP_3 [85]. The difference in the potencies of Ca^{2+} releasing activity obtained may be due to different assay systems used.

IV - 3 - 3) Cooperativity of ligand binding and Ca^{2+} releasing activity of IP_3R1 by adenophostin and IP_3

The extent of cooperativity of Ca^{2+} release is an important and fundamental issue for understanding the channel opening mechanism. In previous reports, there is controversy about the cooperativity of IICR, i.e., no cooperativity [92, 104] or positive cooperativity ($n_H = 2$) [90,

93] (n_H = 4) [91] has been reported. We determined the degree of cooperativity of IP_3R1-mediated Ca^{2+} release by Hill plotting using initial rates of Ca^{2+} release (Figure 4-5B). The slopes in the Hill plots over the range of submaximal concentrations of adenophostin (5 - 15 nM) and IP_3 (20 - 200 nM) were 3.9 ± 0.2 and 1.8 ± 0.1, respectively, indicating that adenophostin-induced Ca^{2+} release by the purified IP_3R1 exhibited a high positive cooperativity (n_H = 3.9 ± 0.2), whereas the IP_3-induced Ca^{2+} release exhibited a moderate one (n_H = 1.8± 0.1). The results suggest that at least four molecules of adenophostin or two molecules of IP_3 per one IP_3R1-channel are needed for Ca^{2+} release.

As both adenophostin- and IP_3-induced Ca^{2+} release consist of two sequential events, i.e., ligand-binding and channel opening, we have studied the cooperativity of ligand binding to the purified IP_3R1. Figure 4-6 shows inhibition curves of [^{3}H] IP_3 binding to the purified IP_3R1 by various concentrations of adenophostin and IP_3. Adenophostin inhibited [^{3}H] IP_3 binding to the purified IP_3R1 with higher potency (IC_{50} = 19 nM) than IP_3 (IC_{50} = 76 nM). The apparent inhibition constants (K_i) for adenophostin and IP_3 were calculated to be 10 nM and 41 nM, respectively, using following equation.

$$K_i = (IC_{50} / (1+C/K_d)) \quad \text{(Eq. 2)}$$

where C represents a total concentration of [^{3}H] IP_3 (C = 9.6 nM) and K_d is dissociation constant of [^{3}H] IP_3 binding (K_d = 11 nM).

The affinities of adenophostin and IP_3 to the purified IP_3R1 were well correlated to their Ca^{2+} releasing activities. Hill coefficients of inhibition of [^{3}H]IP_3 binding to the purified IP_3R1 by adenophostin and IP_3 were 1.9 and 1.1, respectively (Figure 4-6B), indicating that in terms of binding to IP_3R1 adenophostin exhibited a positive cooperativity, whereas IP_3 did not. These results demonstrated that the difference in the cooperativity of ligand-binding may result in the difference in the cooperativity of Ca^{2+} releasing between both agonists.

IV - 3 - 4) Analysis of biphasic and quantal natures of adenophostin-induced Ca^{2+} release

To analyze the kinetic features of adenophostin-induced Ca^{2+} release in detail, we attempted to curve fit the profiles. All profiles of Ca^{2+} release consisted of the sum of two single exponentials as IP_3 did. The rate constants of the fast and slow components differed by a factor of about 10 (Figure 4-7A) similar to those of IP_3-induced Ca^{2+} release (Figure 4-7B). Both the fast and slow rate constants were dependent on the concentrations of adenophostin and IP_3. The amplitudes of both states (A_{fast} and A_{slow}) derived from the curve fitting were plotted as a function of the concentrations of adenophostin and IP_3 (Figure 4-7C and 7D). The amplitudes of the fast component increased as the concentration of adenophostin and IP_3 increased, whereas those of the slow components decreased. Considering these amplitudes with the amounts of total released Ca^{2+}, the amounts of released Ca^{2+} by the fast and slow phases were then calculated. The amounts of released Ca^{2+} by the fast and slow components relative to that of 100 nM adenophostin and 5 μM IP_3 were plotted as the function of the concentrations of adenophostin and IP_3 (Figure 4-8A and 8B). The amounts of released Ca^{2+} by the fast component increased as a function of the concentrations of adenophostin and IP_3, whereas the amounts of the slow component were almost constant, i.e., already saturated, over the concentrations of adenophostin and IP_3 examined. These results suggest that the fast component is kinetically the state of low affinity for both adenophostin and IP_3 and high permeability of Ca^{2+}, but the slow component is of high affinity and low permeability. Since the fast phase of Ca^{2+} release increases with increasing IP_3 concentrations and the slow phase remains constant, our data demonstrates that the fast phase is not only the determinant of the amount of Ca^{2+} release but also responsible for the quantal Ca^{2+} release. In the [^{3}H] IP_3 binding experiments using IP_3, we detected single state of IP_3R1, although two states were observed in Ca^{2+} releasing experiments. The difference of numbers of the state of IP_3R1 may be due to the difference in experimental conditions, i.e., pH, temperature and buffer compositions.

Recently, heterogeneity of IP_3R densities in pools, which had equal sensitivity to IP_3, was reported to be responsible for biphasic Ca^{2+} release [155]. We wish to discuss such possibility.

If this is the reason for biphasic nature of IICR, the amplitudes of the fast and slow components in the curve fitting should be independent to the IP_3 concentrations, and the ratio of the amounts of released Ca^{2+} by the fast and slow components must be constant. Because in such an assumption, the amplitudes and the ratio of the amounts of released Ca^{2+} should reflect the distribution of such heterogeneity, i.e., numbers of IP_3-sensitive Ca^{2+} pools with high and low density of IP_3R reflect the amplitudes and the amounts of the released Ca^{2+} by the fast and slow phases, respectively. However, in our experiments, the amplitudes of the fast and slow components, and the ratio of the total released Ca^{2+} were dependent on IP_3 concentrations, indicating that the biphasic nature of Ca^{2+} release was not due to such heterogeneity of receptor density. A possibility of heterogeneity in the size of individual Ca^{2+} pools was also excluded by the same reasons and by the direct observation using electron microscopy. The average diameter of the liposome was 170 ± 50 nm (n = 300) and the distribution of the size was represented in single peak (Figure 3-2).

Here, we have demonstrated that adenophostin, a novel agonist of the IP_3R, is capable of producing the quantal response of Ca^{2+} release as IP_3 did, but exhibited different positive cooperativity in ligand-binding step and high positive cooperativity in Ca^{2+} release from those of IP_3. The present study has also demonstrated that the purified IP_3R1 has two states with different affinity for both adenophostin and IP_3, i.e., a low affinity and high affinity state. This could arise from alternative splicing leading to the production of variants of IP_3R1. Alternatively, there may be two different states of a single IP_3R due to ligand-dependent inactivation or interconversion.

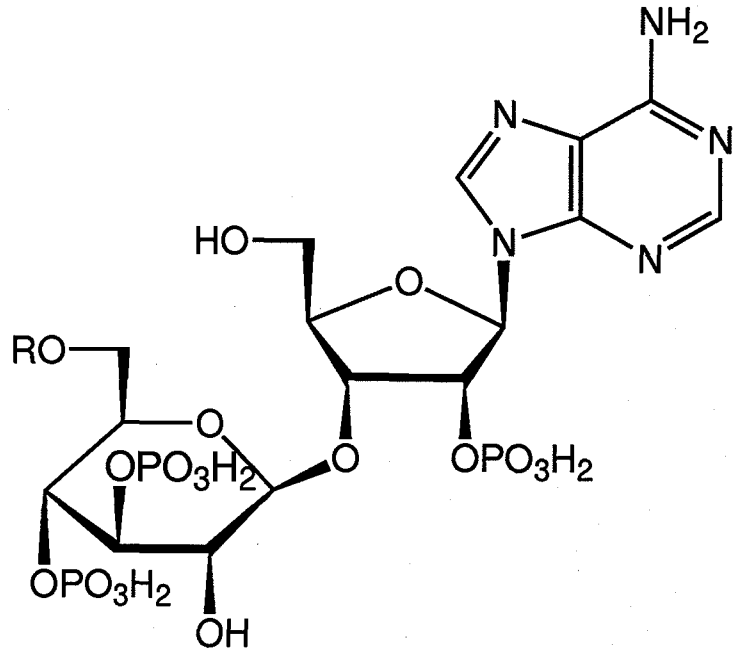

Adenophostin A: R = H
B: R = $COCH_3$

Figure 4-1. Structure of adenophostins

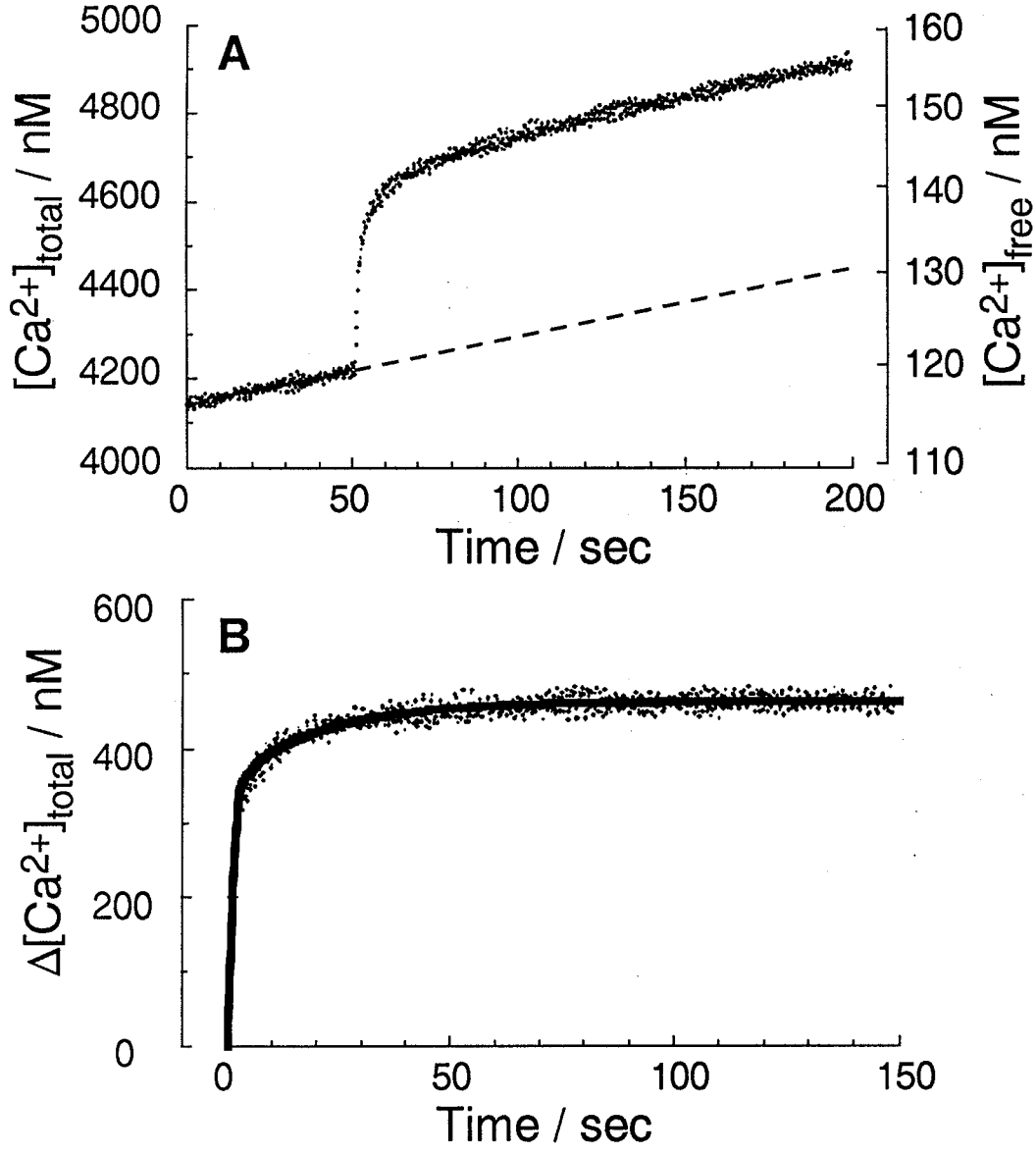

Figure 4-2. Typical profile of Ca^{2+} release by adenophostin in the purified and reconstituted IP_3R1.

Changes of fluorescence of the Ca^{2+} indicator fluo-3 were recorded after injection of 15 nM adenophostin. Adenophostin-induced Ca^{2+} release from the liposomes was followed by a constant leakage of Ca^{2+} (the *dotted line*). B, The net Ca^{2+} release was obtained by extrapolating and subtracting the constant Ca^{2+} leakage from the profile. The profile of net Ca^{2+} release was found to be well fitted by a biexponential (the *solid line*) with the fast and slow rate constants.

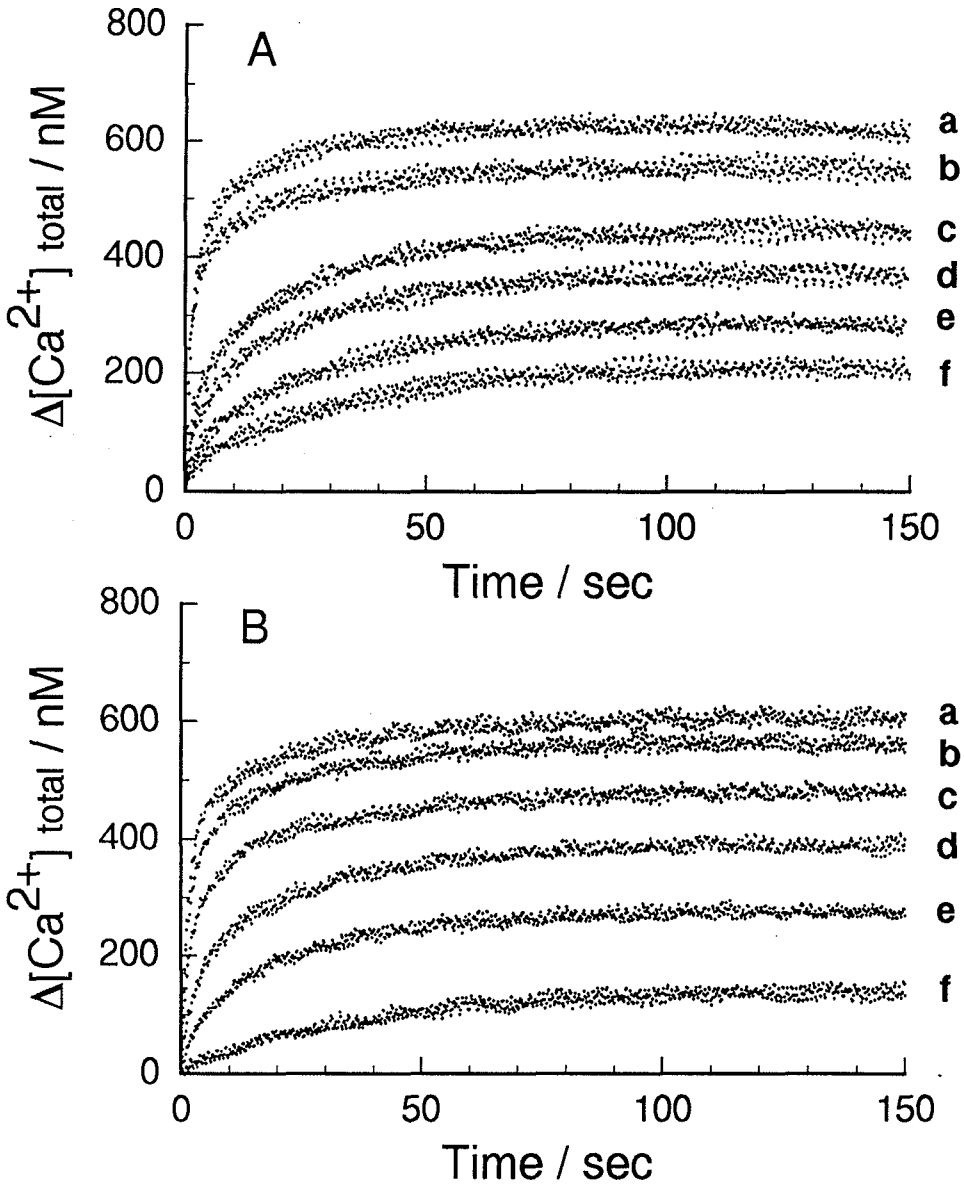

Figure 4-3. Time course of Ca^{2+} release following the injection of different concentrations of agonist.

Adenophostin- and IP_3-induced Ca^{2+} release at different concentrations of IP_3 were performed on a single batch of proteoliposomes. A: [adenophostin] = 100 nM (a), 50 nM (b), 11 nM (c), 9 nM (d), 7 nM (e), 5 nM (f), B: $[IP_3]$ = 5 μM (a), 500 nM (b),200 nM (c), 70 nM (d) 40 nM (e) and 20 nM (f).

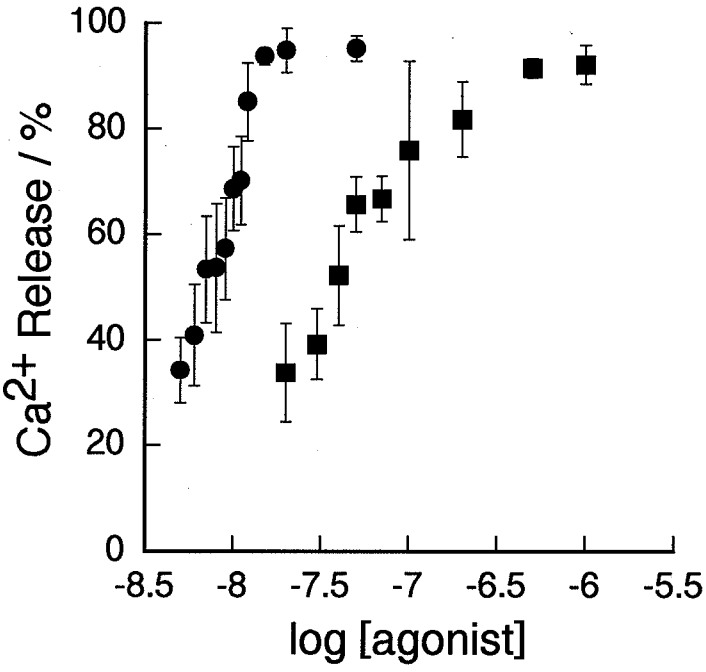

Figure 4-4. The amounts of released Ca^{2+} plotted as a function of concentrations of adenophostin (●) and IP_3 (■).

The amounts of released Ca^{2+} were plotted as a function of adenophostin and IP_3 concentrations. The data were normalized to the amplitude for 100 nM adenophostin and 5.0 μM IP_3 (values are mean ± S. D., n=3 - 4).

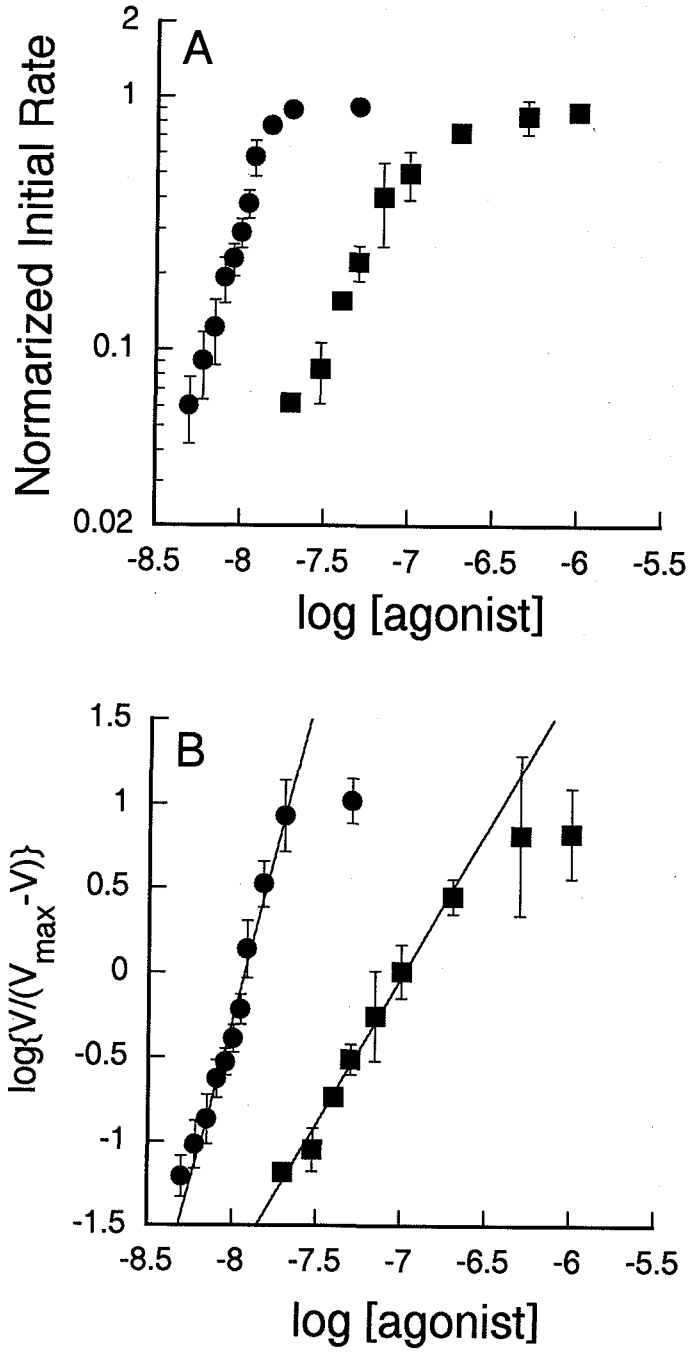

Figure 4-5. Analysis of Ca^{2+} release induced by adenophostin (●) and IP_3 (■).
A: Normalized initial rates of Ca^{2+} release were plotted as a function of the concentration of adenophostin (●) and IP_3 (■). B: Hill plot of Ca^{2+} release by adenophostin (●) and IP_3 (■) (values are mean ± S. D., n=3 - 4).

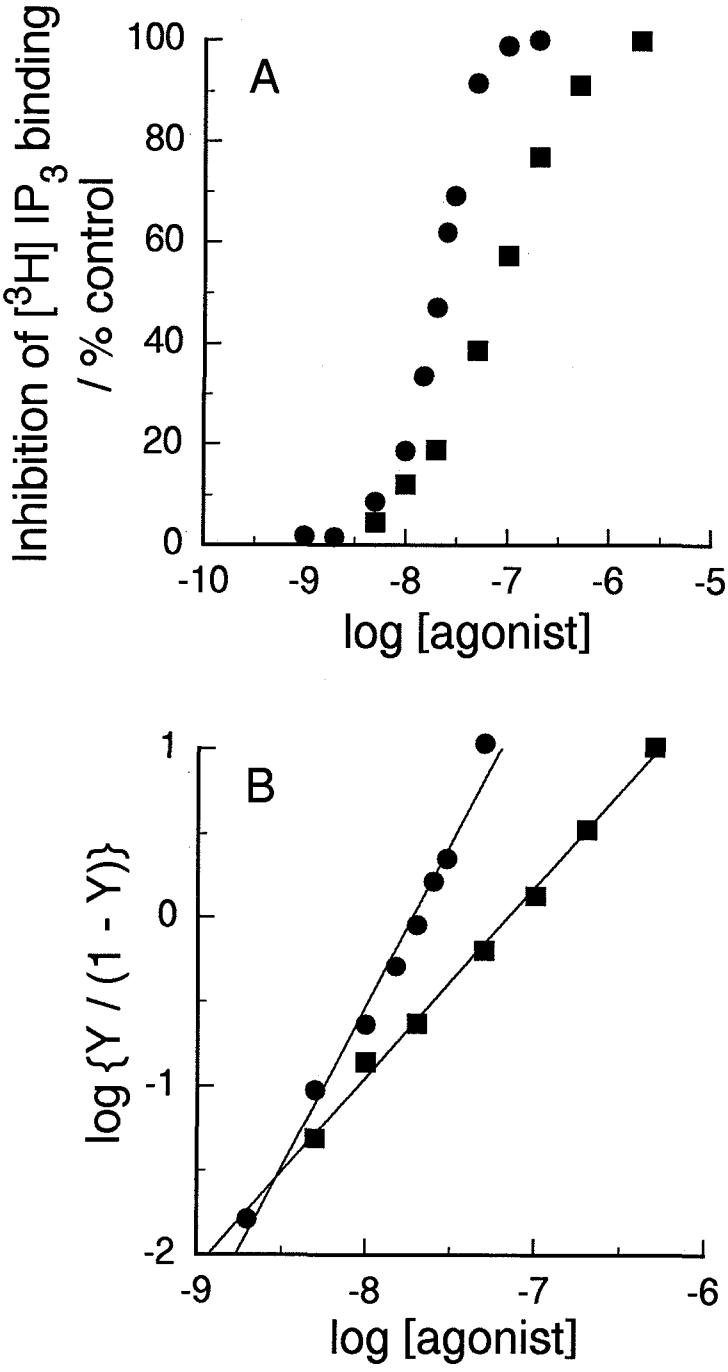

Figure 4-6. Inhibition of [^{3}H]IP_3 binding to the purified IP_3R1 by adenophostin (●) and IP_3 (■).

The [^{3}H]IP_3 binding assay was carried out as described in Materials and methods. A: Displacement curves of [^{3}H]IP_3 binding in the presence of adenophostin (●) and IP_3 (■). B: Hill plot of inhibition of [^{3}H]IP_3 binding (Y / % control) by adenophostin (●) and IP_3 (■). Measurements were duplicated.

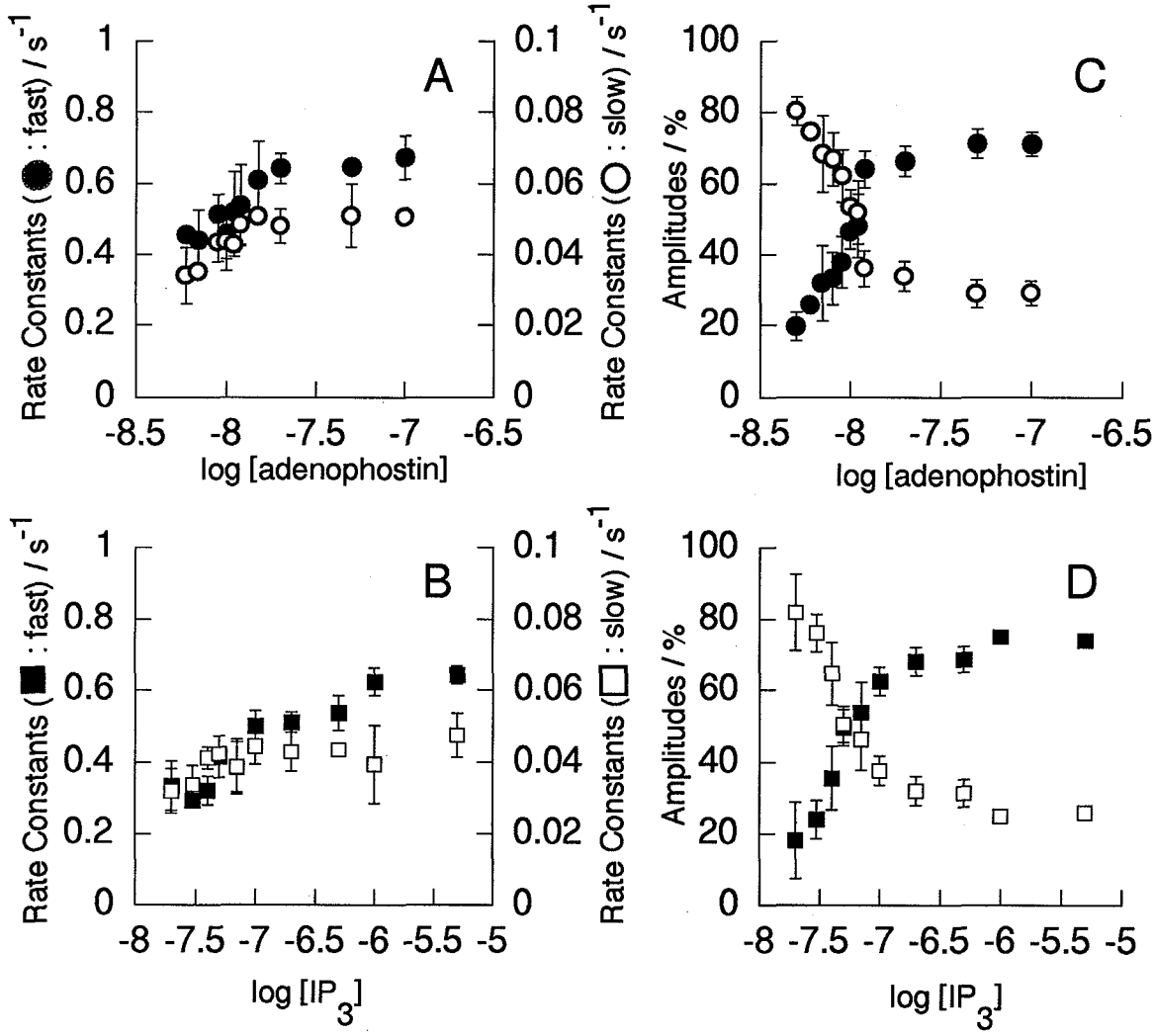

Figure 4-7. Biexponential analysis of adenophostin- and IP_3-induced Ca^{2+} release: Adenophostin dependence of the rate constants (A) and the amplitudes (C). IP_3 dependence of the rate constants (B) and the amplitudes (D).

A and C: the fast (●) and the slow (○) rate constants and amplitudes were plotted as a function of the concentration of adenophostin. B and D: the fast (■) and slow (□) rate constants and amplitudes were plotted as a function of the concentration of IP_3 (values are mean ± S. D., n=3 - 4).

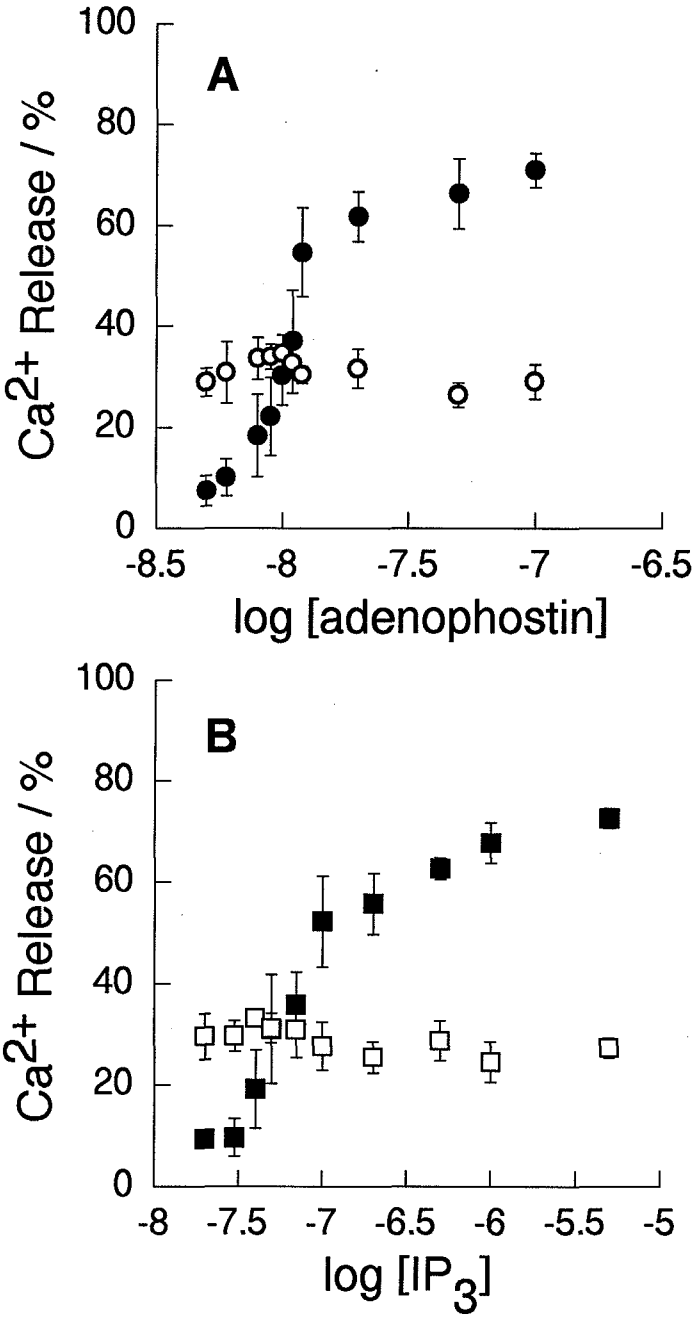

Figure 4-8. The amounts of released Ca^{2+} by the fast and slow components of adenophostin-induced Ca^{2+} release (●: fast and ○: slow) and IP_3-induced Ca^{2+} release (■: fast and □: slow).

The amounts of total released Ca^{2+} (Fig. 4-4) and the amplitude of the two components of adenophostin-induced Ca^{2+} release (Fig. 4-7C) and IP_3-induced Ca^{2+} release (Fig. 4-7D) allowed us to calculate the amounts of released Ca^{2+} by the fast (*the closed symbols*) and slow (*the open symbols*) components (values are mean ± S. D., n=3 - 4).

CHAPTER V

CHARACTERIZATION OF AN ANTIBODY (αM2) AGAINST THE PEPTIDE CORRESPONDING TO THE SPLICING REGION (SII) OF INOSITOL 1,4,5-TRISPHOSPHATE RECEPTOR TYPE 1

V - 1 Introduction

Heterogeneity due to alternative splicing has been found in the rat [50], human [72] and mouse [55] IP_3Rs. One alternatively-splicing segment (named SI for the mouse receptor subtype) is a 45-nucleotide sequence coding for 15 amino acids within the IP_3 binding domain. The other alternatively splicing segment (SII) is a 120-nucleotide sequence (40 amino acids) between the two potential PKA phosphorylation sites [55] (Figure 5-1). Within the SII segment, additional splicing events occur in combination with three more segments, A, B and C coding for 23, 1 and 16 amino acids, respectively [55]. This combination of alternative splicing produces for splicing variants, i.e., SII(A+B+C segments), $SIIB^-$(A+C segments), $SIIBC^-$ (A segment only) and $SIIABC^-$ (deletion of A, B and C). In the mouse central nervous system, the $SIIB^-$ subtype is predominant (50 - 54%), and the $SIIABC^-$ is a predominant splicing subtype in spinal cord (54%). In the peripheral tissues tested, only the $SIIABC^-$-type mRNA was observed. Thus, the SII, $SIIB^-$ and $SIIBC^-$ subtypes may be brain-specific receptors and IP_3R lacking SII is known to be ubiquitous isoform. [55]. This segment is located between the two potential sites for PKA phosphorylation as described in Chapter I. *In vitro* PKA phosphorylation demonstrated that the rat cerebellar receptor (SII^+) is highly phosphorylated at Ser-1756 (Ser-1755 in the mouse receptor) and to a much less extent at Ser-1589 (Ser-1588 in the mouse receptor). By contrast, the rat receptor from the vas deferens (SII^-) is phosphorylated exclusively at Ser-1589 [72]. These results suggested that the phosphorylation of the receptor at the different sites is coupled with the efficiency of the receptor activities.

Recently Michikawa *et al.* raised a polyclonal antibody against a synthetic peptide corresponding to IP_3R1 SII C region (amino acid residues 1718-1731 designated M2: EPSPPLRQLEDHKR) (unpublished data). IP_3R1 isoforms carrying at least one of the subsegments of SII are expressed only neuronal tissue and IP_3R1 isoform lacking SII are known to be expressed ubiquitously, therefore, this antibody is considered to be useful to purify the IP_3R (carrying SII region) expressed from its cDNA by distinguishing the endogenous IP_3R

which lacks the SII region. In this chapter, the polyclonal antibody against a synthetic peptide corresponding to IP_3R1 SII C region was characterized and its utilities are discussed.

V - 2 Experimental Procedures

V - 2 - 1) Materials

Adult ICR mouse were used for immunohistochemical study. ECL Western blotting system, and Nitrocellulose hybridization transfer membranes Hybond ECL from Amersham Corp. All other reagents used were of analytical grade or the highest grade available.

II - 2 - 2) An antibody against a synthetic peptide corresponding IP_3R SII region

A peptide corresponding to a part of SII region of the IP_3R1 (amino acid residues 2736 - 2747 designated M2: EPSPPLRQLEDHKR) was custom-synthesized. The peptide (M2) was conjugated to keyhole limpet hemocyanin (KLH). New Zealand White rabbits were immunized by intradermal injection with a homogenate containing 1 ml of Freund's complete adjuvant and 1 ml of M2-KLH conjugate. Three weeks later, the rabbits were injected with a homogenate containing 1 ml of Freund's incomplete adjuvant and 1 ml of M2-KLH conjugate. Antiserum was collected each week thereafter. Booster injection was performed every 2 weeks until the titer of the antiserum was saturated (Michikawa *et al.* unpublished data).

V - 2 - 3) Expression of deletion mutant IP_3R in NG108-15 cells

To characterize the αM2 antibody against the synthetic peptide corresponding to SII region of IP_3R1, the membrane fractions from NG108-15 cells transfected with the cDNA of IP_3R1 and deletion mutant cDNAs were immunoblotted. For expression experiments, a recombinant plasmid, pBactS-C1-13, was prepared as reported previously [37]. pBactS-C1-13 carries the entire protein-coding sequence of mouse cerebellar IP_3R1 cDNA between a β–actin promoter and a simian virus 40 polyadenylylation sequence. The deletion mutant were obtained by removing various portions of the cDNA from pBactS-C1-13 by using the combinations of restriction endonucleases as reported previously [42]. The deletion mutants D419-735 and D170-1252 lack amino acid residues of IP_3R1 from 419 to 735 and from 170 to 1252, respectively, but contain SII region. ΔSII mutant lacks SII region of IP_3R1 (Figure 5-2).

These cDNAs were introduced into NG108-15 cells by the standard calcium phosphate precipitation technique. 72 hrs after transfection, cells were collected, washed with ice-cold PBS and resuspended with ice cold 0.25M sucrose in buffer A (5 mM Tris-HCl, pH 7.4, 0.1 mM EDTA, 0.1 mM phenylmethylsulfonyl fluoride (PMSF), 10 μM leupeptin, 10 μM pepstatin A, 1 mM 2-mercaptoethanol) and were homogenized using a glass-Teflon Potter homogenizer with 10 strokes at 1,200 rpm. The homogenate was centrifuged at 1000 x g for 5 min at 2 ^{o}C to remove nuclei, and the pellet was homogenized again under the same condition. The combined supernatants were centrifuged at 105,000 x g for 1 hr at 2 ^{o}C to precipitate the membrane fraction.

V - 2- 4) Immunoblots of IP_3R in peripheral tissues with αM2 antibody and monoclonal antibody 18A10

Adult ddY mice were anesthetized and then killed by decapitation, and various tissues were dissected. Thymus, spleen, liver, heart, SK muscle, testis, uterus and adrenal were examined as peripheral tissues and cerebellum and cerebrum as neuronal tissues. The membrane fractions of each tissues were prepared according to the method described above and was electrophoresed (5 % SDS-PAGE) and transferred to a nitrocellulose membrane. The blots were immunostained with αM2 antibody and the monoclonal antibody 18A10 using western blotting system (Amersham).

V - 2 - 5) Immunohistochemistry

After ether anesthetization, an adult ICR mouse killed by injecting PBS followed by freshly prepared Bouin's solution (the mixture solution of saturated picric acid : 4% p-formaldehyde : glacial acetic acid = 15 : 5 : 1), via the left ventricle and washing out from the right atrium. Brain was dissected and postfixed in Bouin's solution for 2 hr at 4 ^{o}C. Paraffin sections (7 μm thick) were prepared by the conventional method. The sections were sequentially pretreated with 0.3% H_2O_2 in methanol for 30 min, 0.05% Triton X-100 in PBS

for 10 min, and 2% skim milk in PBS at 4 °C for 2 hr. The pretreated sections were incubated with the first antibody for 3 hr. The polyclonal antibody αM2 and the monoclonal antibody 18A10 were used as the first antibody. The αM2 antibody used was an IgG fraction purified from rabbit antisera with protein A-Sepharose. The sections reacted with the first antibodies were sequentially treated as follows: washing with PBS three times for 5 min each, incubation for 2 hr with goat biotiylated anti-rabbit (for αM2) or anti- rat (for 18A10) IgG as the second antibody, and incubation for 1 hr with avidin D-conjugated HRP. After washing with PBS, the immunoreacted sections were stained by incubation with DAB solution.

V - 2 - 6) Immunoaffinity purification of IP_3R using αM2 antibody

αM2 antibody was purified using protein A-Sepharose CL-4B column according to the manufacturer's protocol. The purified antibody was conjugated to the CNBr-activated Sepharose 4B according to the method described in Chapter II. IP_3R was purified using αM2 antibody-conjugated immunoaffinity column as described in Chapter II.

Electrophoresis was carried out on a 5 % gradient polyacrylamide gel. The gel was stained with Coomassie Brilliant Blue R-250. The purified IP_3R1 was also electrophoresed (5 % SDS-PAGE) and transferred to a nitrocellulose membrane. The blots were immunostained with the monoclonal antibodies, 18A10 using western blotting system (Amersham).

V - 3 Results and Discussion

V - 3 - 1) αM2 antibody recognizes the alternative splicing region SII of IP_3R1

To characterize the αM2 antibody against the synthetic peptide corresponding to SII region of IP_3R1, the membrane fraction from NG108-15 cells transfected with the cDNA of IP_3R1 and deletion mutant cDNAs were immunoblotted (Figure 5-3). The expressed IP_3R (C1-13) and the deletion mutants (D419-735, D170-1252) which contain the SII region showed immunoreactivity with αM2 as well as 18A10, whereas ΔSII mutant which lack the SII region did not, indicating that αM2 antibody recognizes the splicing region SII of IP_3R1. As the immunoblotting of the deletion mutants of IP_3Rs with αM2 antibody did not have any signals at the position of IP_3R, i.e., endogenous IP_3R, while 18A10 detected it. The results suggested that the endogenous IP_3R in NG108-15 is SII- isoform (non-neural type). Therefore, αM2 antibody is useful to isolate the expressed IP_3R from cDNA from the endogenous type, which enables us to investigate completely homogeneous IP_3R1, i.e., excluding the heterogeneity due to the splicing variants.

V - 3 - 2) Splicing variants of IP_3R containing SII region expressed in central nervous system, not in peripheral tissues

The SII region consist of 120 nucleotides and is located in the coupling domain between the PKA phosphorylation consensus sequences. RNase protection analysis showed that the presence of the insert is a property of neuronal cell types, whereas the shorter form represents a non-neuronal cell types. To confirm this observation, peripheral tissues, thymus, spleen, liver, heart, SK muscle, testis, uterus and adrenal, were immunoblotted with αM2 antibody (Figure 5-4). The immunoblots showed no immunoreactivity with αM2 antibody (weak signals appeared in testis and uterus is considered to be non-specific signals, because the signals remained after preabsorption with M2 peptide), whereas the monoclonal antibody 18A10 which recognize C-terminus of IP_3R1 did, confirming that IP_3R1 without SII region is non-neuronal type as reported previously [55].

V - 3 - 3) Immunohistochemical study of the splicing region SII of IP_3R1 in mouse cerebellum

The cerebellum is known to contain all isoforms of IP_3R due to alternative splicing of SII. These isoforms can be divided into two groups, i.e., neuronal type (carrying at least one of the subsegments of SII) and non-neuronal type (lacking SII). The localization of neuronal and non-neuronal type of IP_3R was investigated using αM2 and 18A10. Figure 5-5 provides a comparison of αM2 and 18A10 for immunohistochemical analysis of the IP_3R. The soma and the dendritic arborization of Purkinje cells were stained strongly with both antibodies in similar way, indicating there seems to be no heterogeneity in the localization of neural and non-neuronal type of IP_3R in the cerebellum.

V - 3 - 4) Immunoaffinity purification of IP_3R using αM2 antibody

Although we could isolate the single type of IP_3R1 from the mouse cerebellum using immunoaffinity column conjugated with the polyclonal antibody against the pep 6 peptide corresponding to the C-terminus of IP_3R as described in Chapter II, it contains the splicing variants of IP_3R1. To avoid such heterogeneity, we need to develop the method accompanied with the expression systems of IP_3R. As the endogenous IP_3R in NG108-15 is SII- isoform (non-neural type) as described above, the αM2 antibody is expected to be useful to isolate the expressed IP_3R from the endogenous type, which enables us to investigate completely homogeneous IP_3R1, i.e., excluding the heterogeneity due to the splicing variants. The utilization of αM2 antibody in the immunoaffinity purification was examined. Figure 5-6 shows SDS-PAGE analysis of the immunopurified IP_3R from mouse cerebellum using the affinity column conjugated with αM2 antibody. The purified IP_3R1 was immunostained with the monoclonal antibody against IP_3R1, 18A10, and was found to be single band, revealing that αM2 is useful in the immunoaffinity purification. Therefore, the αM2 antibody seems to be

useful to purify the IP_3R expressed in NG108-15 cells from its cDNA by distinguishing the endogenous IP_3R which lacks the SII region .

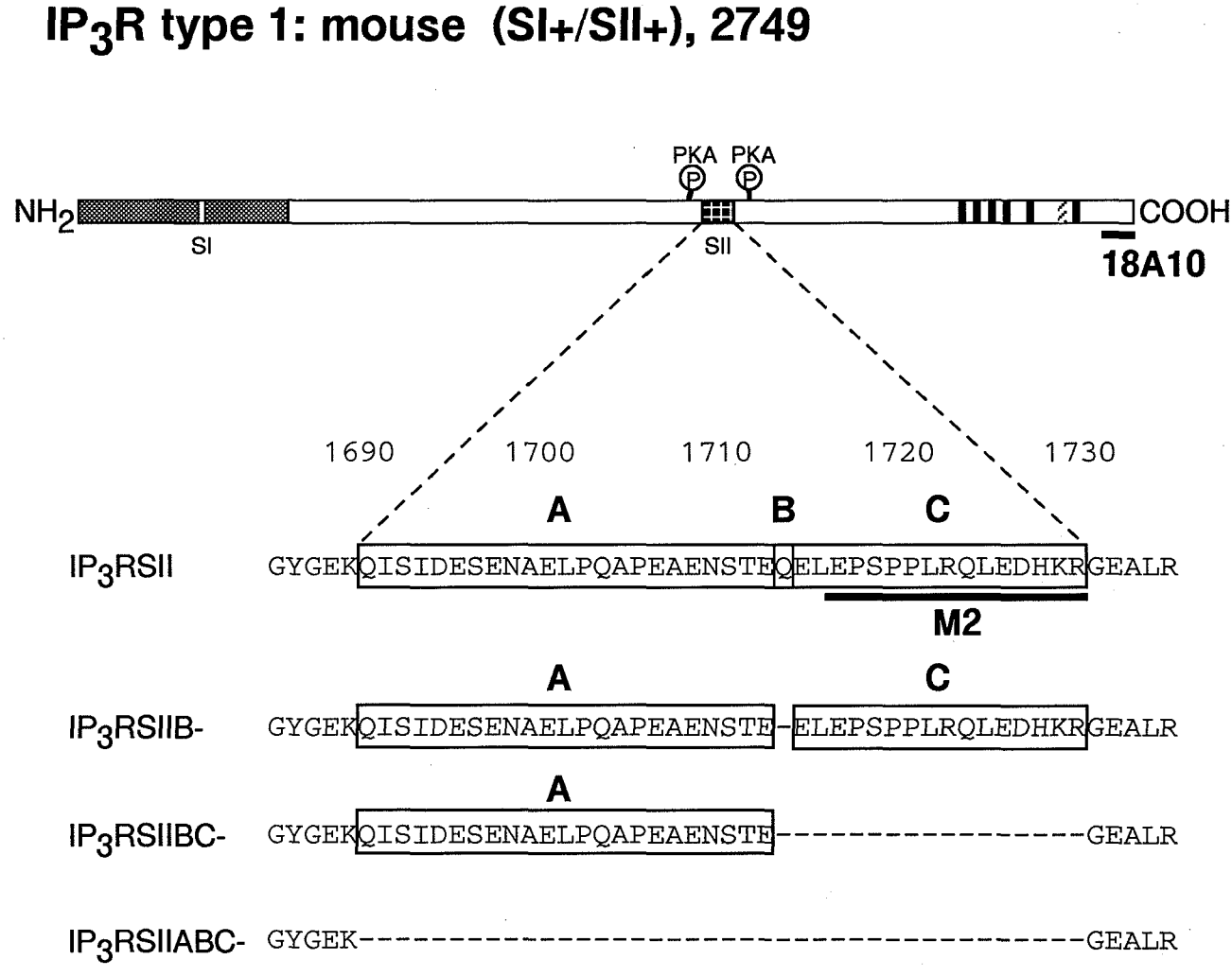

Figure 5-1. Schematic representation of IP_3R1 splicing variants (SII).

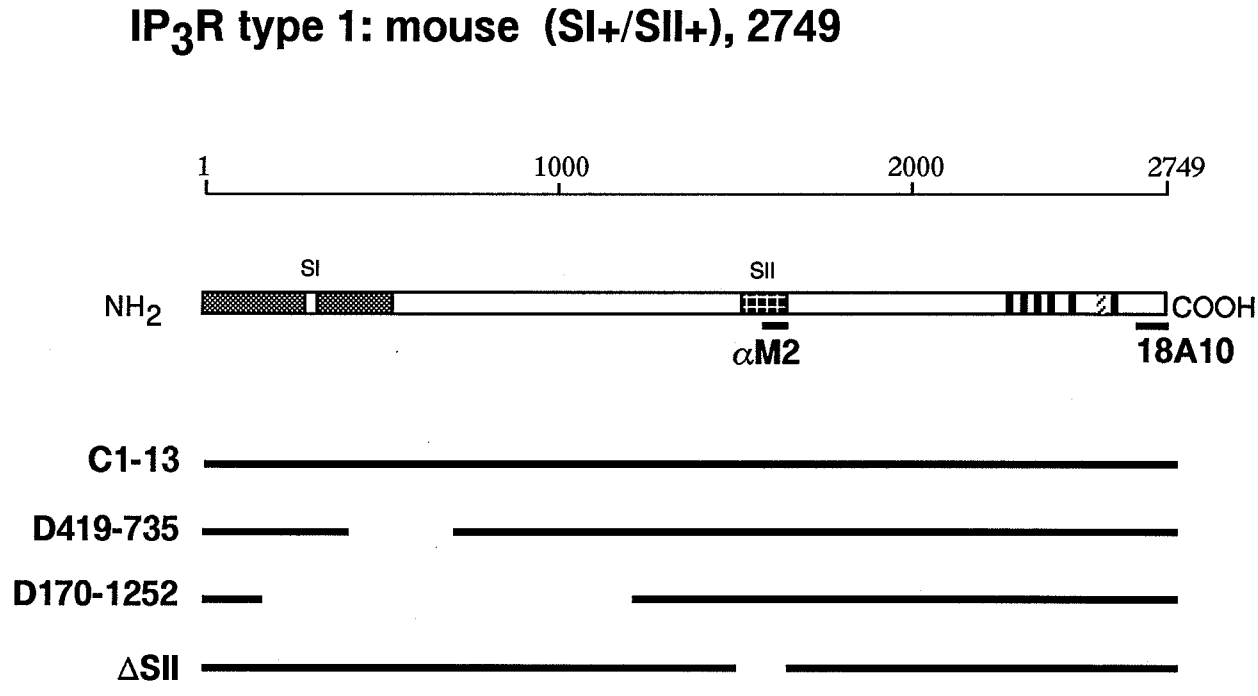

Figure 5-2. Structures of internal deletion mutants.

Horizontal lines represent the region of the receptor carried by the mutants. Mutant names are to the left.

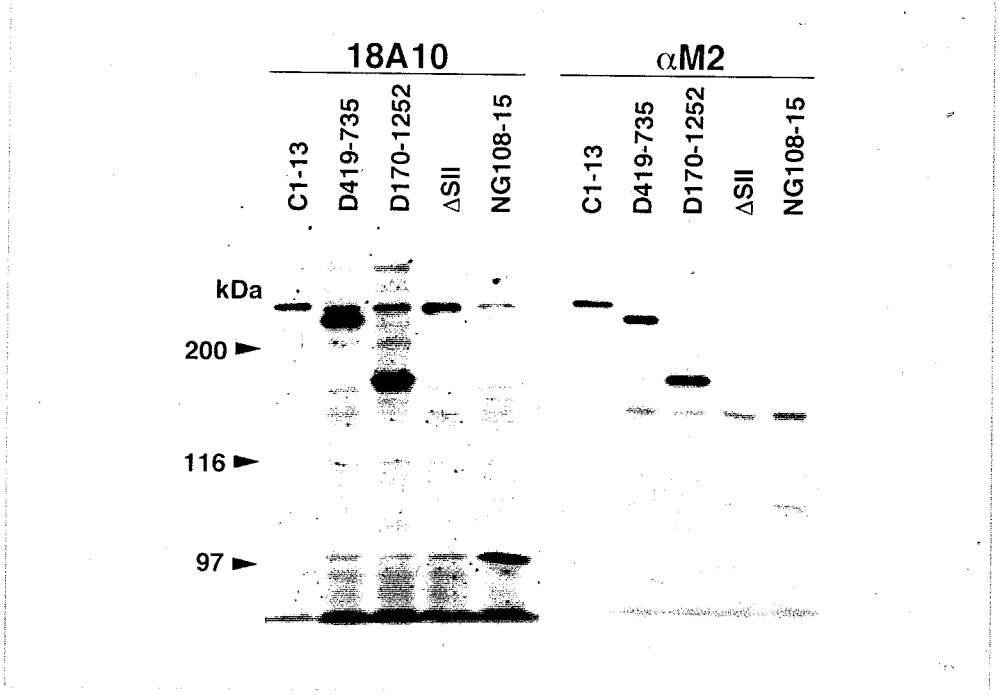

Figure 5-3. Immunoblots of series of deletion mutants of IP_3R1 expressed in NG108-15 from their mutant cDNAs.

The membrane fractions from NG108-15 cells transfected with the cDNA of IP_3R1 (C1-13) and deletion mutant cDNAs (D419-735, D170-1252, ΔSII) were immunoblotted with 18A10 (left) and αM2 (right). NG108-15 is control.

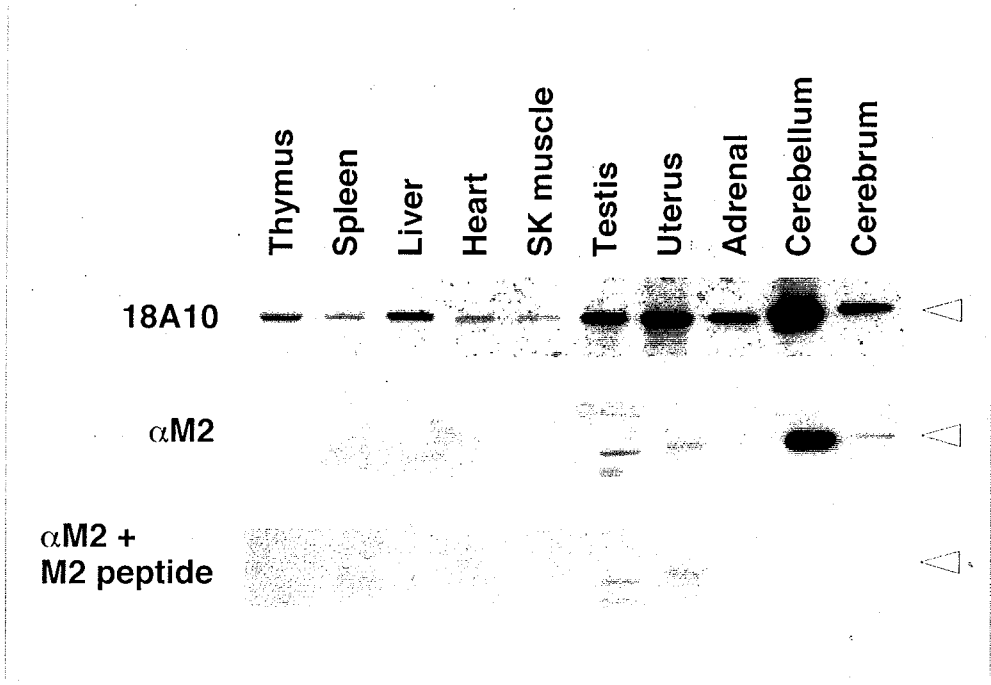

Figure 5-4. Immunoblots of IP_3R in peripheral tissues with the αM2 antibody and the monoclonal antibody 18A10.

The membrane fractions of various peripheral tissues (thymus, spleen, liver, heart, skeletal (SK) muscle, testis, uterus and adrenal) and two neuronal tissues (cerebellum and cerebrum) were applied to SDS-PAGE gel (5 %), followed by immunoblots with 18A10 (top), αM2 (middle) and αM2 preabsorbed with M2 peptide (bottom). The open arrow indicates the position of IP_3R1.

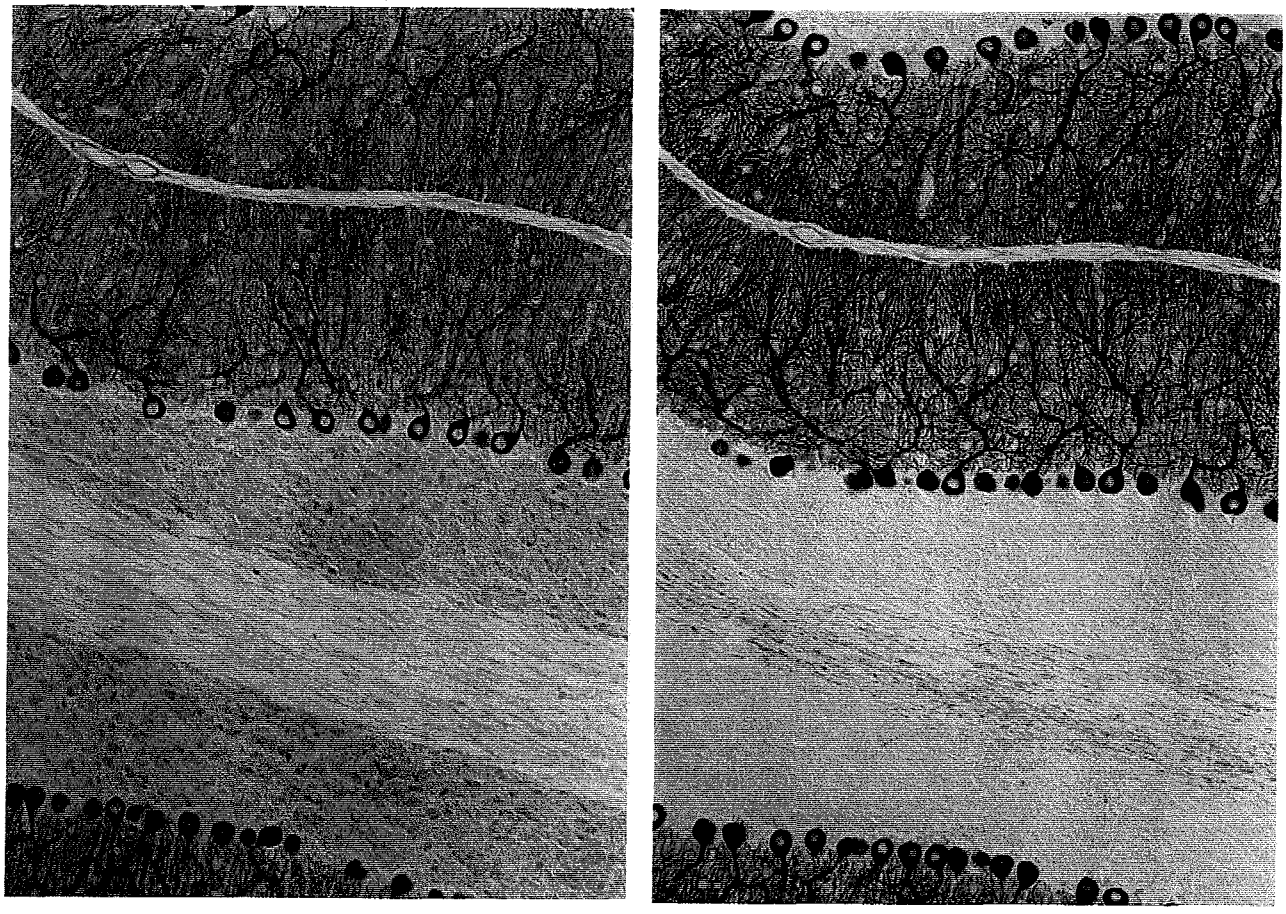

Figure 5-5 (A, B). Immunochistochemical staining of IP_3R in mouse cerebellum with the αM2 antibody and the monoclonal antibody 18A10.

Sagital sections of mouse cerebellum were stained with the polyclonal antibody αM2 (A, C) and the monoclonal antibody 18A10 (B, D). A and B, x 50; C and D, x 250.

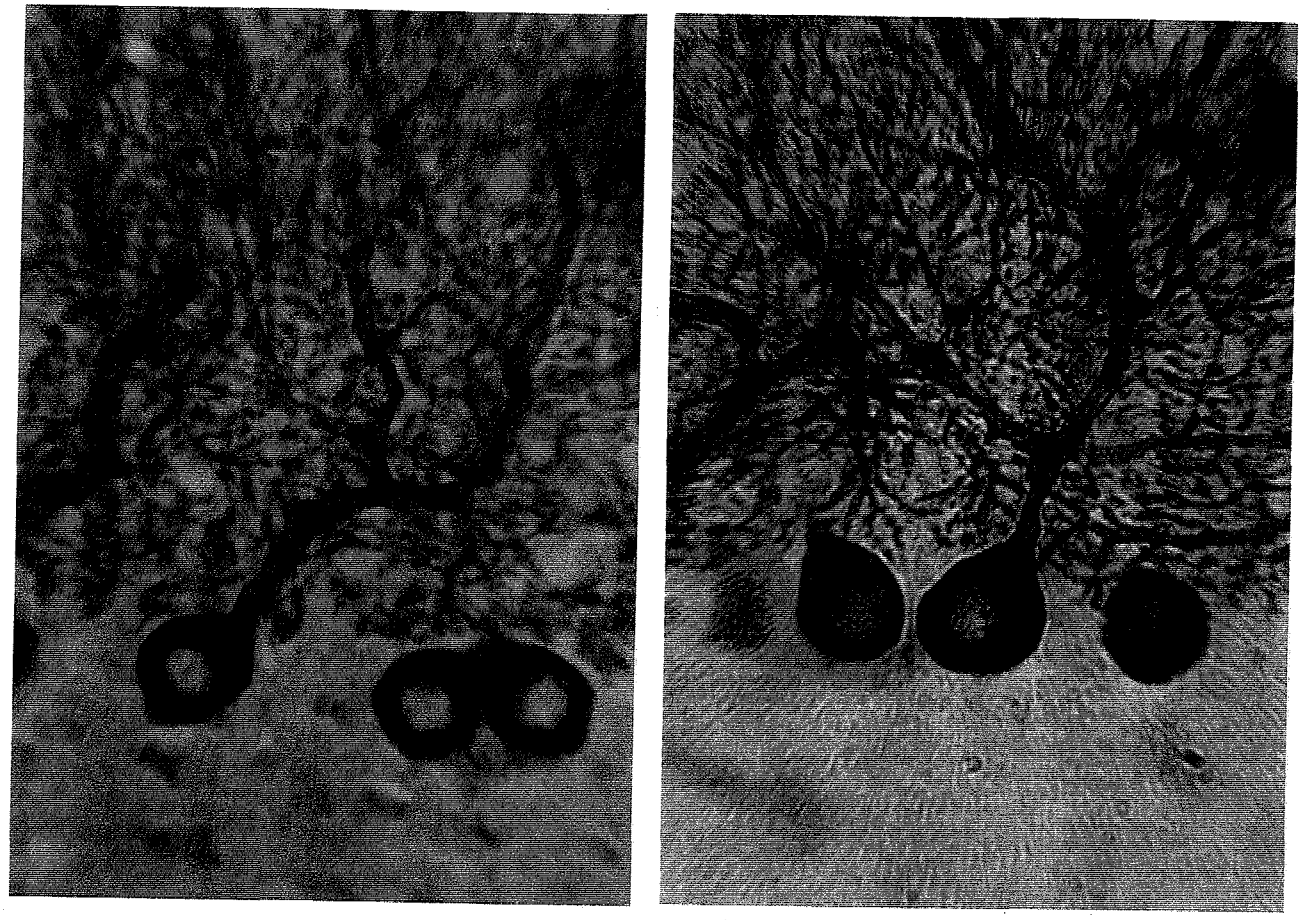

Figure 5-5 (C, D). Immunochistochemical staining of IP_3R in mouse cerebellum with the αM2 antibody and the monoclonal antibody 18A10.

Sagital sections of mouse cerebellum were stained with the polyclonal antibody αM2 (A, C) and the monoclonal antibody 18A10 (B, D). A and B, x 50; C and D, x 250.

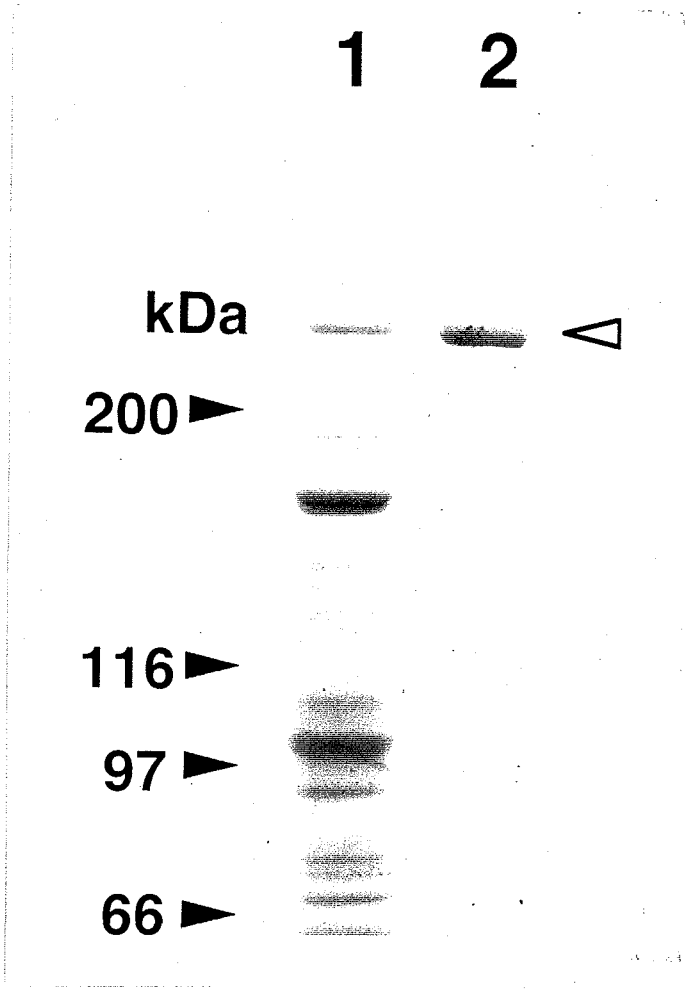

Figure 5-6. SDS-PAGE analysis of the purified IP_3R1 using the αM2 antibody .
Electrophoresis was carried out on a 5 % polyacrylamide gel. The gel was stained with Coomassie Brilliant Blue R-250. The positions of molecular weight markers (in kDa) are shown on the left. The open arrow indicates the position of IP_3R. *Lanes* 1, the cerebellar membrane fraction . *Lanes* 2, the immunopurified IP_3R1.

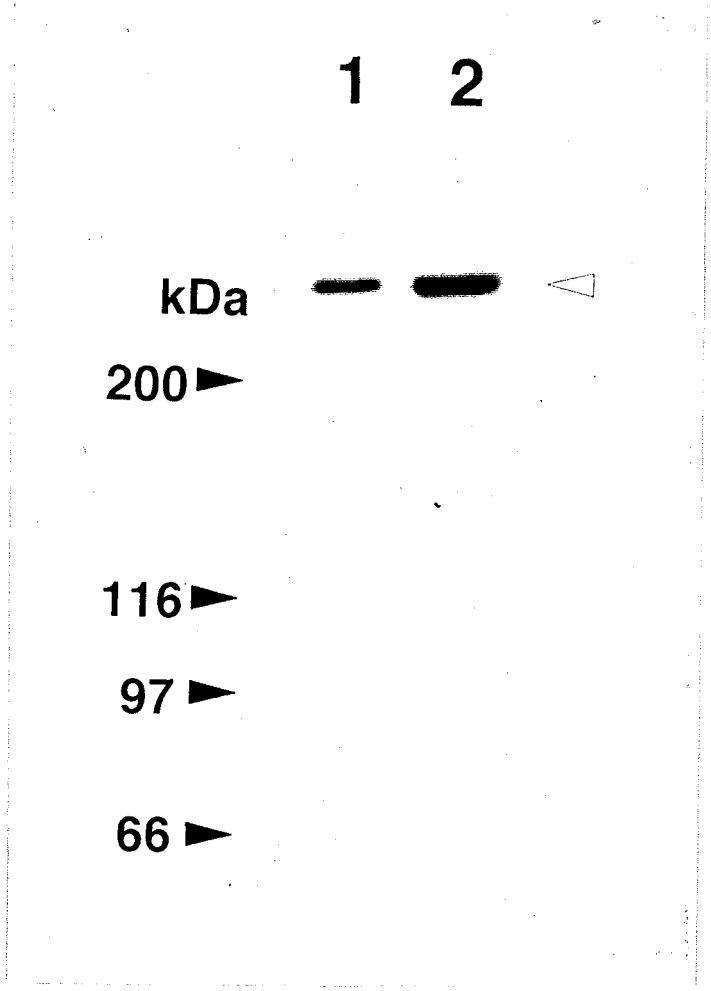

Figure 5-7. Immunoblot of the purified IP_3R1 from mouse cerebellum using the affinity column conjugated with the αM2 antibody . Immunoblots of the purified IP_3R1.

The purified IP_3R1 was analyzed by Western blotting. The cerebellar microsomal fraction and the purified IP_3R1 were applied to the gel, followed by immunoblotting with monoclonal antibodies 18A10. The open arrow indicates the position of IP_3R1. *Lanes* 1, the cerebellar membrane fraction . *Lanes* 2, the immunopurified IP_3R1.

CHAPTER VI

CONCLUSION

Despite of intensive studies on the kinetics of Ca^{2+} release, some properties of channel opening and the effects of modulators on IICR so often differ among the reports. The previous reports used permeabilized cells and microsomal preparations have been complicated by many factors ((i) composition of subtypes of IP_3Rs, (ii) metabolism of IP_3, (iii) Ca^{2+} pump, (iv) molecules sensing changes in Ca^{2+} concentration, (v) heterogeneity of IICR-Ca^{2+} pools). No works concerning the cooperativity and biphasic nature of Ca^{2+} release analyzed by using the purified single type of IP_3R have been reported yet.

In this study, I have investigated the kinetics of Ca^{2+} release mediated by the purified single type of IP_3R1 using the fluorescent Ca^{2+} indicator fluo-3. I have demonstrated that the population of the immunopurified purified IP_3Rs has been found to be almost homogeneous, predicting that the purified IP_3R exists in a homotetrameric structure of IP_3R1 (Chapter II).

The novel system to investigate the IICR-mediated the purified IP_3R have been established. Using this system, the positive cooperativity of IICR and the biphasic nature and the quantal Ca^{2+} release of IICR by a single type of IP_3R1 have been defined (Chapter III). IP_3-induced Ca^{2+} release of the purified IP_3R1 exhibited positive cooperativity; the Hill coefficient was 1.8 ± 0.1. The half maximal initial rate for Ca^{2+} release occurred at 100 nM IP_3. At the submaximal concentrations of IP_3, the purified IP_3R1 showed quantal Ca^{2+} release, revealing that a single type of IP_3R (IP_3R1) is capable of producing the phenomenon of quantal Ca^{2+} release. The profiles of the IP_3-induced Ca^{2+} release of the purified IP_3R1 were found to be biexponential with the fast and slow rate constants ($k_{fast} = 0.3 \sim 0.7\ s^{-1}$, $k_{slow} = 0.03 \sim 0.07\ s^{-1}$), indicating that IP_3R1 has two states to release Ca^{2+}. The amount of released Ca^{2+} by the slow phase was constant, whereas that by the fast phase increased in proportion to added IP_3. This provides evidence to support the view that the fast phase of Ca^{2+} release is mediated by the low affinity state and the slow phase by the high affinity state of the IP_3R1. This also suggests that the fast component of Ca^{2+} release is responsible for the process of quantal Ca^{2+} release.

I have also investigated the kinetics of Ca^{2+} release induced by the novel agonist of IP_3R, adenophostin, and compared the kinetics with that by the native ligand IP_3 in terms of the cooperativity, quantal and biphasic nature of IP_3R1-mediated Ca^{2+} release (Chapter IV). The phenomenon of the quantal Ca^{2+} release occurred by the novel agonist of IP_3R, adenophostin, as well as by the native ligand IP_3. Adenophostin B-induced Ca^{2+} release by the purified IP_3R1 exhibited a high positive cooperativity (n_H = 3.9 ± 0.2, EC_{50} = 11 nM), whereas the IP_3-induced Ca^{2+} release did a moderate one (n_H = 1.8± 0.1, EC_{50} = 100 nM). Inhibition of $[^3H]IP_3$ binding to the purified IP_3R1 by adenophostin B and IP_3 exhibited a positive cooperativity (n_H = 1.9, Ki = 10 nM) and no cooperativity (n_H = 1.1, Ki = 41 nM), respectively. These results suggested that the difference in the cooperativity of ligand-binding resulted in the difference in the cooperativity of Ca^{2+} release.

To develop the immuno-affinity purification method for the expression system of IP_3R1 from its cDNA, a polyclonal antibody (αM2 antibody) against peptide corresponding to the SII region (neuron type) was raised and characterized (Chapter V). The αM2 antibody have recognized the neuron type of IP_3R1 and seems to be useful to purify the IP_3R1 expressed in NG108-15 cells from its cDNA by distinguishing the endogenous IP_3R which lacks the SII region .

In future investigations using the present system, the purification and reconstitution of other types of IP_3Rs and the mutated IP_3Rs may reveal new insights into IICR and may allow us to relate any differences in the kinetic properties of IICR to the differences in the structure of the different types of IP_3R. Also, this will allow us to observe the effects of modulators, such as PKA, ATP and Ca^{2+} etc. on type-specific IICR.

REFERENCES

[1] Berridge, M.J., and Irvine, R.F. Inositol phosphates and cell signalling. *Nature* **1989** 341, 197-205.

[2] Berridge, M.J. Inositol trisphosphate and calcium signalling. *Nature* **1993** 361, 315-325.

[3] Furuichi, T., Kohda, K., Miyawaki, A., and Mikoshiba, K. Intracellular channels. *Curr. Opin. Neurobiol.* **1994** 4, 294-303.

[4] Pederson. P, L., and Carafoli. E. Ion motive ATPases. I. Ubiquity, properties, and significance to cell function. *Trends Biochem. Sci.* **1987** 12, 146-150.

[5] Pozzan, T., Rizzuto, R., Volpe, P., and Meldolesi, J. Molecular and cellular physiology of intracellular calcium stores. [Review]. *Physiological Reviews* **1994** 74, 595-636.

[6] Blackford, S., Rea, P.A., and Sanders, D. Voltage sensitivity of $H+/Ca^{2+}$ antiport in higher plant tonoplast suggests a role in vacuolar calcium accumulation. *J. Biol. Chem.* **1990** 265, 9617-9620.

[7] Lai, F.A., Erickson, H.P., Rousseau, E., Liu, Q.Y., and Meissner, G. Purification and reconstitution of the calcium release channel from skeletal muscle. *Nature* **1988** 331, 315-319.

[8] Takeshima, H., Nishimura, S., Matsumoto, T., Ishida, H., Kangawa, K., Minamino, N., Matsuo, H., Ueda, M., Hanaoka, M., Hirose, T., and Numa, S. Primary structure and expression from complementary DNA of skeletal muscle ryanodine receptor. *Nature* **1989** 339, 439-445.

[9] Otsu, K., Willard, H.F., Khanna, V.K., Zorzato, F., Green, N.M., and MacLennan, D.H. Molecular cloning of cDNA encoding the Ca^{2+} release channel (ryanodine receptor) of rabbit cardiac muscle sarcoplasmic reticulum. *J. Biol. Chem.* **1990** 265, 13472-13483.

[10] Zorzato, F., Fujii, J., Otsu, K., Phillips, M., Green, N.M., Lai, F.A., Meissner, G., and MacLennan, D.H. Molecular cloning of cDNA encoding human and rabbit forms of the

Ca^{2+} release channel (ryanodine receptor) of skeletal muscle sarcoplasmic reticulum. *J. Biol. Chem.* **1990** 265, 2244-2256.

[11] Giannini, G., Clementi, E., Ceci, R., Marziali, G., and Sorrentino, V. Expression of a ryanodine receptor-Ca^{2+} channel that is regulated by TGF-beta. *Science* **1992** 257, 91-94.

[12] Hakamata, Y., Nakai, J., Takeshima, H., and Imoto, K. Primary structure and distribution of a novel ryanodine receptor/calcium release channel from rabbit brain. *FEBS Lett.* **1992** 312, 229-235.

[13] Ma, J., Fill, M., Knudson, C.M., Campbell, K.P., and Coronado, R. Ryanodine receptor of skeletal muscle is a gap junction-type channel. *Science* **1988** 242, 99-102.

[14] Coronado, R., Morrissette, J., Sukhareva, M., and Vaughan, D.M. Structure and function of ryanodine receptors. *Am. J. Physiol. Cell Physiol.* **1994** 266, C1485-1504.

[15] Brillantes, A.M.B., Ondrias, K., Scott, A., Kobrinsky, E., Ondriasove, E., Moschella, M.C., Jayaraman, T., Landers, M., Ehrlich, B.E., and Marks, A.R. Stabilization of calcium release channel (ryanodine receptor) function by FK506-binding protein. *Cell* **1994** 77, 513-523.

[16] Meszaros, L.G., Bak, J., and Chu, A. Cyclic ADP-ribose as an endogenous regulator of teh non-skeletal type ryanodine receptor Ca^{2+} channel. *Nature* **1993** 364, 76-79.

[17] Thorn, P., Gerasimenko, O., and Petersen, O.H. Cyclic ADP-ribose regulation of ryanodine receptors involved in agonist-evoked cytosolic Ca^{2+} oscillations in pancreatic acinar cells. *EMBO J.* **1994** 13, 2038-2043.

[18] Clapham, D.E. Calcium signaling. [Review]. *Cell* **1995** 80, 259-68.

[19] Streb, H., Irvine, R.F., Berridge, M.J., and Schulz, I. Release of Ca^{2+} from a nonmitochondrial intracellular store in pancreatic acinar cells by inositol-1,4,5-trisphosphate. *Nature* **1983** 306, 67-69.

[20] Biden, T.J., and Wollheim, C.B. Ca^{2+} regulates the inositol tris/tetrakisphosphate pathway in intact and broken preparations of insulin-secreting RINm5F cells. *J. Biol. Chem.* **1986** 261, 11931-11934.

[21] Johanson, R.A., Hansen, C.A., and Williamson, J.R. Purification of D-myo-inositol 1,4,5-trisphosphate 3-kinase from rat brain. *J. Biol. Chem.* **1988** 263, 7465-7471.

[22] Yamaguchi, K., Hirata, M., and Kuriyama, H. Purification and characterization of inositol 1,4,5-trisphosphate 3-kinase from pig aortic smooth muscle. *Biochem. J.* **1988** 251, 129-134.

[23] Sim, S.S., Kim, J.W., and Rhee, S.G. Regulation of D-myo-inositol 1,4,5-trisphosphate 3-kinase by cAMP-dependent protein kinase and protein kinase C. *J. Biol. Chem.* **1990** 265, 10367-10372.

[24] Tarver, A.P., King, W.G., and Rittenhouse, S.E. Inositol 1,4,5-trisphosphate and inositol 1,2-cyclic 4,5-trisphosphate are minor components of total mass of inositol trisphosphate in thrombin-stimulated platelets. Rapid formation of inositol 1,3,4-trisphosphate. *J. Biol. Chem.* **1987** 262, 17268-17271.

[25] Bradford, P.G., and Rubin, R.P. Quantitative changes in inositol 1,4,5-trisphosphate in chemoattractant-stimulated neutrophils. *J. Biol. Chem.* **1986** 261, 15644-15647.

[26] Palmer, S., Hughes, K.T., Lee, D.Y., and Wakelam, M.J. Development of a novel, Ins(1,4,5)P3-specific binding assay. Its use to determine the intracellular concentration of Ins(1,4,5)P3 in unstimulated and vasopressin-stimulated rat hepatocytes. *Cellular Signalling* **1989** 1, 147-156.

[27] Palmer, S., and Wakelam, M.J. Mass measurement of inositol phosphates. [Review]. *Biochimica et Biophysica Acta* **1989** 1014, 239-246.

[28] Hirota, J., Furuichi, T., and Mikoshiba, K. Inositol 1,4,5-trisphosphate receptor as Ca^{2+} releasing channel on the endoplasmic reticulum. *Genes and Development* **1995** 81-96.

[29] Mikoshiba, K., Huchet, M., and Changeux, J.P. Biochemical and immunological studies on the P400 protein, a protein characteristic of the Purkinje cell from mouse and rat cerebellum. *Dev. Neurosci.* **1979** 2, 254-275.

[30] Mikoshiba, K., Okano, H., and Tsukada, Y. P400 protein characteristic to Purkinje cells and related proteins in cerebella from neuropathological mutant mice: autoradiographic study by ^{14}C-leucine and phosphorylation. *Dev. Neurosci.* **1985** 7, 179-187.

[31] Maeda, N., Niinobe, M., Nakahira, K., and Mikoshiba, K. Purification and characterization of P400 protein, a glycoprotein characteristic of Purkinje cell, from mouse cerebellum. *J. Neurochem.* **1988** 51, 1724-1730.

[32] Maeda, N., Niinobe, M., Inoue, Y., and Mikoshiba, K. Developmental expression and intracellular location of P400 protein characteristic of Purkinje cells in the mouse cerebellum. *Dev. Biol.* **1989** 133, 67-76.

[33] Yamamoto, H., Maeda, N., Niinobe, M., Miyamoto, E., and Mikoshiba, K. Phosphorylation of P400 protein by cyclic AMP-dependent protein kinase and Ca^{2+}/calmodulin-dependent protein kinase II. *J. Neurochem.* **1989** 53, 917-923.

[34] Supattapone, S., Worley, P.F., Baraban, J.M., and Snyder, S.H. Solubilization, purification, and characterization of an inositol trisphosphate receptor. *J. Biol. Chem.* **1988** 263, 1530-1534.

[35] Worley, P.F., Baraban, J.M., and Snyder, S.H. Inositol 1,4,5-trisphosphate receptor binding: autoradiographic localization in rat brain. *J. Neurosci.* **1989** 9, 339-346.

[36] Maeda, N., Niinobe, M., and Mikoshiba, K. A cerebellar Purkinje cell marker P400 protein is an inositol 1,4,5-trisphosphate (InsP3) receptor protein. Purification and characterization of InsP3 receptor complex. *EMBO J.* **1990** 9, 61-67.

[37] Furuichi, T., Yoshikawa, S., Miyawaki, A., Wada, K., Maeda, N., and Mikoshiba, K. Primary structure and functional expression of the inositol 1,4,5-trisphosphate-binding protein P400. *Nature* **1989** 342, 32-38.

[38] Mignery, G.A., Newton, C.L., Archer, B.T., and Sudhof, T.C. Structure and expression of the rat inositol 1,4,5-trisphosphate receptor. *J. Biol. Chem.* **1990** 265, 12679-12685.

[39] Yoshikawa, S., Tanimura, T., Miyawaki, A., Nakamura, M., Yuzaki, M., Furuichi, T., and Mikoshiba, K. Molecular cloning and characterization of the inositol 1,4,5-trisphosphate receptor in Drosophila melanogaster. *J. Biol. Chem.* **1992** 267, 16613-16619.

[40] Kume, S., Muto, A., Aruga, J., Nakagawa, T., Michikawa, T., Furuichi, T., Nakade, S., Okano, H., and Mikoshiba, K. The Xenopus IP3 Receptor: Structure, Function, and Localization in Oocytes and Eggs. *Cell* **1993** 73, 555-570.

[41] Yamada, N., Makino, Y., Clark, R.A., Pearson, D.W., Mattei, M.G., L., G.J., Ohama, E., Fujino, I., Miyawaki, A., Furuichi, T., and Mikoshiba, K. Human inositol 1,4,5-trisphosphate type 1 receptor, InsP3R1: structure, function, regulation of expression and cromosomal localization. *Biochem. J* **1994** 302, 781-790.

[42] Miyawaki, A., Furuichi, T., Ryou, Y., Yoshikawa, S., Nakagawa, T., Saitoh, T., and Mikoshiba, K. Structure-function relationships of the mouse inositol 1,4,5-trisphosphate receptor. *Proc. Natl. Acad. Sci. USA* **1991** 88, 4911-4915.

[43] Mignery, G.A., Johnston, P.A., and Sudhof, T.C. Mechanism of Ca^{2+} inhibition of inositol 1,4,5-trisphosphate (InsP3) binding to the cerebellar InsP3 receptor. *J. Biol. Chem.* **1992** 267, 7450-7455.

[44] Yamada, M., Miyawaki, A., Saito, K., Nakajima, T., Yamamoto-Hino, M., Furuichi, T., and Mikoshiba, K. The calmodulin binding domain in mouse type 1 inositol 1,4,5-trisphosphate receptor. *Biochem. J.* **1995** 308, 83-85.

[45] Maeda, N., Kawasaki, T., Nakade, S., Yokota, N., Taguchi, T., Kasai, M., and Mikoshiba, K. Structural and functional characterization of inositol 1,4,5-trisphosphate receptor channel from mouse cerebellum. *J. Biol. Chem.* **1991** 266, 1109-1116.

[46] Supattapone, S., Danoff, S.K., Theibert, A., Joseph, S.K., Steiner, J., and Snyder, S.H. Cyclic AMP-dependent phosphorylation of a brain inositol trisphosphate receptor decreases its release of calcium. *Proc Natl Acad Sci U S A* **1988** 85, 8747-8750.

[47] Komalavilas, P., and Lincoln, T.M. Phosphorylation of the inositol 1,4,5-trisphosphate receptor by cyclic GMP-dependent protein kinase. *J. Biol. Chem.* **1994** 269, 8701-8707.

[48] Ferris, C.D., Huganir, R.L., Bredt, D.S., Cameron, A.M., and Snyder, S.H. Inositol trisphosphate receptor: phosphorylation by protein kinase C and calcium calmodulin-dependent protein kinases in reconstituted lipid vesicles. *Proc Natl Acad Sci U S A* **1991** 88, 2232-2235.

[49] Furuichi, T., and Mikoshiba, K. Inositol 1,4,5-Trisphosphate Receptor-Mediated Ca^{2+} Signaling in the Brain. *Journal Neurochemistry* **1995** 64, 953-960.

[50] Mignery, G.A., and Sudhof, T.C. The ligand binding site and transduction mechanism in the inositol-1,4,5-triphosphate receptor. *EMBO J.* **1990** 9, 3893-3898.

[51] Ross, C.A., Danoff, S.K., Schell, M.J., Snyder, S.H., and Ullrich, A. Three additional inositol 1,4,5-trisphosphate receptors: molecular cloning and differential localization in brain and peripheral tissues. *Proc. Natl. Acad. Sci. U. S. A.* **1992** 89, 4265-4269.

[52] Sudhof, T.C., Newton, C.L., Archer III, B.T., Ushkaryov, Y.A., and Mignery, G.A. Structure of a novel InsP3 receptor. *EMBO J.* **1991** 10, 3199-3206.

[53] Michikawa, T., Hamanaka, H., Otsu, H., Yamamoto, A., Miyawaki, A., Furuichi, T., Tashiro, Y., and Mikoshiba, K. Transmembrane topology and sites of N-glycosylation of inositol 1,4,5-trisphosphate receptor. *J. Biol. Chem.* **1994** 269, 9184-9189.

[54] Nakanishi, S., Maeda, N., and Mikoshiba, K. Immunohistochemical localization of an inositol 1,4,5-trisphosphate receptor, P400, in neural tissue: studies in developing and adult mouse brain. *J. Neurosci.* **1991** 11, 2075-2086.

[55] Nakagawa, T., Okano, H., Furuichi, T., Aruga, J., and Mikoshiba, K. The subtypes of the mouse inositol 1,4,5-trisphosphate receptor are expressed in a tissue-specific and developmentally specific manner. *Proc. Natl. Acad. Sci. USA* **1991** 88, 6244-6248.

[56] Furuichi, T., Shiota, C., and Mikoshiba, K. Distribution of inositol 1,4,5-trisphosphate receptor mRNA in mouse tissues. *FEBS Lett.* **1990** 267, 85-88.

[57] Otsu, H., Yamamoto, A., Maeda, N., Mikoshiba, K., and Tashiro, Y. Immunogold localization of inositol 1, 4, 5-trisphosphate (InsP3) receptor in mouse cerebellar Purkinje cells using three monoclonal antibodies. *Cell Struc. Funct.* **1990** 15, 163-173.

[58] Ross, C.A., Meldolesi, J., Milner, T.A., Satoh, T., Supattapone, S., and Snyder, S.H. Inositol 1,4,5-trisphosphate receptor localized to endoplasmic reticulum in cerebellar Purkinje neurons. *Nature* **1989** 339, 468-470.

[59] Mignery, G.A., Sudhof, T.C., Takei, K., and De Camilli, P. Putative receptor for inositol 1,4,5-trisphosphate similar to ryanodine receptor. *Nature* **1989** 342, 192-195.

[60] Satoh, T., Ross, C.A., Villa, A., Supattapone, S., Pozzan, T., Snyder, S.H., and Meldolesi, J. The inositol 1,4,5,-trisphosphate receptor in cerebellar Purkinje cells: quantitative immunogold labeling reveals concentration in an ER subcompartment. *J. Cell Biol.* **1990** 111, 615-624.

[61] Yamamoto, A., Otsu, H., Yoshimori, T., Maeda, N., Mikoshiba, K., and Tashiro, Y. Stacks of flattened smooth endoplasmic reticulum highly enriched in inositol 1,4,5-trisphosphate ($InsP_3$) receptor in mouse cerebellar Purkinje cells. *Cell Struc. Funct.* **1991** 16, 419-432.

[62] Takei, K., Stukenbrok, H., Metcalf, A., Mignery, G.A., Sudhof, T.C., Volpe, P., and De, C.P. Ca^{2+} stores in Purkinje neurons: endoplasmic reticulum subcompartments demonstrated by the heterogeneous distribution of the $InsP_3$ receptor, Ca^{2+}-ATPase, and calsequestrin. *J. Neurosci.* **1992** 12, 489-505.

[63] Restrepo, D., Miyamoto, T., Bryant, B.P., and Teeter, J.H. Odor stimuli trigger influx of calcium into olfactory neurons of the channel catfish. *Science* **1990** 249, 1166-1168.

[64] Fadool, D.A., and Ache, B.W. Plasma membrane inositol 1,4,5-trisphosphate-activated channels mediate signal transduction in lobster olfactory receptor neurons. *Neuron* **1992** 9, 907-918.

[65] Kuno, M., and Gardner, P. Ion channels activated by inositol 1,4,5-trisphosphate in plasma membrane of human T-lymphocytes. *Nature* **1987** 326, 301-304.

[66] Khan, A.A., Steiner, J.P., Klein, M.G., Schneider, M.F., and Snyder, S.H. IP_3 receptor: localization to plasma membrane of T cells and cocapping with the T cell receptor. *Science* **1992** 257, 815-818.

[67] Khan, A.A., Steiner, J.P., and Snyder, S.H. Plasma membrane inositol 1,4,5-trisphosphate receptor of lymphocytes: selective enrichment in sialic acid and unique binding specificity. *Proc. Natl. Acad. Sci. U. S. A.* **1992** 89, 2849-2853.

[68] Parys, J.B., Sernett, S.W., DeLisle, S., Snyder, P.M., Welsh, M.J., and Campbell, K.P. Isolation, characterization, and localization of the inositol 1,4,5-trisphosphate receptor protein in Xenopus laevis oocytes. *J. Biol. Chem.* **1992** 267, 18776-18782.

[69] Mourey, R.J., Verma, A., Supattapone, S., and Snyder, S.H. Purification and characterization of the inositol 1,4,5- trisphosphate receptor protein from rat vas deferens. *Biochem. J.* **1990** 272, 383-389.

[70] Worley, P.F., Baraban, J.M., Supattapone, S., Wilson, V.S., and Snyder, S.H. Characterization of inositol trisphosphate receptor binding in brain. Regulation by pH and calcium. *J. Biol. Chem.* **1987** 262, 12132-12136.

[71] Miyawaki, A., Furuichi, T., Maeda, N., and Mikoshiba, K. Expressed cerebellar-type inositol 1,4,5-trisphosphate receptor, P400, has calcium release activity in a fibroblast L cell line. *Neuron* **1990** 5, 11-18.

[72] Danoff, S.K., Ferris, C.D., Donath, C., Fischer, G.A., Munemitsu, S., Ullrich, A., Snyder, S.H., and Ross, C.A. Inositol 1,4,5-trisphosphate receptors: distinct neuronal and nonneuronal forms derived by alternative splicing differ in phosphorylation. *Proc. Natl. Acad. Sci. U. S. A.* **1991** 88, 2951-2955.

[73] Ferris, C.D., Cameron, A.M., Bredt, D.S., Huganir, R.L., and Snyder, S.H. Inositol 1,4,5-trisphosphate receptor is phosphorylated by cyclic AMP-dependent protein kinase at serines 1755 and 1589. *Biochem. Biophys. Res. Commun.* **1991** 175, 192-198.

[74] Hajnoczky, G., Gao, E., Nomura, T., Hoek, J.B., and Thomas, A.P. Multiple mechanisms by which protein kinase A potentiates inositol 1,4,5-trisphosphate-induced Ca^{2+} mobilization in permeabilized hepatocytes. *Biochem. J.* **1993** 293, 413-422.

[75] Nakade, S., Rhee, S.K., Hamanaka, H., and Mikoshiba, K. Cyclic AMP-dependent phosphorylation of an immunoaffinity-purfied homotetrameric inositol 1,4,5-trisphosphate

receptor (type I) increases Ca^{2+} flux in reconstituted lipid vesicles. *J. Biol. Chem.* **1994** 269, 6735-6742.

[76] Ferris, C.D., Huganir, R.L., and Snyder, S.H. Calcium flux mediated by purified inositol 1,4,5-trisphosphate receptor in reconstituted lipid vesicles is allosterically regulated by adenine nucleotides. *Proc Natl Acad Sci U S A* **1990** 87, 2147-2151.

[77] Bennett, V. Spectrin-based membrane skeleton: a multipotential adaptor between plasma membrane and cytoplasm [published errata appear in Physiol Rev 1991 Jan;71(1):preceding Table of Contents and 1991 Oct;71(4):following 1193]. [Review]. *Physiological Reviews* **1990** 70, 1029-1065.

[78] Lokeshwar, V.B., and Bourguignon, L.Y. The lymphoma transmembrane glycoprotein GP85 (CD44) is a novel guanine nucleotide-binding protein which regulates GP85 (CD44)-ankyrin interaction. *J. Biol. Chem.* **1992** 267, 22073-22078.

[79] Joseph, S.K., and Samanta, S. Detergent solubility of the inositol trisphosphate receptor in rat brain membranes. Evidence for association of the receptor with ankyrin. *J. Biol. Chem.* **1993** 268, 6477-6486.

[80] Bourguignon, L.Y., Jin, H., Iida, N., Brandt, N.R., and Zhang, S.H. The involvement of ankyrin in the regulation of inositol 1,4,5-trisphosphate receptor-mediated internal Ca^{2+} release from Ca^{2+} storage vesicles in mouse T-lymphoma cells. *J. Biol. Chem.* **1993** 268, 7290-7297.

[81] Lilly, Y.W.B., and Hengtao, J. Identification of the ankyrin-binding domain of the mouse T-lymphoma cell inositol 1,4,5-trisphosphate (IP3) receptor and its role in the regulation of IP3-mediated internal Ca^{2+} release. *J. Biol. Chem.* **1995** 270, 7257-7260.

[82] Cameron, A.M., Steiner, J.P., Sabatini, D.M., Kaplin, A.I., Walensky, L.D., and Snyder, S.H. Immunophilin FK506 binding protein associated with inositol 1,4,5-trisphosphate receptor modulates calcium flux. *Proc. Natl. Acad. Sci. USA* **1994** 92, 1784-1788.

[83] Yoo, S.H. pH-dependent interaction of chromogranin A with integral membrane proteins of secretory vesicle including 260-kDa protein reactive to inositol 1,4,5-triphosphate receptor antibody. *J. Biol. Chem.* **1994** 269, 12001-12006.

[84] Ferris, C.D., Huganir, R.L., Supattapone, S., and Snyder, S.H. Purified inositol 1,4,5-trisphosphate receptor mediates calcium flux in reconstituted lipid vesicles. *Nature* **1989** 342, 87-89.

[85] Takahashi, M., Tanzawa, K., and Takahashi, S. Adenophostins, newly discovered metabolites of Penicillium brevicompactum, act as potent agonists of the inositol 1,4,5-trisphosphate receptor. *J. Biol. Chem.* **1994** 269, 369-372.

[86] Newton, C.L., Mignery, G.A., and Sudhof, T.C. Co-expression in Vertebrate Tissues and Cell Lines of Multiple Inositol 1,4,5-Trisphosphate Reeptors with Distinct Affinities for IP3. *J. Biol. Chem.* **1994** 269, 28613-28619.

[87] Yamamoto-Hino, M., Sugiyama, T., Hikichi, K., Mattei, M.G., Hasegawa, K., Sekine, S., Sakurada, K., Miyawaki, A., Furuichi, T., Hasegawa, M., and Mikoshiba, K. Cloning and characterization of human type 2 and type 3 inositol 1, 4, 5-trisphosphate receptors. *Recepters and Channels* **1994** 2, 9-22

[88] Blondel, O., Takeda, J., Janssen, H., Seino, S., and Bell, G.I. Sequence and functional characterization of a third inositol trisphosphate receptor subtype, IP3R-3, expressed in pancreatic islets, kidney, gastrointestinal tract, and other tissues. *J. Biol. Chem.* **1993** 268, 11356-11363.

[89] Maranto, A.R. Primary structure, ligand binding, and localization of the human type 3 inositol 1,4,5-trisphosphate receptor expressed in intestinal epithelium. *J. Biol. Chem.* **1994** 269, 1222-1230.

[90] Champeil, P., Combettes, L., Berthon, B., Doucet, E., Orlowski, S., and Claret, M. Fast kinetics of calcium release induced by myo-inositol trisphosphate in permeabilized rat hepatocytes. *J. Biol. Chem.* **1989** 264, 17665-17673.

[91] Meyer, T., Wensel, T., and Stryer, L. Kinetics of calcium channel opening by inositol 1,4,5-trisphosphate. *Biochemistry* **1990** 29, 32-37.

[92] Finch, E.A., Turner, T.J., and Goldin, S.M. Calcium as a coagonist of inositol 1,4,5-trisphosphate-induced calcium release. *Science* **1991** 252, 443-446.

[93] Somlyo, A.V., Horiuti, K., Trentham, D.R., Kitazawa, T., and Somlyo, A.P. Kinetics of Ca^{2+} release and contraction induced by photolysis of caged D-myo-inositol 1,4,5-trisphosphate in smooth muscle. The effects of heparin, procaine, and adenine nucleotides. *J. Biol. Chem.* **1992** 267, 22316-22322.

[94] Kindman, L.A., and Meyer, T. Use of intracellular Ca^{2+} stores from rat basophilic leukemia cells to study the molecular mechanism leading to quantal Ca^{2+} release by inositol 1,4,5-trisphosphate. *Biochemistry* **1993** 32, 1270-1277.

[95] Ghosh, T.K., Mullaney, J.M., Tarazi, F.I., and Gill, D.L. GTP-activated communication between distinct inositol 1,4,5-trisphosphate-sensitive and -insensitive calcium pools. *Nature* **1989** 340, 236-239.

[96] Hajnoczky, G., Lin, C., and Thomas, A.P. Luminal communication between intracellular calcium stores modulated by GTP and the cytoskeleton. *J. Biol. Chem.* **1994** 269, 10280-10287.

[97] Iino, M. Biphasic Ca^{2+} dependence of inositol 1,4,5-trisphosphate-induced Ca^{2+} release in smooth muscle cells of the guinea pig taenia caeci. *J. Gen. Physiol.* **1990** 95, 1103-1122.

[98] Iino, M., and Endo, M. Calcium-dependent immediate feedback control of inositol 1,4,5-trisphosphate-induced Ca^{2+} release. *Nature* **1992** 360, 76-78.

[99] Missiaen, L., De Smedt, H., Droogmans, G., and Casteels, R. Luminal Ca^{2+} controls the activation of the inositol 1,4,5-trisphosphate receptor by cytosolic Ca^{2+}. *J. Biol. Chem.* **1992** 267, 22961-22966.

[100] Combettes, L., and Champeil, P. Calcium and inositol 1,4,5-trisphosphate-induced Ca^{2+} release [letter]. *Science* **1994** 265, 813-815.

[101] Missiaen, L., De Smedt, H., Parys, J.B., and Casteels, R. Co-activation of inositol trisphosphate-induced Ca^{2+} release by cytosolic Ca^{2+} is loading-dependent. *J. Biol. Chem.* **1994** 269, 7238-7242.

[102] Missiaen, L., Parys, J.B., De Smedt, H., Himpens, B., and Casteels, R. Inhibition of inositol trisphosphate-induced calcium release by caffeine is prevented by ATP. *Biochem. J.* **1994** 300, 81-84.

[103] Muallem, S., Pandol, S.J., and Beeker, T.G. Hormone-evoked calcium release from intracellular stores is a quantal process. *J. Biol. Chem.* **1989** 264, 205-12.

[104] Watras, J., Bezprozvanny, I., and Ehrlich, B.E. Inositol 1,4,5-trisphosphate-gated channels in cerebellum: presence of multiple conductance states. *J. Neurosci.* **1991** 11, 3239-3245.

[105] Meyer, T., Holowka, D., and Stryer, L. Highly cooperative opening of calcium channels by inositol 1,4,5-trisphosphate. *Science* **1988** 240, 653-656.

[106] Meyer, T., and Stryer, L. Transient calcium release induced by successive increments of inositol 1,4,5-trisphosphate. *Proc. Natl. Acad. Sci. USA* **1990** 87, 3841-3845.

[107] Pietri, F., Hilly, M., and Mauger, J.P. Calcium mediates the interconversion between two states of the liver inositol 1,4,5-trisphosphate receptor. *J. Biol. Chem.* **1990** 265, 17478-17485.

[108] Taylor, C.W., and Potter, B.V. The size of inositol 1,4,5-trisphosphate-sensitive Ca^{2+} stores depends on inositol 1,4,5-trisphosphate concentration. *Biochem. J.* **1990** 266, 189-194.

[109] Missiaen, L., De Smedt, H., Droogmans, G., and Casteels, R. Ca^{2+} release induced by inositol 1,4,5-trisphosphate is a steady-state phenomenon controlled by luminal Ca^{2+} in permeabilized cells. *Nature* **1992** 357, 599-602.

[110] Loomis-Husselbee, J.W., and Dawson, A.P. A steady-state mechanism can account for the properties of inositol 2,4,5-trisphosphate-stimulated Ca^{2+} release from permeabilized L1210 cells. *Biochem. J.* **1993** 289, 861-866.

[111] Bootman, M.D. Quantal Ca^{2+} release from InsP3-sensitive intracellular Ca^{2+} stores. [Review]. *Molecular & Cellular Endocrinology* **1994** 98, 157-166.

[112] Bootman, M.D., Cheek, T.R., Moreton, R.B., Bennett, D.L., and Berridge, M.J. Smoothly graded Ca^{2+} release from inositol 1,4,5-trisphosphate-sensitive Ca^{2+} stores. *J. Biol. Chem.* **1994** 269, 24783-24791.

[113] Combettes, L., Claret, M., and Champeil, P. Calcium control on InsP3-induced discharge of calcium from permeabilised hepatocyte pools. *Cell Calcium* **1993** 14, 279-292.

[114] Oldershaw, K.A., Nunn, D.L., and Taylor, C.W. Quantal Ca^{2+} mobilization stimulated by inositol 1,4,5-trisphosphate in permeabilized hepatocytes. *Biochem. J.* **1991** 278, 705-708.

[115] Sayers, L.G., Brown, G.R., Michell, R.H., and Michelangeli, F. The effects of thimerosal on calcium uptake and inositol 1,4,5-trisphosphate-induced calcium release in cerebellar microsomes. *Biochem. J.* **1993** 289, 883-887.

[116] Ferris, C.D., Cameron, A.M., Huganir, R.L., and Snyder, S.H. Quantal calcium release by purified reconstituted inositol 1,4,5-trisphosphate receptors. *Nature* **1992** 356, 350-352.

[117] Bezprozvanny, I., Watras, J., and Ehrlich, B.E. Bell-shaped calcium-response curves of Ins(1,4,5)P_3- and calcium-gated channels from endoplasmic reticulum of cerebellum. *Nature* **1991** 351, 751-754.

[118] Missiaen, L., Parys, J.B., De Smedt, H., Oike, M., and Casteels, R. Partial calcium release in response to submaximal inositol 1,4,5-trisphosphate receptor activation. [Review]. *Molecular & Cellular Endocrinology* **1994** 98, 147-156.

[119] Zhang, B.X., Zhao, H., and Muallem, S. Ca^{2+}-dependent kinase and phosphatase control inositol 1,4,5-trisphosphate-mediated Ca^{2+} release. Modification by agonist stimulation. *J. Biol. Chem.* **1993** 268, 10997-1001.

[120] Luttrell, B.M. The biological relevance of the binding of calcium ions by inositol phosphates. *J. Biol. Chem.* **1993** 268, 1521-1524.

[121] Magnusson, A., Haug, L.S., Walaas, S.I., and Ostvold, A.C. Calcium-induced degradation of the inositol (1,4,5)-trisphosphate receptor/Ca^{2+}-channel. *FEBS Lett.* **1993** 323, 229-232.

[122] Brass, L.F., and Joseph, S.K. A role for inositol triphosphate in intracellular Ca^{2+} mobilization and granule secretion in platelets. *J. Biol. Chem.* **1985** 260, 15172-15179.

[123] Varney, M.A., Rivera, J., Lopez, B.A., and Watson, S.P. Are there subtypes of the inositol 1,4,5-trisphosphate receptor? *Biochem. J.* **1990** 269, 211-216.

[124] Chilvers, E.R., Challiss, R.A., Willcocks, A.L., Potter, B.V., Barnes, P.J., and Nahorski, S.R. Characterisation of stereospecific binding sites for inositol 1,4,5-trisphosphate in airway smooth muscle. *British Journal of Pharmacology* **1990** 99, 297-302.

[125] Enouf, J., Giraud, F., Bredoux, R., Bordeau, N., and Toledano-Levy, S. Possible role for cAMP-dependent phosphorylation in the calcium release mediated bi inositol 1,4,5-trisphosphate in human platelet membrane vesicles. *Biochem. Biophys. Acta* **1987** 928, 7682.

[126] Burgess, G.M., Bird, G.S., Obie, J.F., and Putney, J.J. The mechanism for synergism between phospholipase C- and adenylylcyclase-linked hormones in liver. Cyclic AMP-dependent kinase augments inositol trisphosphate-mediated Ca^{2+} mobilization without increasing the cellular levels of inositol polyphosphates. *J. Biol. Chem.* **1991** 266, 4772-4781.

[127] Volpe, P., and Alderson, L.B. Regulation of inositol 1,4,5-trisphosphate-induced Ca^{2+} release. II. Effect of cAMP-dependent protein kinase. *Am J Physiol* **1990** 258, 1086-1091.

[128] Quinton, T.M., and Dean, W.L. Cyclic AMP-dependent phosphorylation of the inositol-1,4,5-trisphosphate receptor inhibits Ca^{2+} release from platelet membranes. *Biochem. Biophys. Res. Commun.* **1992** 184, 893-899.

[129] Tsukioka, M., Iino, M., and Endo, M. pH dependence of inositol 1,4,5-trisphosphate-induced Ca^{2+} release in permeabilized smooth muscle cells of the guinea-pig. *J. Physiol.* **1994** 475, 369-375.

[130] Irvine, R.F. 'Quantal' Ca^{2+} release and the control of Ca^{2+} entry by inositol phosphates--a possible mechanism. [Review]. *FEBS Lett.* **1990** 263, 5-9.

[131] Nunn, D.L., and Taylor, C.W. Luminal Ca^{2+} increases the sensitivity of Ca^{2+} stores to inositol 1,4,5-trisphosphate. *Molecular Pharmacology* **1992** 41, 115-119.

[132] Combettes, L., Claret, M., and Champeil, P. Do submaximal InsP3 concentrations only induce the partial discharge of permeabilized hepatocyte calcium pools because of the concomitant reduction of intraluminal Ca^{2+} concentration? *FEBS Lett.* **1992** 301, 287-290.

[133] Gyorke, S., and Fill, M. Ryanodine receptor adaptation: control mechanism of Ca^{2+}-induced Ca^{2+} release in heart. *Science* **1993** 260, 807-809.

[134] Hajnoczky, G., and Thomas, A.P. The inositol trisphosphate calcium channel is inactivated by inositol trisphosphate. *Nature* **1994** 370, 474-477.

[135] Mark, D.D., and Foskett, J.K. Single-channel inositol 1,4,5-trisphosphate receptor currents revealed by patch clamp of isolated Xenopus oocyte nuclei. *J. Biol. Chem.* **1994** 269, 29375-29378.

[136] Berridge, M.J., and Galione, A. Cytosolic calcium oscillators. *FASEB J.* **1988** 2, 3074-3082.

[137] Berridge, M.J. Calcium oscillations. *J. Biol. Chem.* **1990** 265, 9583-9586.

[138] Rooney, T.A., and Thomas, A.P. Organization of intracellular calcium signals generated by inositol lipid-dependent hormones. [Review]. *Pharmacology & Therapeutics* **1991** 49, 223-237.

[139] Meyer, T., and Stryer, L. Calcium spiking. [Review]. *Annual Review of Biophysics & Biophysical Chemistry* **1991** 20, 153-174.

[140] Nathanson, M.H., Padfield, P.J., O'Sullivan, A.J., Burgstahler, A.D., and Jamieson, J.D. Mechanism of Ca^{2+} wave propagation in pancreatic acinar cells. *J. Biol. Chem.* **1992** 267, 18118-18121.

[141] Lechleiter, J., Girard, S., Peralta, E., and Clapham, D. Spiral calcium wave propagation and annihilation in Xenopus laevis oocytes. *Science* **1991** 252, 123-126.

[142] Swann, K. Different triggers for calcium oscillations in mouse eggs involve a ryanodine-sensitive calcium store. *Biochem. J.* **1992** 287, 79-84.

[143] Rooney, T.A., and Thomas, A.P. Intracellular calcium waves generated by Ins(1,4,5)P3-dependent mechanisms. [Review]. *Cell Calcium* **1993** 14, 674-690.

[144] Miyazaki, S., Yuzaki, M., Nakada, K., Shirakawa, H., Nakanishi, S., Nakade, S., and Mikoshiba, K. Block of Ca^{2+} wave and Ca^{2+} oscillation by antibody to the inositol 1,4,5-trisphosphate receptor in fertilized hamster eggs [published erratum appears in Science 1992 Oct 9;258(5080):following 203]. *Science* **1992** 257, 251-255.

[145] Sanchez, and Cobbold, P.H. Agonist-specificity in the role of Ca^{2+}-induced Ca^{2+} release in hepatocyte Ca^{2+} oscillations. *Biochem. J.* **1993** 291, 169-172.

[146] Hirota, J., Kohda, K., Miyawaki, A., Furuichi, T., and Mikoshiba, K. Analysis of IP3 receptor / Ca^{2+} release channel. *Saibou Kougaku* **1994** 13, 637-648.

[147] Yamamoto-Hino, M., Miyawaki, A., Kawano, H., Sugiyama, T., Furuichi, T., Hasegawa, M., and Mikoshiba, K. Immunohistochemical study of inositol 1,4,5-trisphosphate receptor type 3 in rat central nervous system. *Neuro Report* **1995** 6, 273-276.

[148] Sugiyama, T., Furuya, A., Monkawa, T., Yamamoto-Hino, M., Satoh, S., Ohmori, K., Miyawaki, A., Hanai, N., Mikoshiba, K., and Hasegawa, M. Monoclonal antibodys recognizing the subtypes of inositol 1,4,5-trisphosphate receptor: Application to the studies on inflammatory cells. *FEBS Lett.* **1994** 354, 149-154.

[149] Monkawa, T., Miyawaki, A., Sugiyama, T., Yoneshima, H., Yamamoto-Hino, M., Furuichi, T., Saruta, T., Hasegawa, M., and Mikoshiba, K. Heterotetrameric complex formation of inositol 1,4,5-trisphosphate receptor subunits. *J. Biol. Chem.* **1995** 270, 14700-14704.

[150] Hirota, J., Michikawa, T., Miyawaki, A., Takahashi, M., Tanzawa, K., Okura, I., Furuichi, T., and Mikoshiba, K. Adenophostin-mediated quantal Ca^{2+} release in the

purified and reconstituted inositol 1,4,5-trisphosphate receptor type 1. *FEBS Lett.* **1995** 368, 248-252.

[151] Renard-Rooney, D.C., Hajnoczky, G., Seitz, M.B., Schneider, T.G., and Thomas, A.P. Imaging of inositol 1,4,5-trisphosphate-induced Ca^{2+} fluxes in single permeabilized hepatocytes. Demonstration of both quantal and nonquantal patterns of Ca^{2+} release. *J. Biol. Chem.* **1993** 268, 23601-23610.

[152] Takei, K., Mignery, G.A., Mugnaini, E., Sudhof, T.C., and De Camilli, P. Inositol 1,4,5-trisphosphate receptor causes formation of ER cisternal stacks in transfected fibroblasts and in cerebellar Purkinje cells. *Neuron* **1994** 12, 327-342.

[153] Richardson, A., and Taylor, C.W. Effects of Ca^{2+} chelators on purified inositol 1,4,5-trisphosphate (InsP3) receptors and InsP3-stimulated Ca^{2+} mobilization. *J. Biol. Chem.* **1993** 268, 11528-11533.

[154] Pietri, F., Hilly, M., Claret, M., and Mauger, J.P. Characterisation of 2 reversible states of the inositol 1,4,5-trisphosphate receptor in rat hepatocytes. *Gastroenterol Clin Biol* **1990** 14, 710-714.

[155] Hirose, K., and Iino, M. Heterogeneity of channel density in inositol-1,4,5-trisphosphate-sensitive Ca^{2+} stores. *Nature* **1994** 372, 791-794.

[156] Takahashi, M., Kagasaki, T., Hosoya, T., and Takahashi, S. *Journal of Antibiotics* **1993** 46, 1643-1647.

[157] Hirota, J., Michikawa, T., Miyawaki, A., Furuichi, T., Okura, I. and Mikoshiba, K. Kinetics of calcium release by the immunoaffinity-purified inositol 1,4,5-trisphosphate receptor reconstituted into lipid vesicles. *J. Biol. Chem.* **1995,** 270, 19046-19051